Roles of Alkali Metals *tert*-Butoxide as Catalysts and Activators in Organic Transformations

Chandresh K. Patel,[a] Sourav Banerjee,[a] Kamal Kant,[a] Ragini Sengupta,[b] Nayyef Aljaar,[c] and Chandi C. Malakar*[a]

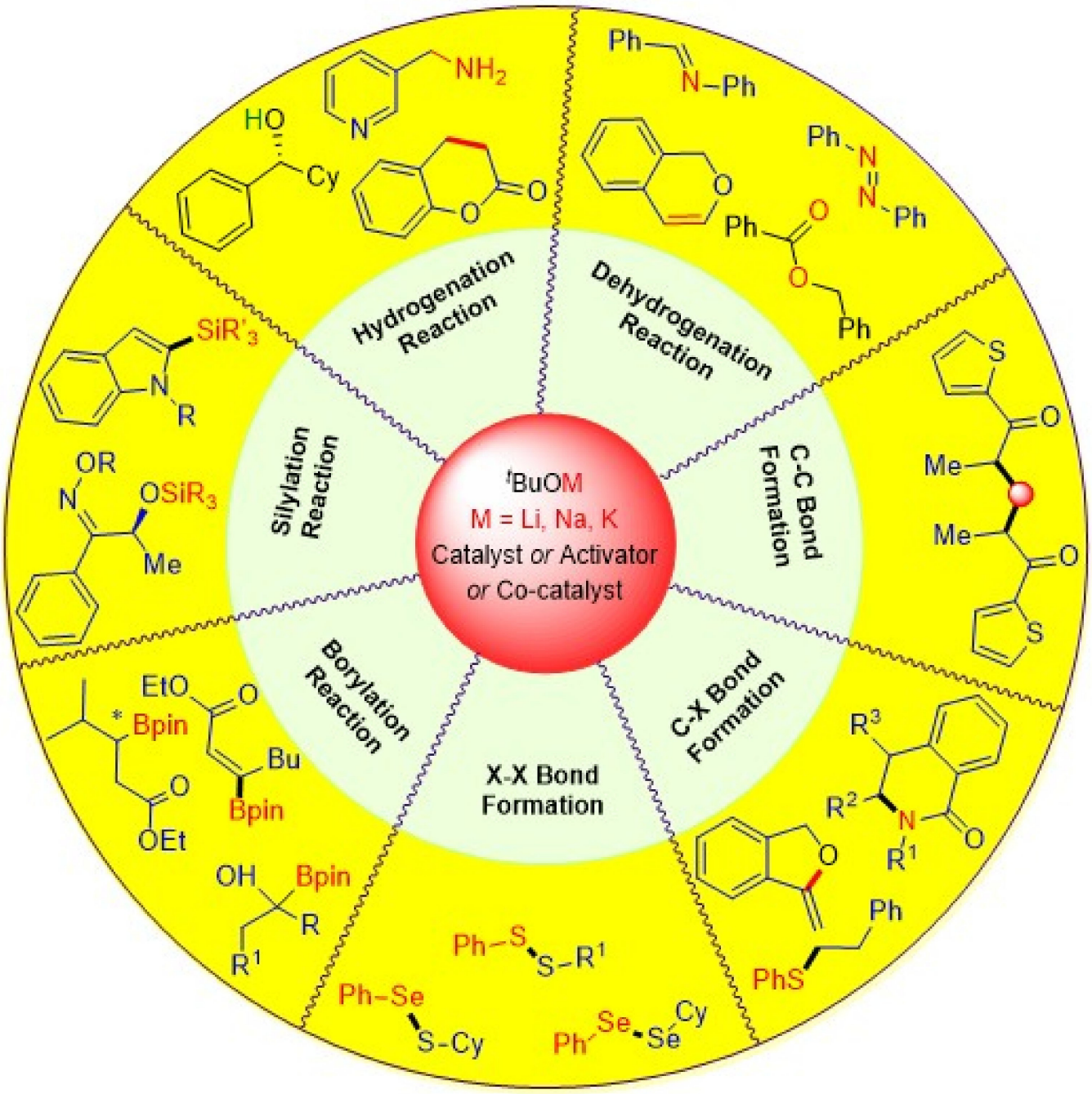

The alkali metal *tert*-butoxides have found wide application as catalysts and activators for the conversion of numerous organic molecules. These formidable additives in catalytic amounts are extensively employed in the transition metal-free approaches to serve for the single-electron transfer processes towards the formation of C–C and C-heteroatom bond formation. This review elucidates their multifaceted roles encompassing a series of novel synthetic methodologies, in-depth analyses of their reactivity patterns, and catalytic efficiencies across a myriad of reactions. The involvement of alkali metal *tert*-butoxides either directly or in combination with other metals as catalysts are discussed along with the detailed mechanistic pathways in various reactions. Overall, this article summarises approximately all reactions those have been influenced by the catalytic amounts of *tert*-butoxides and reported in the last decades.

1. Introduction

In recent years, the development of novel reagents in organic transformations has generated extensive interest in the construction of biologically important N, O, and S containing heterocycles.[1–3] The alkali metal *tert*-butoxides are among these significant class of reagents, which are commercially available chemical compounds with the general formula $(CH_3)_3COM$, where M is (Li, Na, or K). Recently, the unexampled reactivity of these reagents has prompted the search for a new area of research due to their unique ways of involvement in organic transformations as catalysts or activators. The basic strength of *tert*-butoxides has been found to be solvent dependent, which is highest in DMSO solvent and lowest in nonpolar solvents like benzene and others.[4] In the previous years, *tert*-butoxides have witnessed enormous utilization in organic reactions and have been found to be effective surrogates of transition metals. For instance, one of the most industrially important transformations in organic chemistry refers to the cross-coupling reactions of arylhalides with activated or non-activated arenes to furnish biaryl products, and these types of reactions can be generously affected by *tert*-butoxides through a single electron transfer mechanism.[5–8] In recent years two review articles have been published on KO^{t}Bu mediated reactions;[9,10] whereas, a broad perspective of organic transformations using catalytic amounts of all alkali metal *tert*-butoxides would attract the attention of readers in organic chemistry.

The alkali metal *tert*-butoxides in catalytic amounts, have mostly been discovered as either activators or co-catalysts in combination with transition metals or have even been directly used as catalysts. More recently, Jenkins and Krenske in 2020, reviewed a mechanistic study on $HSiR_3$/KO^{t}Bu-mediated reactions[11] and Yoshida in 2016 has shown the combination of base/metal catalysis for the borylation of alkynes.[12] In this review article, in detail we have described various approaches related to alkali metal *tert*-butoxides as catalysts or activators in a wide range of organic transformations.

[a] *C. K. Patel, S. Banerjee, K. Kant, Dr. C. C. Malakar*
Department of Chemistry,
National Institute of Technology Manipur
Langol, Imphal-795004, Manipur (India)
E-mail: chdeepm@gmail.com
cmalakar@nitmanipur.ac.in

[b] *R. Sengupta*
Institute for Photon Science and Synchrotron Radiation (IPS), Karlsruhe Institute of Technology (KIT),
Helmholtz-Platz 1, 76344 Eggenstein-Leopoldshafen (Germany)

[c] *Dr. N. Aljaar*
Department of Chemistry, Faculty of Science
The Hashemite University
P.O. Box 330127, Zarqa 13133 (Jordan)

2. Role of catalytic amounts of alkali metal (Li, Na, and K) *tert*-butoxides in efficient organic transformations: In transition metal-free synthetic procedures

2.1. Silylation reactions

Grubbs *et al.*[13] in 2015 demonstrated a mild approach for the dehydrogenative C–H silylation of substantial numbers of heteroarenes **1** at the C2 centre using ^{t}BuOK as a catalyst and hydrosilanes **2** as a silylating reagent, producing C2 silylated products with good yield and regioselectivity (> 20:1, C-2:C-3), which is presented in Scheme 1.

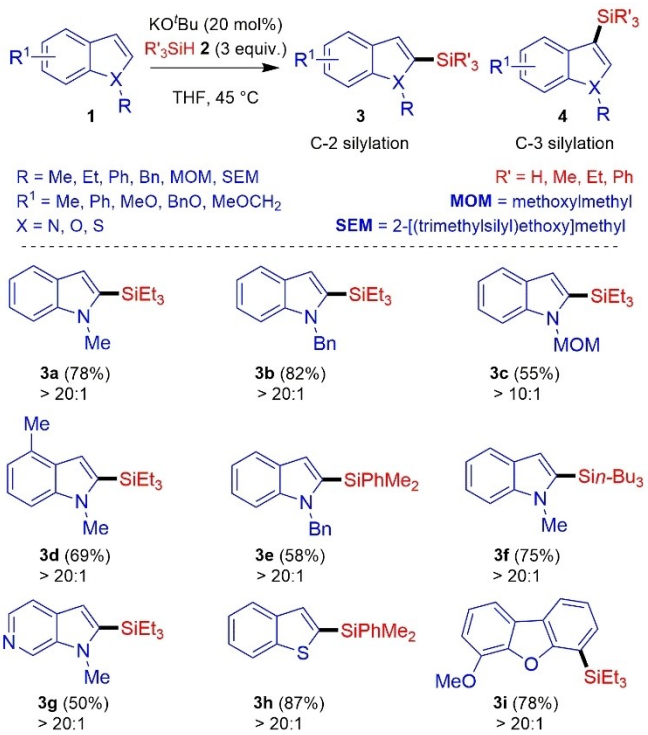

Scheme 1. KO^{t}Bu Catalyzed cross dehydrogenative C–H silylation of heteroarene.

After stabilizing the methodology, various heteroarenes containing N, O, and S were tested and successfully converted into C-2 silylated product **3** in moderate to good yields and exhibited good functional group tolerance having neutral or electron-donating heterocycles, whereas indoles having electron-withdrawing substituents were unreactive. Further, the application of heteroaryl silanes has been performed to investigate the efficiency of this described protocol.

Based on the literature precedents[13] and extensive experimental and computational studies, Stoltz *et al.*[14] published an article in 2017 depicting the detailed reaction mechanism of C–H bond silylation of heteroarenes using environmentally benign potassium *tert*-butoxide as a catalyst. This research introduced the concept of utilizing the earth-abundant main group metal alkoxide, i.e. KO^{t}Bu as a catalyst for the effective direct dehydrogenative C–H silylation of many important

heteroarenes including 1-methyl indole **1 a** in the presence of hydrosilanes. Alkali metal alkoxides embedded with small cations like NaO^{t}Bu were found to be inactive. Silylation at the C2 position of 1-methyl indole was observed to be the major product, whereas silylation at the C3 was realized as a minor product. However, the reverse was observed with an increased temperature and prolonged reaction time, provided that the C2 functionalization is the kinetically controlled product and the C3 silylation is the thermodynamically controlled product.

Moreover, the KO^{t}Bu-catalyzed silylation of heteroarenes was observed to be reversible in the cross-over experiments. The use of stoichiometric 2,2,6,6-tetramethyl-1-piperidinyloxy (TEMPO) as a radical inhibitor indicated that the reaction proceeds *via* a radical mechanism, and the mixture of KO^{t}Bu with Et_3SiH in THF was found to be electron paramagnetic resonance (EPR) active at the temperature of 45 °C. Based on these observations, it was postulated that a silyl radical species is involved in the catalytic C–H silylation reaction. Furthermore, to understand the involved reaction mechanism, many studies and experiments were performed including a radical clock experiment, a kinetic isotope effect, an NMR study, and a ReactIR *in situ* study. A computational study, Density Functional Theory (DFT), was carried out that sheds light on the radical chain process. Considering the crucial role of heteroarenes in medicinal chemistry, natural products, and polymer chemistry the direct dehydrogenative C–H silylation using this approach is worth mentioning. The proposed approach is environmentally-friendly with a simple experimental procedure that has good functional group tolerance.

The proposed reaction mechanism in Scheme 2 indicates the addition of triethylsilyl radical at the C2 position of the indole moiety to form benzylic radical **II**, as the silyl radical addition to the double bond occurs readily which facilitates the formation of a more stable σ-bond in the expense of a less stable π-bond. Hydrogen gas is liberated when the C2-H bond α-position to the radical centre gets fragmented by β-H scission and then aromaticity gets restored in the system. The chaining process is restored when the generated silicate radical anion **III** reacts with triethylsilane **2 a** to form triethylsilyl radical.

An alternative reaction mechanism has also been proposed in Scheme 3, where $(KO^tBu)_4$ plays the role of hydrogen atom transfer catalyst by abstracting one hydrogen atom from **II** and forming silylated moiety **3 a** in addition to the base-hydrogen adduct **IV**. The adduct **IV** reacts with **2 a** to form a triethylsilyl radical and the catalytic cycle is continued.

Interestingly, in the same year (2017), Zare *et al.*[15] brought two more possible reaction mechanisms into the limelight for the C–H silylation of heteroarenes using potassium *tert*-butoxide as a catalyst. After going through extensive experimental and computational studies including DFT calculations, they proposed a mechanism that involves an ionic pathway, and another proposal is based on a neutral pathway.

In the proposed ionic pathway (Scheme 4), the electron-rich heteroarene **1** in the companionship of potassium ion forms a cation-π complex **I**, and in the presence of *tert*-butoxide ion, silane moiety **2** forms an intermediate **V** which deprotonates C2-H and C3-H to form the complexes **IIa** and **IIb** respectively, in addition to the release of hydrogen gas. From the complexes **IIa** and **IIb**, reactive carbanions **IIIa** and **IIIb** are formed which form pentacoordinated silicon intermediates **IVa** and **IVb** in the presence of silyl ether **VI**. Finally, products **3** and **4** were formed by the dissociation of *tert*-butoxide from **IVa** and **IVb**.

In the neutral mechanism (Scheme 5), the intermediates are neutral, otherwise, it resembles the ionic pathway. One silicon-oxygen bond is formed in the reaction between Me_3SiH and the KO^{t}Bu tetramer giving rise to pentacoordinated intermediate **II**. The KO^{t}Bu tetramer does not dissociate in the neutral mechanism. In the next step, the silicon-hydrogen bond of intermediate **II** is reported to undergo heterolysis followed by the formation of complex **III** in which the hydride ion remains

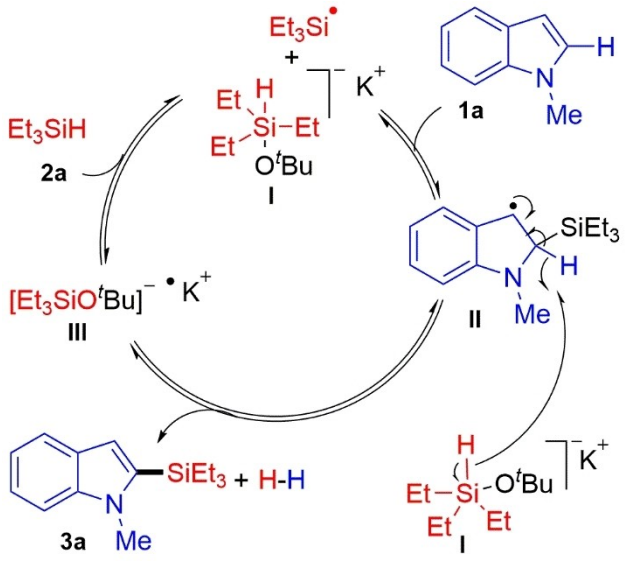

Scheme 2. Proposed mechanism *via* radical pathway promoted by penta-coordinated silicon.

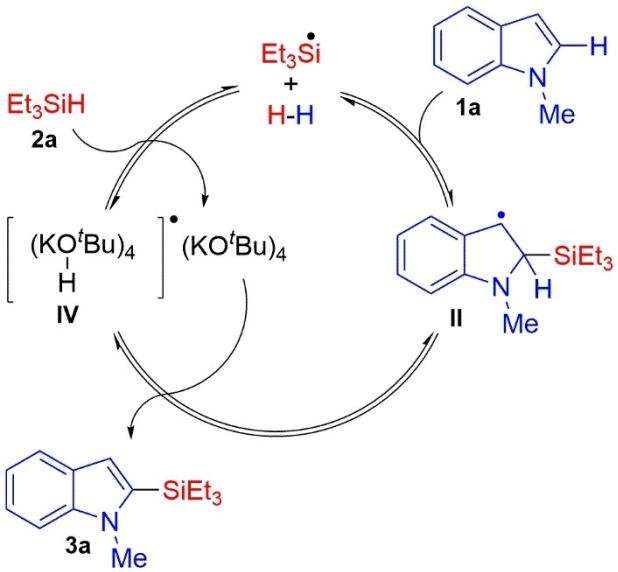

Scheme 3. Radical pathway promoted by tetrameric KO^{t}Bu.

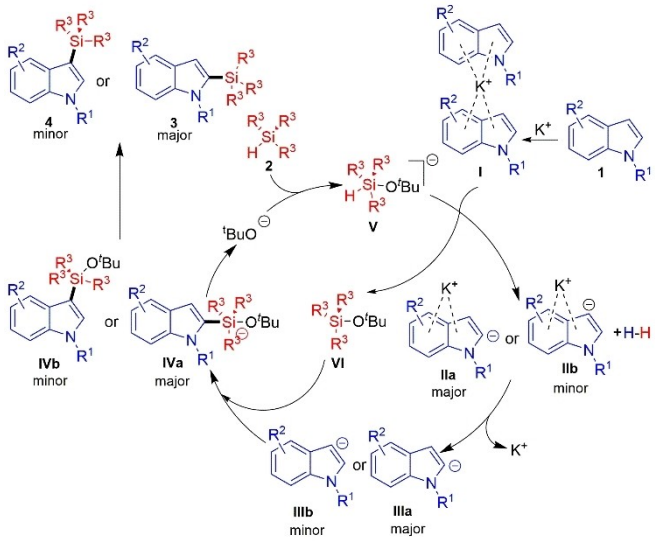

Scheme 4. Proposed ionic mechanism for silylation reaction.

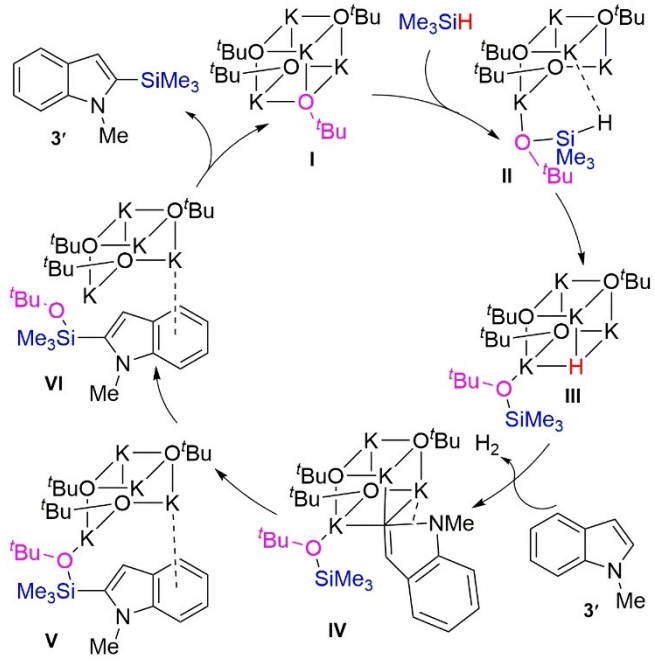

Scheme 5. Neutral mechanism for silylation reaction.

attached to one corner of intermediate **III**. In the next step, carbanion complex **IV** is formed *via* deprotonation, and hydrogen is liberated. In the consecutive steps, intramolecular silicon-carbon bond formation takes place in intermediate **V**, and a pseudorotation in intermediate **VI** is reported to happen. Finally, *tert*-butoxide is dissociated, silylated heteroarene **3** is generated, and the cycle is continued.

An article published by Kim *et al.*[16] has focused on the site-selective Si–H functionalization of hydrosilane using a continuous flow sequential organolithium reaction catalyzed by potassium *tert*-butoxide. The purpose of the research was to develop a continuous flow system for the functionalization of hydrosilanes, especially to synthesize functionalized silanes in a highly efficient and sustainable manner (Scheme 6).

The authors achieved this goal by using a sequential organolithium reaction catalyzed by potassium *tert*-butoxide. This reaction was found to be highly effective and produces high yields of functionalized silanes in a short amount of reaction time. In addition, it was highly scalable, allowing for large-scale production of functionalized silanes. This novel method does not require the use of transition metals and is atom-economic with high yields of the functionalized synthetically important organosilanes. The proposed reaction mechanism highlights that potassium *tert*-butoxide assisted in the generation of a pentacoordinated silyl moiety **I** in combination with hydrosilane. The generation of pentacoordinated silyl moiety is pivotal in the rapid transformation of the reactant.

In the proposed reaction mechanism (Scheme 7), initially, the potassium *tert*-butoxide reacts with hydrosilane **2**, forming a penta-coordinated silyl species **I**. The activated silyl moiety **I** reacts with **5** to generate silylated product **II** and regenerates the *tert*-butoxide ion. It has been reported that the intermediate **I** can decompose in the absence of **5**, which has been verified by the formation of gas with the excess reaction time in the flow method. It is noteworthy to mention that an instant *tert*-butoxide-catalyzed reaction between **I** and **5** is crucial to generate a silylated product **II**.

2.2. Carbon-Carbon bond forming reactions

In 2018, Boris *et al.*[17] investigated the reaction between ketimine **7** and arylacetylene **8** in the presence of 50 mol% of ^{t}BuOK in DMSO to obtain propargylamine **9** as a targeted product. The ^{t}BuOK has been found to be an effective catalyst to complete the reaction, while the transformation was ineffective when carried out using other bases. The reaction condition shows good potential over the diversity of both substrates **7** and **8** (Scheme 8) and produces the required

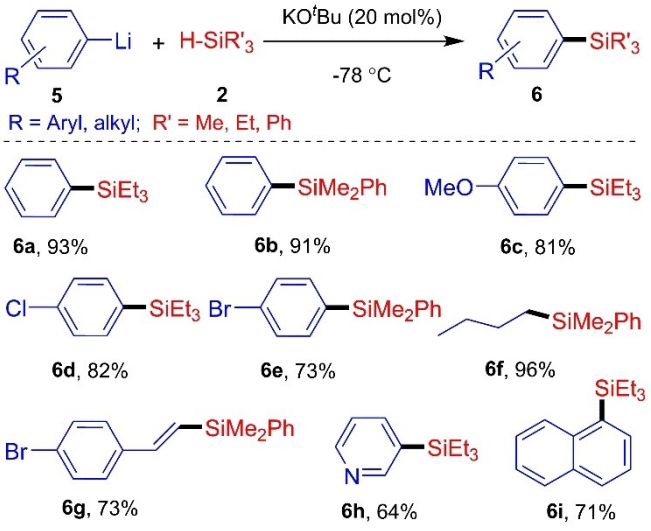

Scheme 6. Si–H Functionalization by KO^{t}Bu.

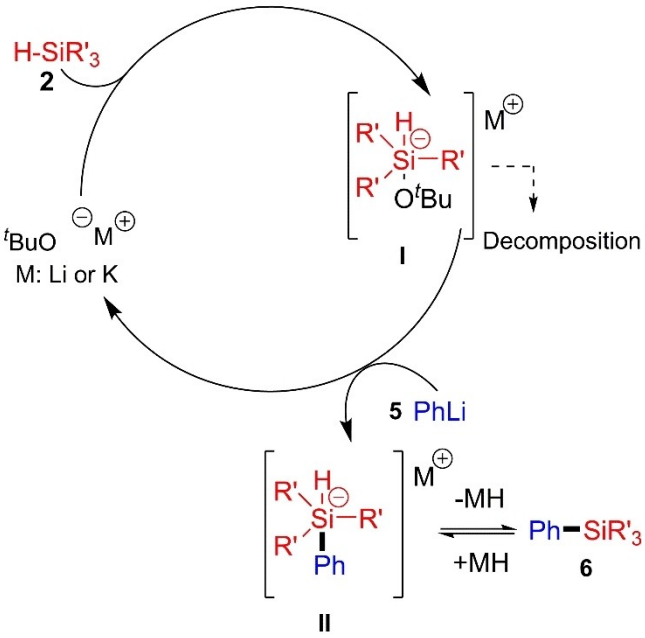

Scheme 7. Proposed reaction mechanism for Si–H.

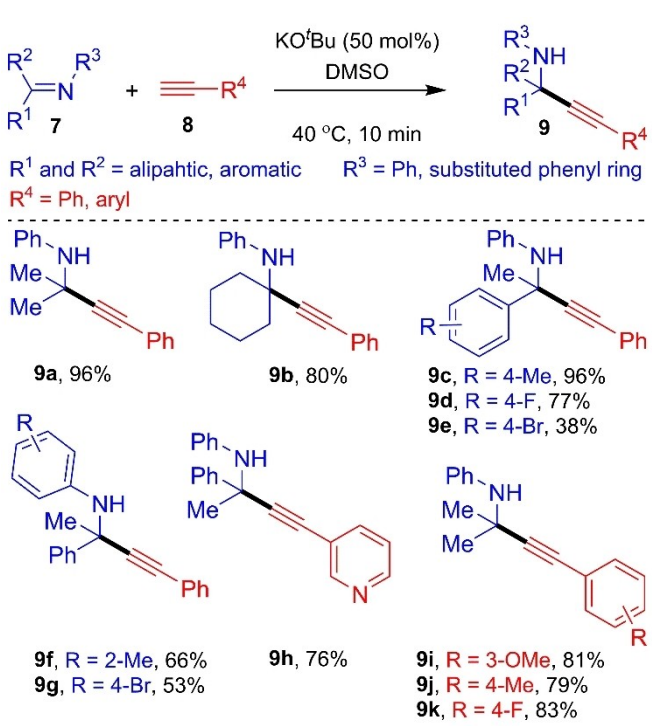

Scheme 8. 'BuOK Catalysed addition of arylacetylenes to ketimines.

products in good to excellent yields. It has been mentioned that, using the Br-substituted substrates **7**, the corresponding products **9e** and **9g** were found to have in lower yields (38% and 53%, respectively) because of their solubility in the 'BuOK/DMSO system.

Based on this assumption, a mechanistic path has been provided (Scheme 9) for this reaction, in which the first step of the reaction involves deprotonation of substrate **8** to yield the intermediate **I** in the presence of a base. Afterwards, the nucleophilic addition of intermediate **I** may occur over the substrate **7** to form the intermediate **II** and lastly upon protonation, the final product **9** could be obtained (Scheme 9).

Using a similar catalytic approach with a combination of 'BuOK/DMSO, Claus and co-workers have reported 4-exo-dig-cyclization of substituted-propionamides **10** to synthesize the different substituted derivatives of α-methylene-β-lactams **11** (Scheme 10).[18] To achieve the required cyclization, 30 mol% of KO'Bu has been shown to be most effective and they have proved this methodology to be efficient by synthesizing diversely substituted β-lactams through different propiolamides.

Based on the experimental evidence, the mechanism of this reaction has been proposed. The mechanism for cyclization of propionamides proceeds with the formation of dimesyl anion through the mixture of potassium *tert*-butoxide and DMSO solvent. The intermediate **I** is obtained by deprotonation of **10** and then as a result of the nucleophilic attack of anionic carbon

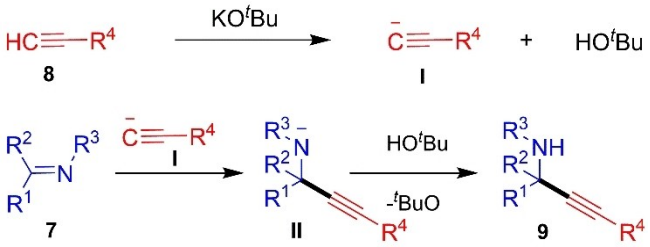

Scheme 9. Provisional mechanism for the addition of arylacetylenes to ketimines.

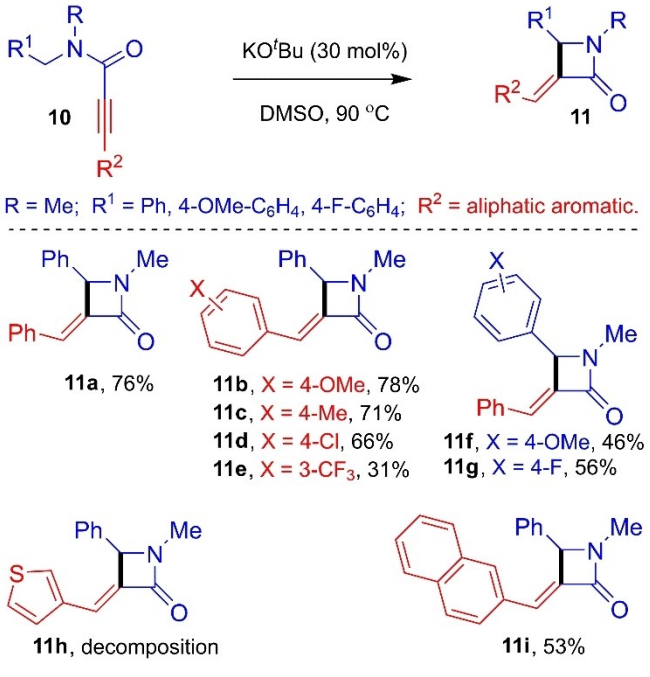

Scheme 10. Method for the synthesis of α-methylene-β-lactams.

over the C–C triple bond, the intermediate **II** could be obtained. Next, upon protonation, the cyclized product **11** has been found (Scheme 11).

Milstein and co-workers[19] in 2019 reported a transition metal-free, highly efficient, and supportable approach for the construction of the C–C bond by performing the reaction between benzyl alcohols **12** and arylacetylene **8** in the presence of 5 mol% of ^{t}BuOK. A wide range of α-alkylated ketones **13** were prepared by employing the different benzyl alcohols and substituted phenyl acetylenes (Scheme 12).

To investigate the possible mechanistic path, the authors have performed several controlled experiments, EPR spectrometry analysis, and DFT studies. Upon the experimental observations, the first step of the mechanism involves the proton abstraction of benzyl alcohol **12a** in the presence of catalytic amounts of ^{t}BuOK and then the reaction may be initiated by hydrogen atom transfer from intermediate **I** to form intermediates **II** and **III**. The radical chain reaction starts with the insertion of the radical anion **I** to phenylacetylene **8a** to produce **B** and may be converted into **A** *via* a 1,2-hydrogen shift. The species **A** and **B** can be transformed into either **C** or **D** by hydrogen shifting and then protonation occurs by **12** to form molecules **E** and **I**. The radical anion **E** can then be transformed into **F** *via* hydrogen atom transfer from **I** and regenerated the intermediate **II**. Finally, **F** can be transformed into product **13a** (Scheme 13).

The synthesis of polysubstituted naphthalenes (Scheme 14) was investigated by Wang *et al.*[20] in 2019 using an alkoxide catalyst. It is a transition metal-free transformation *via* the C–C coupling reaction to form 1-cyano-3-acylnaphthalenes **16** from 2-(2-alkynylphenyl)acetonitriles **14** and alkynones **15** as substrates with complete regioselectivity. The optimization of the reaction was started by considering 2-(2-(phenylethynyl)phenyl)acetonitrile and alkynone as starting materials and taking 10 mol% K_2CO_3 in DMF as solvent at 40 °C. The expected product was obtained with 56% yield. Further experiments for screening of the reaction have been performed and it was found that a higher yield of the product was obtained with 10 mol% loading of LiO^{t}Bu, and hence, it is considered as the ideal condition for the reaction. To find the application of various substrates, a broad scope of reactions has been developed with complete regioselectivity, excellent functional group tolerance, high atom-economy and good to excellent isolated yields.

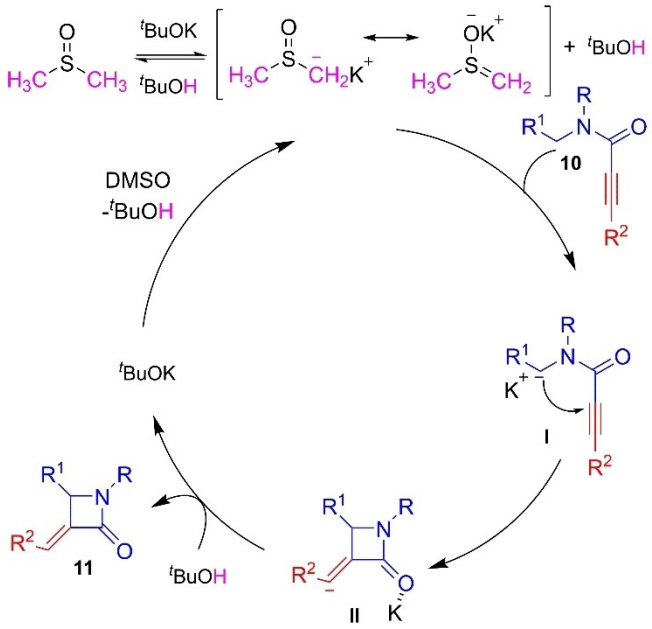

Scheme 11. Proposed mechanism for cyclization of substituted propiolamides.

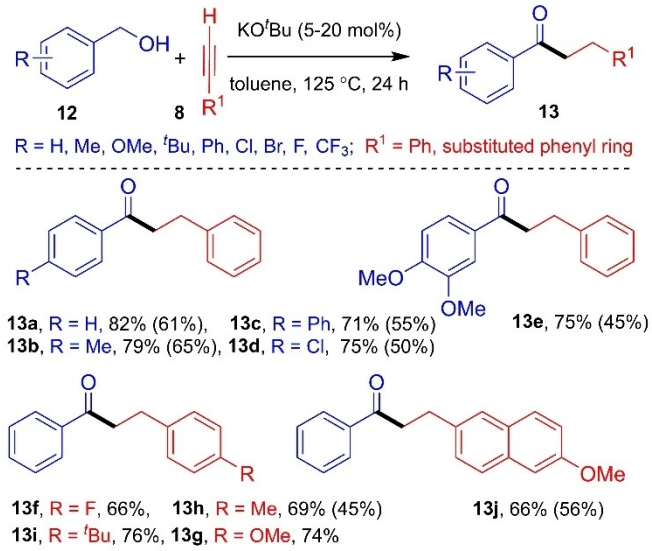

Scheme 12. Synthesis of α-alkylated ketones.

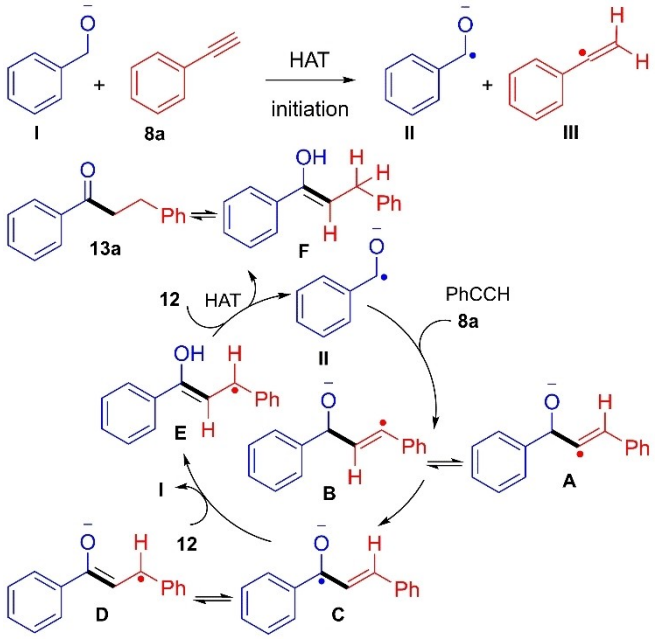

Scheme 13. Proposed mechanism for the synthesis of α-alkylated ketones.

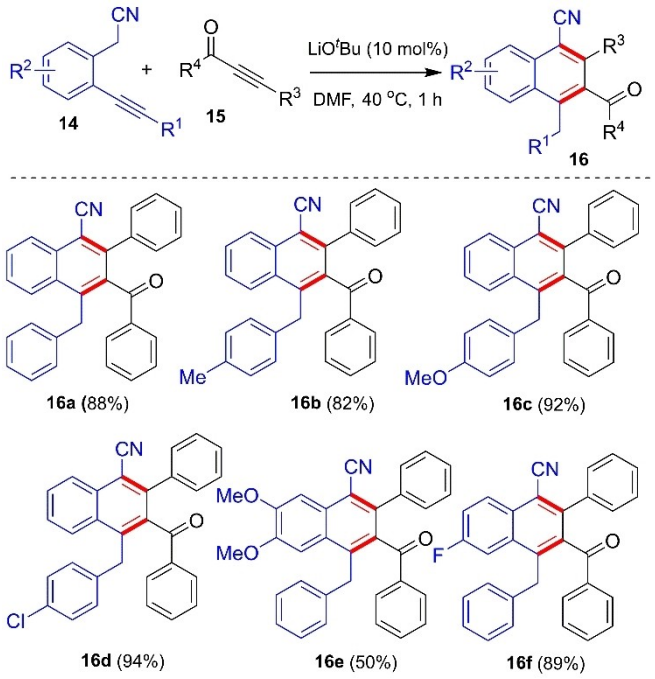

Scheme 14. Synthesis of 1-cyano-3-acylnaphthalenes from 2-(2-alkynylphenyl)acetonitriles and alkynones.

The plausible mechanism starts with the formation of intermediate **A** in the presence of LiO^{t}Bu by the deprotonation of compound **14** and intermediate **B** is formed by the nucleophilic attack of intermediate anion **A** on compound **15**. Then, the intermediate **C** is formed by intramolecular cyclization of **B**, which followed by the proton abstraction gives the intermediate **D**. Finally, the product **16** was formed through the aromatization process (Scheme 15).

A recent article published by Wang and co-workers which introduces a novel method utilizing potassium *tert*-butoxide as a catalyst for the C–C bond forming reaction *via* alpha homo-allylic alkylation of lactams in the presence of 1,3-dienes.[21] This method produces a quaternary carbon centre with high regioselectivity and very good yields. This transformation avoids the use of precious transition metals. The proposed mechanism shows that the cation-pi interaction of potassium enolate with diene plays a vital role in the transformation, which proceeds *via* the 1,2-addition pathway. This method includes a broad substrate scope, environmentally benign, high atom-economic pathways, which has been reported to give a high yield (in gram-scale) transformation as well (Scheme 16).

From the proposed reaction mechanism (Scheme 17), it is evident that a cation-pi interaction occurred between potassium enolate **I** and aryl-substituted diene **18a**. Due to this cation-pi interaction-based carbon-carbon bond formation, the inter-

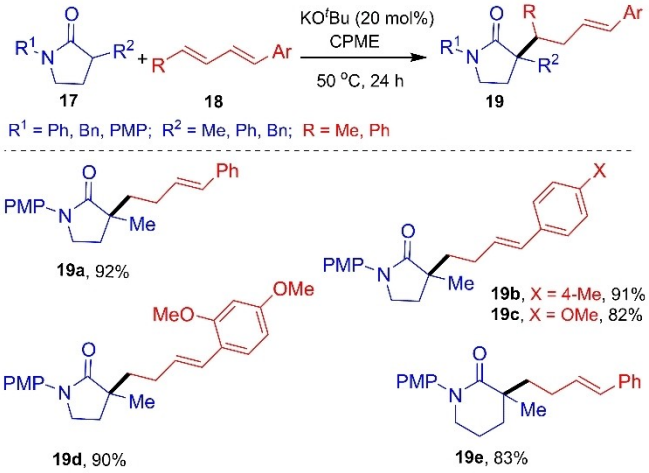

Scheme 16. Alpha homo-allylic alkylation of lactams.

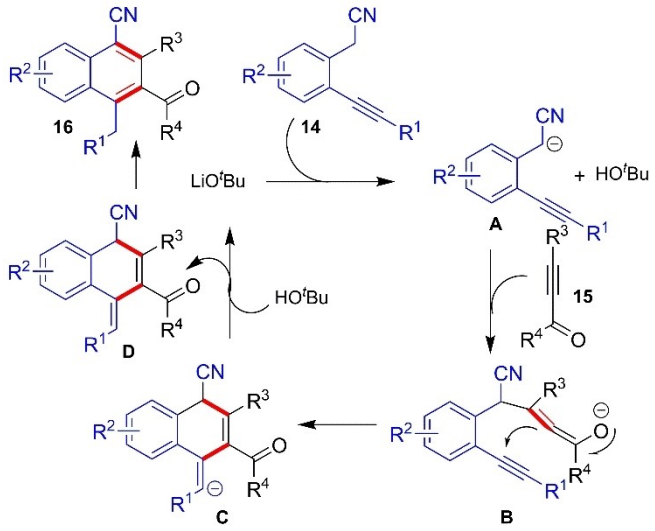

Scheme 15. Reaction mechanism for the synthesis of 1-cyano-3-acylnaphthalenes naphthalenes.

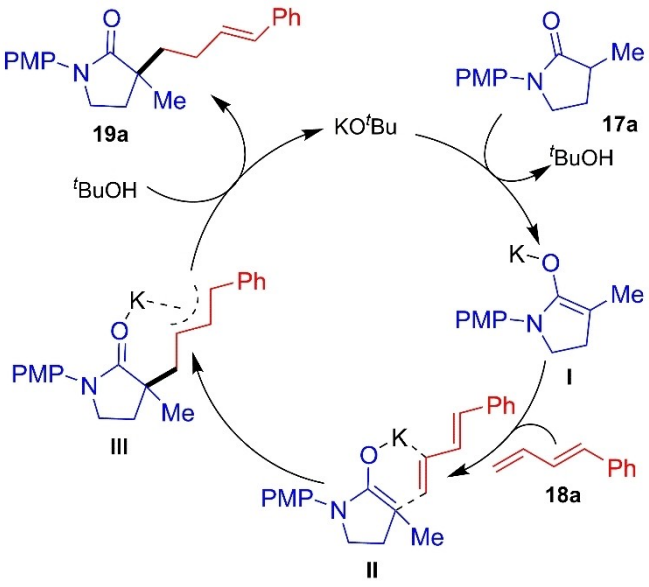

Scheme 17. Proposed reaction mechanism for alpha homo-allylic alkylation of lactams.

mediate **III** is generated. The interaction of intermediate **III** with ^{t}BuOH delivers the product of interest **19 a**.

Recently in 2022, Xing *et al.*[22] reported the C–C bond formation approach for the synthesis of α-alkylated amides *via* C–H functionalization at α-position in the presence of catalytic (20 mol%) amounts of ^{t}BuOK. From a catalytic point of view, the reaction was inactive in the absence of ^{t}BuOK. Different catalysts were attempted in order to substitute ^{t}BuOK; whereas, all catalysts were found to be ineffective for this reaction. Upon employing the reaction conditions, a broad range of substrate scope was developed (Scheme 18).

With the help of controlled experiments, a plausible mechanism has been proposed (Scheme 19). According to the mechanism, enolate species **I** is afforded from the reaction of ^{t}BuOK with substrate **20**, then as a result of the potassium cation and π-interaction of intermediate **I**, a six-membered species **II** is formed. The intermediate **III** may result in the generation of C–C bond, which followed by protonation gives the final product **21**.

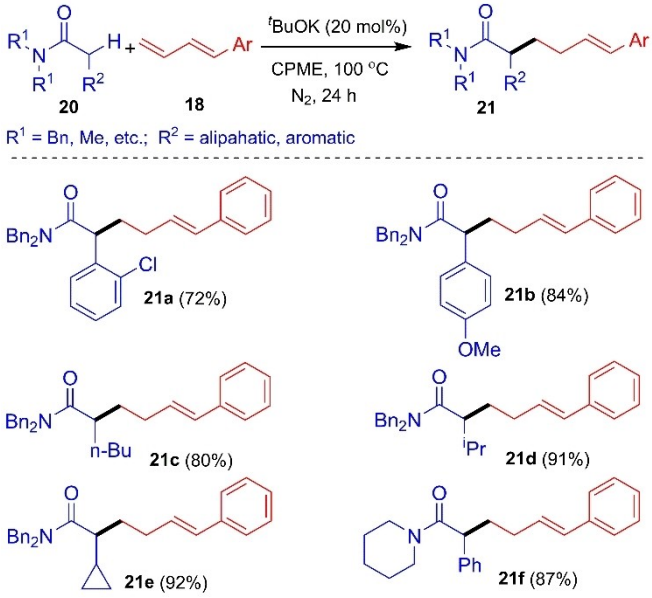

Scheme 18. The α-alkylation of acyclic amides.

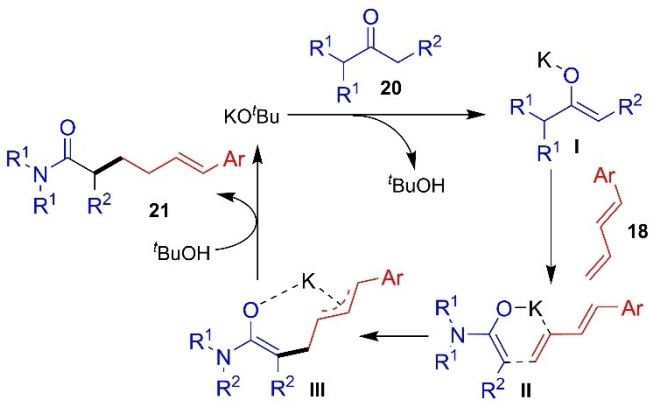

Scheme 19. Plausible mechanism for α-alkylation of acyclic amides.

2.3. Carbon-heteroatom (N, O, S, and Se) bond forming reactions

Li and co-workers[23] in 2014, reported that the alkeynols and alkynylamines can be cyclized with transition metal-free catalysis in the presence of 10 mol% of ^{t}BuOK with excellent selectivity and good to excellent yields of the generated compounds. In terms of synthetic potential, they have developed a broad range of substrate scope by employing various alkynols and alkynylamines in DMSO at 80 °C. For the cyclization of alkynols, it was seen that the type and position of substituents on aromatic rings do not show any remarkable effects on the outcome of the reaction (Scheme 20).

With the support of previous literature, they have proposed a plausible reaction mechanism. According to that, the substrate **22** involves in the hydrogen abstraction process in the presence of ^{t}BuOK to deliver the intermediate **I**. After which as a result of nucleophilic addition the intermediate **II** could be formed. Finally, the protonation of intermediate **II** leads to the formation of exo-cyclized product **23** (Scheme 21).

An intramolecular cyclization method to develop the various substituted benzofuroazepines **25** derivatives has been achieved successfully by performing the reaction of 2-alkynyl benzyloxy nitriles **24** in the presence of catalytic amounts (20 mol%) of ^{t}BuOK (Scheme 22), which is reported by Zeni *et al.*[24] A wide range of compounds **25** can be synthesized with

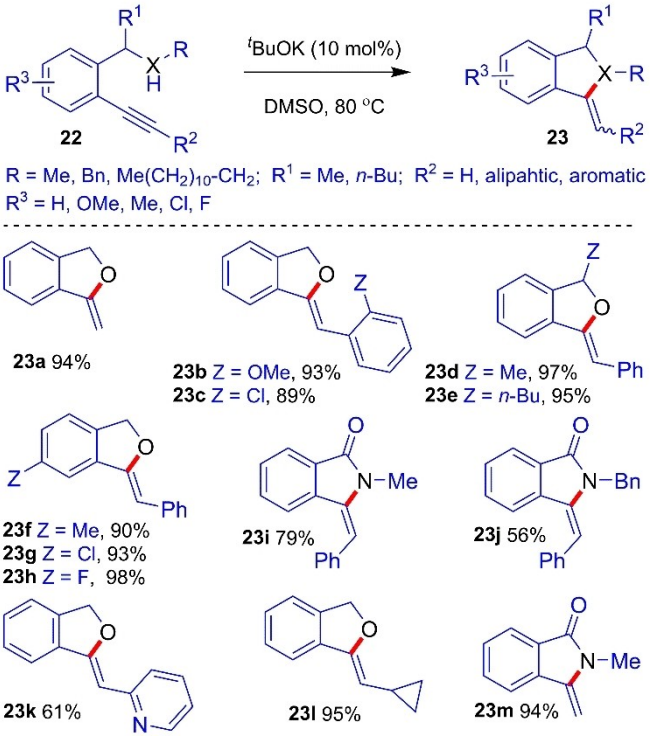

Scheme 20. Cyclisation of alkynyols and alkynylamines.

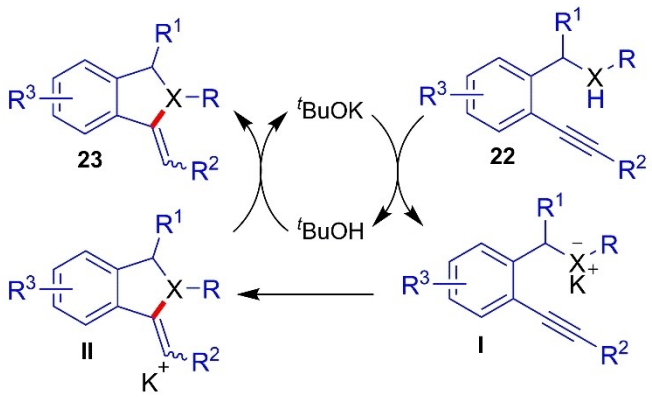

Scheme 21. Proposed mechanism for cyclization of alkynols and alkynylanimens.

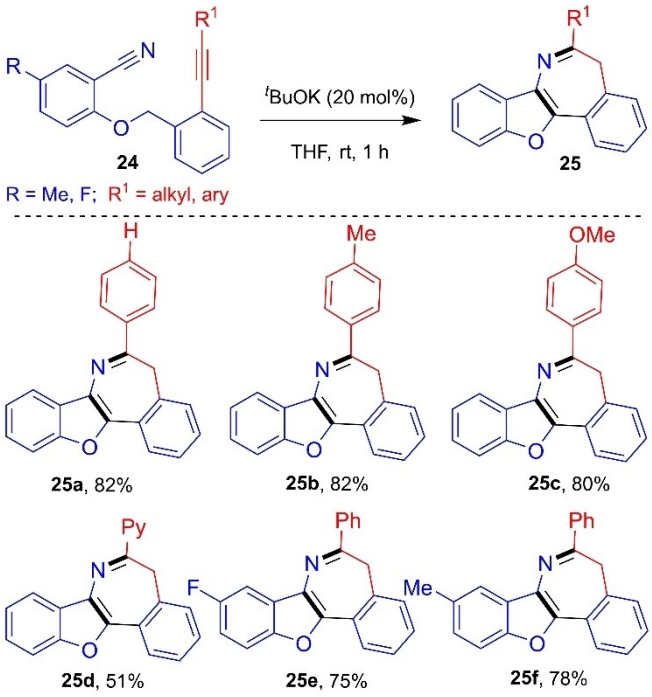

Scheme 22. Synthesis of benzofuroazepines.

the application of developed reaction conditions and it was mentioned that the electron-donating groups present at the acetylene terminus have no effect on the yields of the products; whereas, the bulkiness of the substituents delivers the products in comparatively lower yields. An electron-deficient phenyl ring shows effective yields due to the partial polarization of the C–C triple bond.

A mechanism of the reaction has been proposed based on the controlled experiments, which starts with the abstraction of proton of **24a** by *tert*-butoxide anion to give the intermediate **I**, which can undergo 5-exo-dig cyclization to give intermediate **II**. The intermediate **II** followed by the consecutive 7-endo-dig mode of cyclization delivers the intermediate **III**, which upon protonation the intermediate **IV** can be formed that can further undergo [1,5]-H shift to give the final product **25**, or intermediate **V** and **VI** might be involved to furnish the product **25**. In the second way, if the 6-exo-dig cyclization mode engages, the intermediate **II** can be converted into **VII** and then *via* the formation of intermediates **VIII** and **IX**, the isoquinoline moiety **25** can be formed (Scheme 23).

A mechanism of the reaction has been proposed based on the controlled experiments, which starts with the abstraction of proton of **24a** by *tert*-butoxide anion to give the intermediate **I** that can undergo 5-exo-dig cyclization to give the intermediate **II**. The intermediate **II** followed by the consecutive 7-endo-dig mode of cyclization delivers the intermediate **III**, which upon protonation the intermediate **IV** can be formed, that can further undergo [1,5]-H shift to give the final product **25**, or intermediate **V** and **VI** might be involved to furnish the product **25**. In the second way, if the 6-exo-dig cyclization mode engages, the intermediate **II** can be converted into **VII** and then *via* the formation of intermediates **VIII** and **IX**, the isoquinoline moiety **25** can be formed (Scheme 23).

Yan *et al.*[25] have reported the intramolecular C–N coupling reaction of *ortho*-vinyl benzamides **26** in the presence of catalytic amounts of ^{t}BuOK and DMF as a solvent to produce a valuable nitrogen-containing compounds such as isoquinolinone **27** (Scheme 24) and isoindolinone (Scheme 25) derivatives **29**. This straightforward and sustainable methodology shows good functional group tolerance towards the formation of products **27** and **29** in good yields. Based on several controlled experiments and with the support of previous literature, a provisional mechanism has been postulated (Scheme 26).

According to the mechanism, upon deprotonation of DMF in the presence of ^{t}BuOK followed by a single electron-transfer process, the radical species **III** is formed. After that, the intermediate **III** might abstract the proton from **26a** and another radical species **IV** can be generated. Next, the species **IV** can undergo radical cyclization to form species **V** and finally DMF can donate a proton to **V** to generate the final product **27a** and carbamoyl radical **III**.

Reddy and co-workers[26] developed a synthetic method for acquiring functionally rich tricyclic-oxadiazines using *p*-quinols and azomethine imines (Scheme 27) as starting materials through [3 + 3]-cycloaddition pathways, using catalytic potassi-

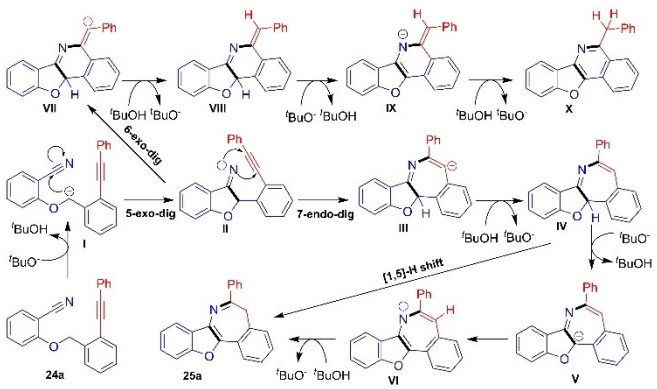

Scheme 23. Mechanistic proposal for the synthesis of benzofuroazepines.

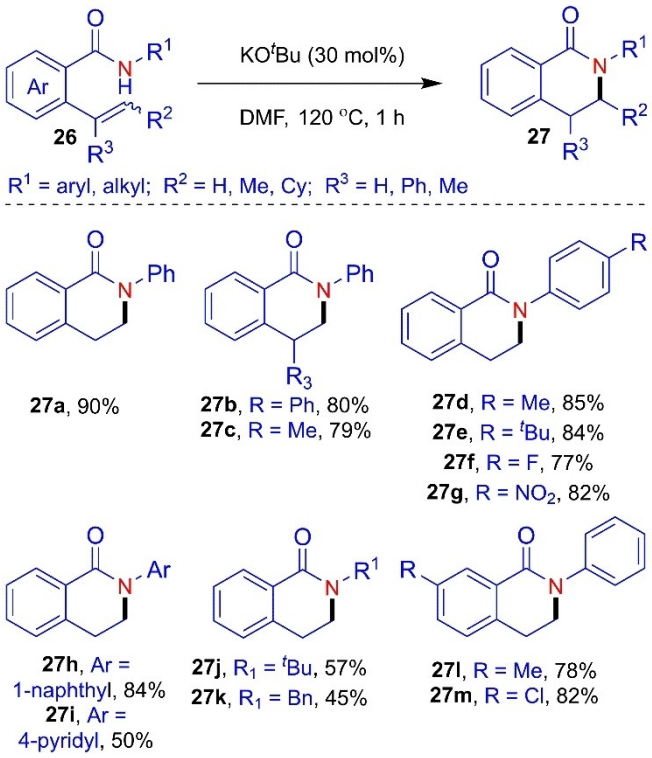

Scheme 24. Intramolecular hydroamination of *ortho*-Vinyl Benzamides.

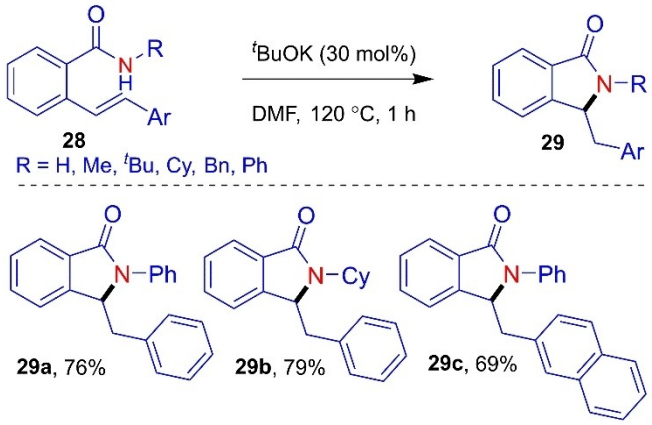

Scheme 25. Intramolecular hydro-amination of stilbene derived amides.

um *tert*-butoxide. The reaction was investigated in the presence of 20 mol% DBU as a catalyst to observe a very low yield (< 5%) of the product. Different types of catalysts such as tertiary amines, Lewis bases, organic bases, inorganic bases, and organic acids and solvents were examined successively. The bases such as sodium tertiary butoxide, sodium methoxide, and potassium tertiary butoxide catalyzed the reaction by furnishing product yields 54%, 67%, and 70% respectively. However, the yield was much less when 1.5 equiv. of NaH was used, and it was also noted that some of the catalysts such as DMAP, DABCO, quinine, triphenylphosphine, potassium carbonate, and *p*-TSA were unable to catalyze the reaction.

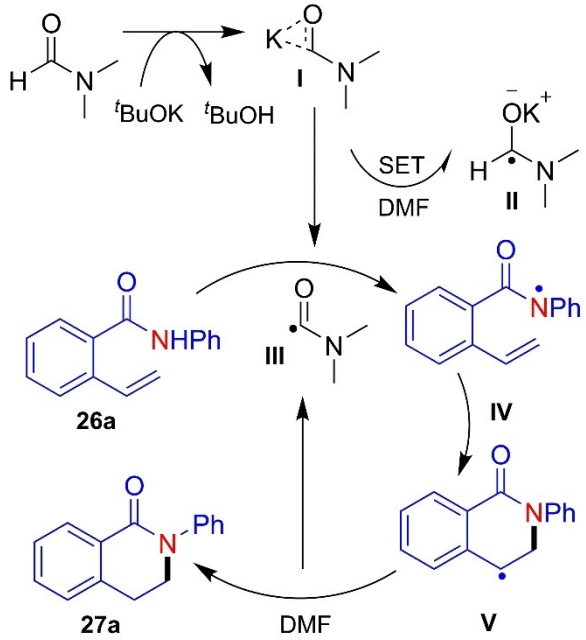

Scheme 26. Proposed reaction mechanism of intramolecular hydroamination.

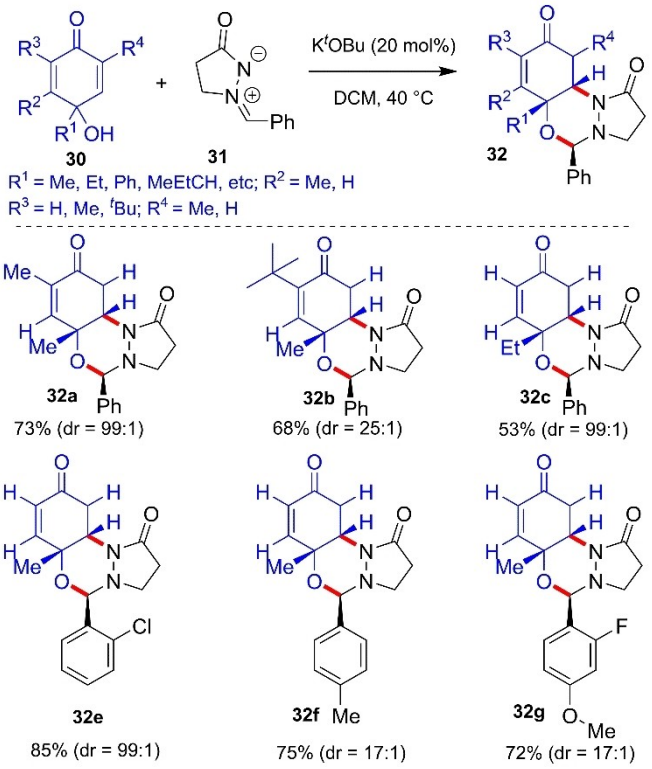

Scheme 27. Regioselective preparation of tricyclic oxadiazines.

It was mentioned that the mechanism of this reaction has no proof whether it involves a concerted or stepwise pathway (Scheme 28); but as there was no intermediate obtained, this is depicted as a concerted mechanism. It starts with an abstraction of protons from *p*-quinols **30** and produces intermediate **I**.

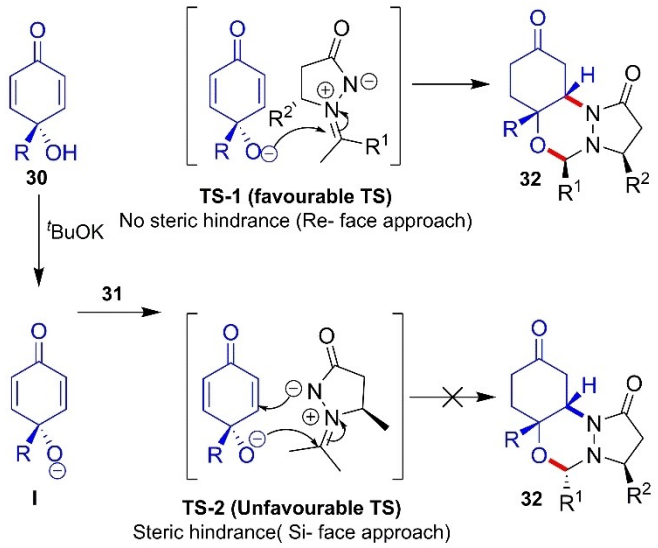

Scheme 28. Proposed reaction mechanism.

A transition state **TS1** is formed, when **I** reacts with compound **35**. Transition state **TS2** is less selective due to steric hindrance and electrostatic repulsions and lastly, *in situ* chemoselective intramolecular addition of the nitrogen anion to the Michael acceptor system would take place instantaneously in a highly diastereoselective 1,4-addition mode to result in the product **32**.

Govindarajan and co-workers have described the carboalkoxylation of styrene **33** in transition metal-free reaction conditions (Scheme 29) using phenyl diazoniumtetrafluoroborate **34**, phenalenyl ligand **36** and the catalytic amount of KO^{t}Bu in the presence of alcohols as sources of carboalkoxylation.[27]

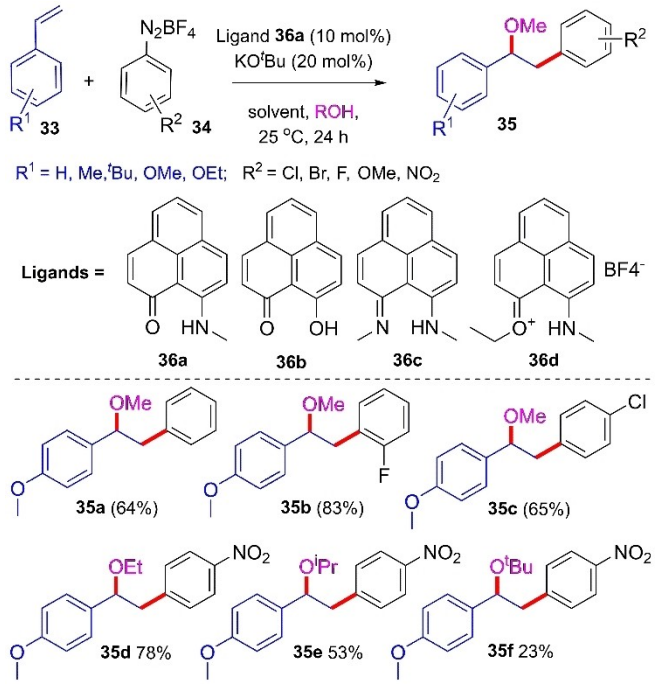

Scheme 29. Carboalkoxylation of styrenes in the presence of various alcohols.

The reaction was optimized by using 4-methoxystyrene and phenyl diazoniumtetrafluoroborate as starting materials with KO^{t}Bu and ligand in DMSO as solvent. These conditions have been applied to various substrates in good to excellent yields and it was observed that employing electron-withdrawing effects on the aryl diazonium salt and 4-methoxy styrene, the reactions delivered unsatisfactory results. The yields of reaction were reduced up to 38% when simple styrene was used with 4-nitrophenyldizonium salt for the developed carboalkoxylation process. This protocol was executed in the presence of various alcohols to provide **35** as well as in the absence of alcohols to provide compound **37** (Scheme 30).

This reaction progressed through the single electron-transfer (SET) mechanism (Scheme 31), which was witnessed by performing a DFT calculation of the catalytic cycle. In order to explain, firstly a (PLY-N,O)-K complex was formed by reacting the ligand PLY-N,O with KO^{t}Bu, which was then reduced by other KO^{t}Bu to form a (PLY-N,O)-K radical anion complex. In the catalytic cycle, electron transfer occurs from the radical anion complex to compound **34** to give aryl radicals **I** and this aryl

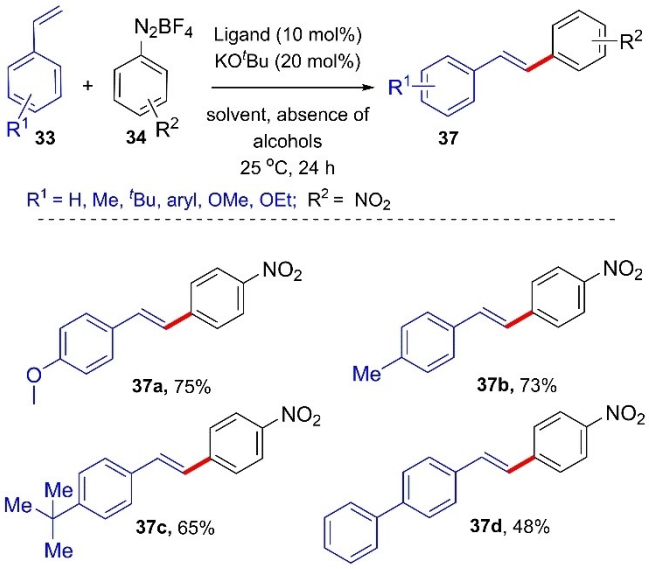

Scheme 30. Carboalkoxylation of styrenes in the absence of various alcohols.

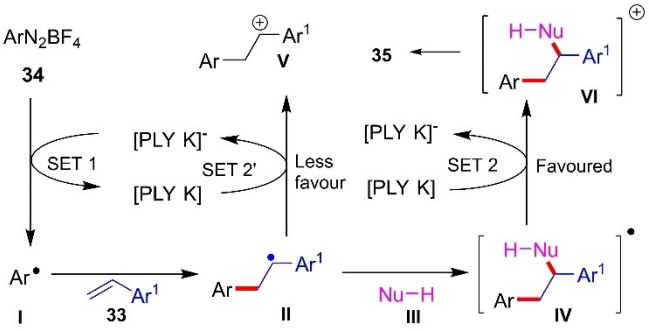

Scheme 31. Catalytic pathways for carboalkoxylation of styrenes.

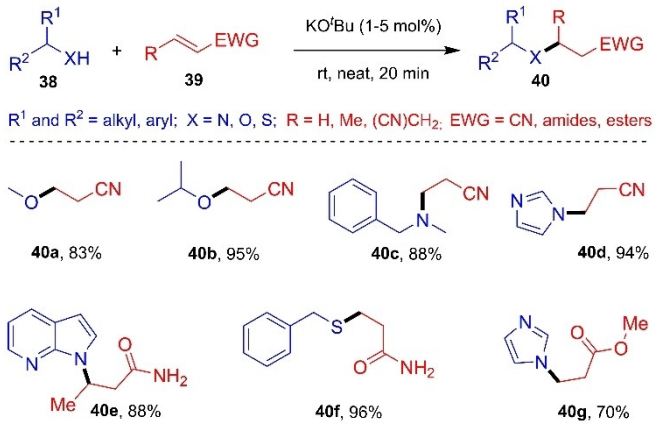

Scheme 32. KO^{t}Bu Catalysed Michael addition reaction.

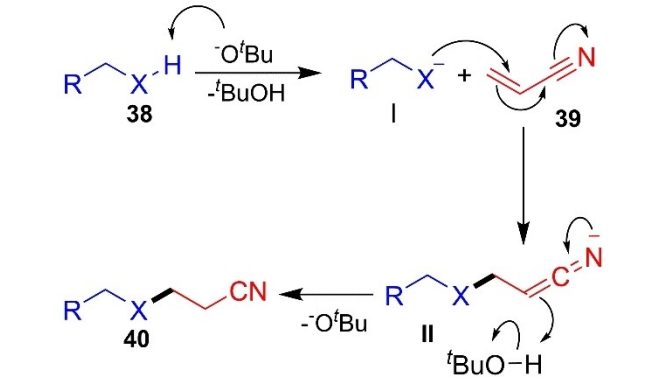

Scheme 33. Proposed mechanism.

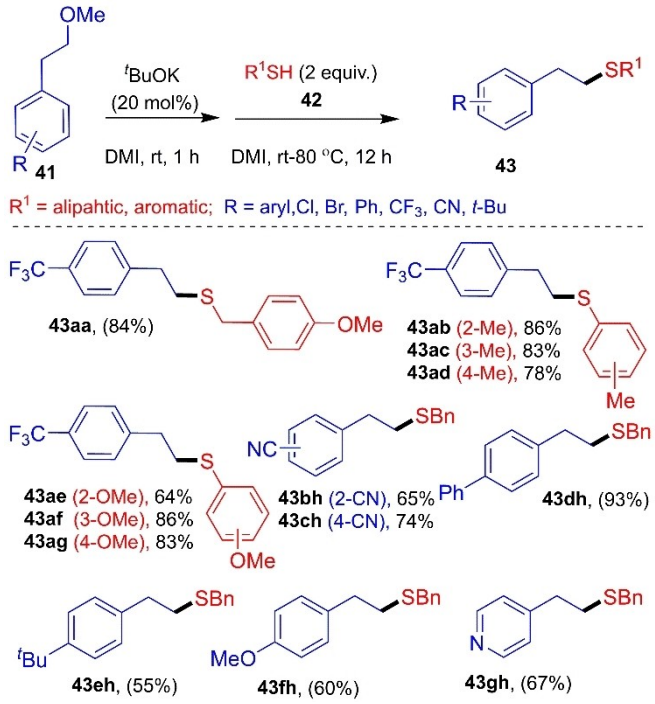

Scheme 34. Hydrothiolation of β-(hetero) arylethyl ethers.

radical **I** is converted into benzylic radical **II** by the nucleophilic attack of aryl radicals on alkene **33**. The catalyst is regenerated by the benzylic radicals **II** through SET 2, and forms a benzylic cation **V**.

Recently, Thiyagarajan and co-workers[28] have witnessed an efficient ^{t}BuOK catalyzed Michael addition reaction between nucleophile **38** and Michael acceptor **39** to obtain the product **40**. A wide range of different substituted alcohols, thiols, and amines can be treated with various substituted nitriles, amides, and esters that show good functional group tolerance and produce the required products in excellent yields (Scheme 32).

In the proposed mechanism (Scheme 33), a nucleophilic intermediate species **I** was generated by the proton abstraction of **38** in the presence of ^{t}BuOK, which further underwent conjugated nucleophilic addition or Michael addition to form the intermediate **II** that upon protonation gave the final product **40**.

Shigeno and co-workers have demonstrated the ^{t}BuOK catalyzed anti-Markovnikov hydrothiolation of various aliphatic and aromatic β-(hetero) arylethyl ethers to produce the corresponding thioethers in good to excellent yields (Scheme 34).[29] In the preliminary investigation of the reaction, 20 mol% of ^{t}BuOK was found to be an effective catalyst and successfully employed for hydrothiolation reaction. The reaction conditions have been applied to diverse β-(hetero) arylethyl ethers using different aliphatic and aromatic thiols.

According to the mechanism, the first step involves the elimination of MeOH in the presence of ^{t}BuOK to give styrene compound **33**. Then, in the second step deprotonation of thioalcohol occurs, and as a result species **I** is obtained. The species **II** was formed by the addition reaction of **33** with **I** and finally, the protonation of **II** afforded the final product **43** (Scheme 35).

The article published by Malakar *et al.*[30] presents a new method for the synthesis of benzimidazoles through a transition metal-free, transfer hydrogenative cascade reaction process. The reaction utilizes nitroarenes **44** and amines/alcohols **45** as starting materials, and potassium *tert*-butoxide as a catalyst, which proceeds through a series of redox-economical steps to produce the desired benzimidazoles **46**. Compared to the traditional transition metal-mediated, expensive, and complex

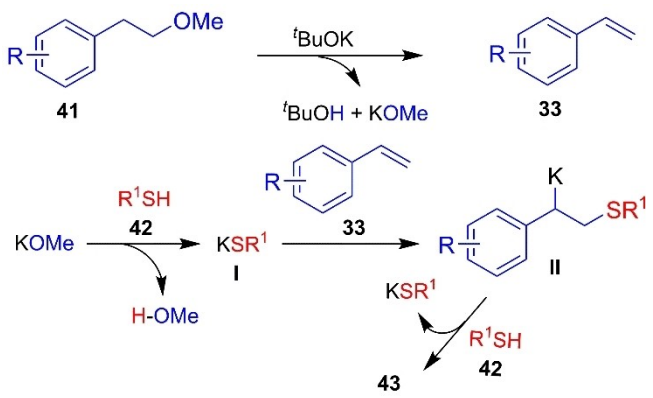

Scheme 35. Proposed reaction mechanism for hydro-thiolation reaction.

methods for the reduction of nitro compounds, this new method utilizes a transfer hydrogenative cascade reaction that involves the transfer of hydrogen from amines or alcohols to nitroarenes.

This reaction is redox-economical and that requires less energy input than traditional methods, and is an environmentally benign process. The effectiveness of this method has been demonstrated by synthesizing a variety of benzimidazoles using different nitroarenes and amines/alcohols. It has been shown that the yields of these compounds are high and that the reaction is highly selective, producing only the desired product. Lower cost and ease of execution make this process very attractive for large-scale synthetic applications (Scheme 36).

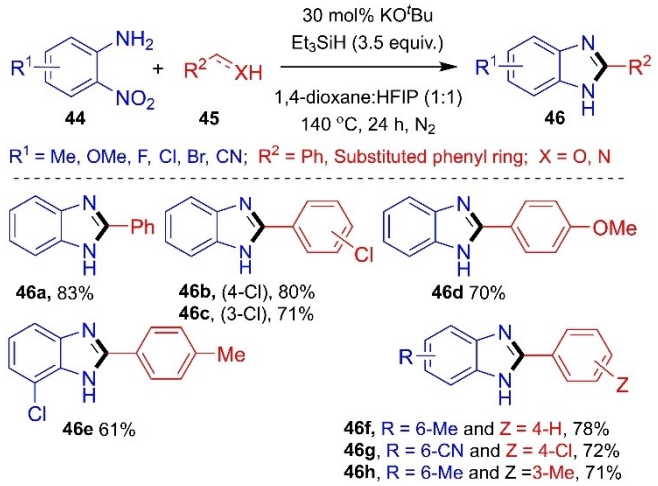

Scheme 36. Reaction scheme and substrate scope for TH cascade reaction of nitroarenes.

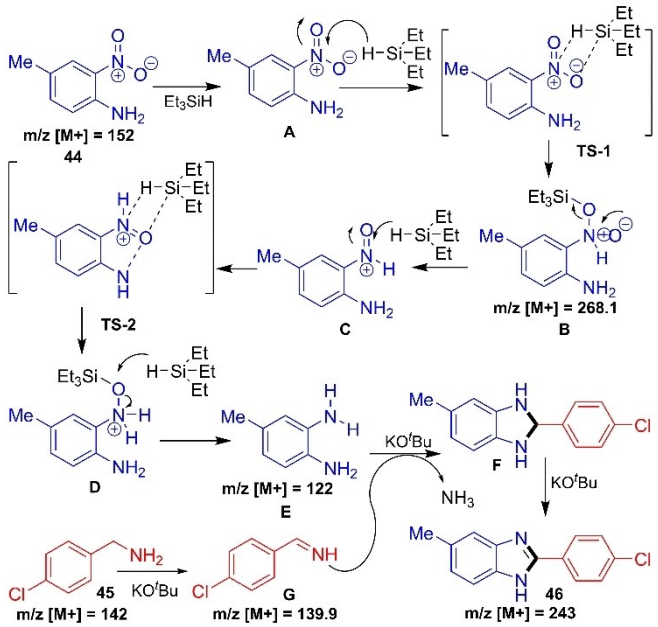

Scheme 37. Proposed reaction mechanism for transfer hydrogenative cascade reaction.

The proposed cascade reaction pathways (Scheme 37) for the above reaction have been established by investigations through control experiments including the timely monitoring of intermediate formation by GC-MS and DFT calculations. The experimental supports reveal that the *in situ* reduction of the nitro group into aniline results in the formation of *o*-phenylenediamine **E** from 2-nitro aniline **44**. It was reported by the authors that the use of HFIP was pivotal in nitro group reduction through its hydrogen bonding capability.

2.4. Other reactions

The article by Hashimoto *et al.*[31] provides new insights into the dehydrogenation reaction of NH-NH bonds to form N=N bonds using cost-effective potassium *tert*-butoxide as a catalyst in the presence of liquid ammonia as a solvent at room temperature with air. It has been reported that the presence of air is important in this transformation; whereas, the presence of nitrogen inhibits the reaction. The application of this novel method ranges from the efficient synthesis of azo compounds with high yield in a very short period of reaction time (3 minutes) to the one-pot facile synthesis of diazirines, which has importance in photoaffinity labeling. The broad substrate scope, synthetic utility in chemical biology, dehydrogenation of phenylhydrazine, time and cost-effectiveness, and gram scale transformation are the uniqueness of this reported method (Scheme 38).

Xu and co-workers have demonstrated the efficient catalytic activity of KO^{t}Bu for the construction of unsymmetrical disulfide S–S, S–Se, Se–Se, N=N and C=N bonds.[32] The potential of reaction conditions has been demonstrated by the synthesis of various unsymmetrical disulfide compounds in excellent yields (Scheme 39). Furthermore, they have utilized 5 mol% of ^{t}BuOK in THF at 25 °C to carry out the reaction of substrates **42**, **49** and **53** to construct the symmetrical S–S, Se–Se, and Se–S bonds (Scheme 40). Finally, the scope of this method has been extended to the construction of N=N and C=N bonds (Scheme 41).

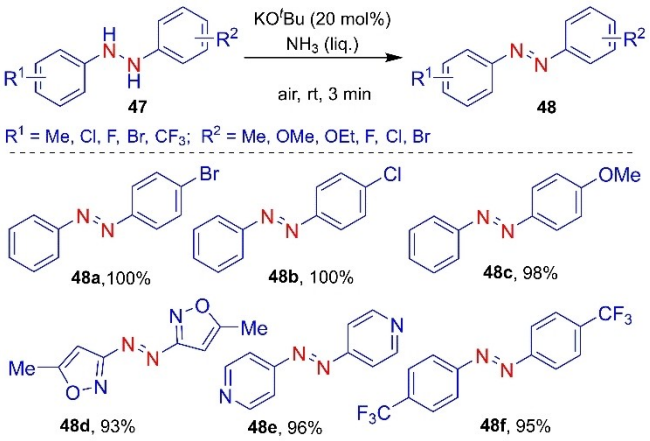

Scheme 38. Substrate scope for KO^{t}Bu catalysed dehydrogenation of NH-NH bond.

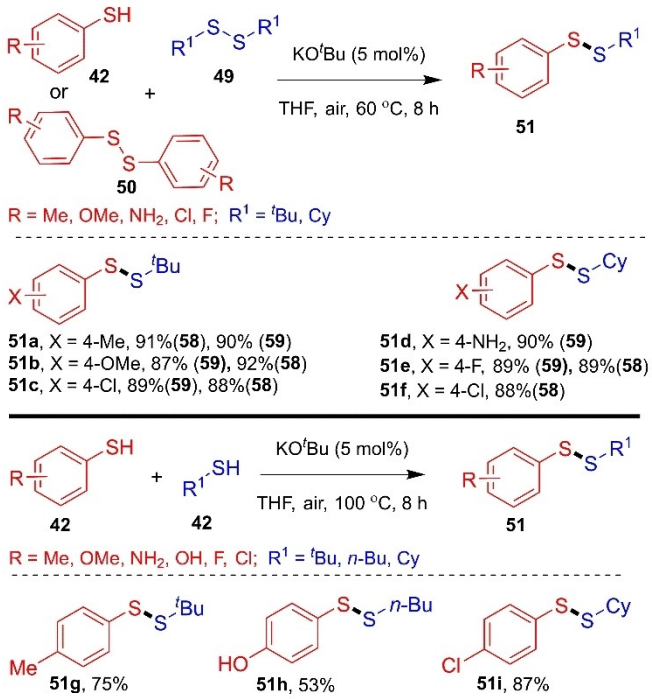

Scheme 39. KO^{t}Bu Catalysed unsymmetrical S–S bond formation.

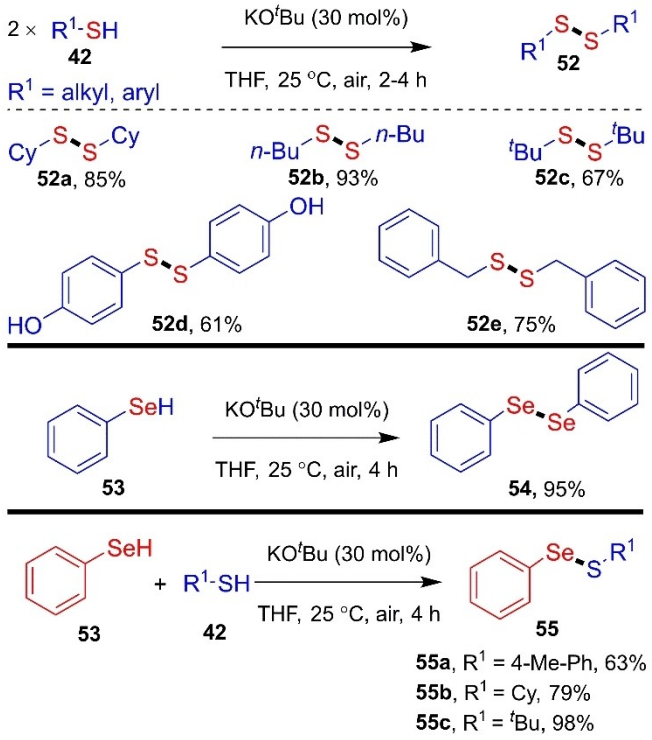

Scheme 40. KO^{t}Bu Catalysed symmetrical S–S, Se–Se, and Se–S bond forming reactions.

The article published by Kim and co-workers[33] presents a thorough and well-executed study on the use of lithium *tert*-butoxide as a catalyst for the hydroboration of carbonyl compounds under mild reaction conditions. The authors clearly

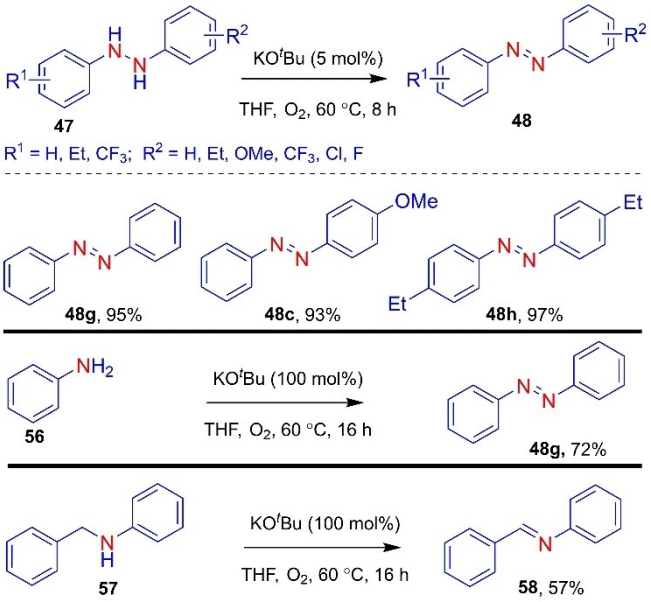

Scheme 41. KO^{t}Bu Catalysed N=N and C=N bond formation.

describe their experimental methods and results, and provided a detailed analysis of the mechanism of the developed reaction (Scheme 42).

This article includes a comprehensive survey of the different carbonyl compounds that are suitable for this reaction and the yields of the corresponding products. The authors also presented a comparison of the results obtained with lithium *tert*-butoxide as a catalyst with other catalysts, which provides valuable insight into the efficiency of this catalytic system. Stoichiometric conversion of aldehydes and ketones as well as of ester moieties under the optimized conditions was obtained

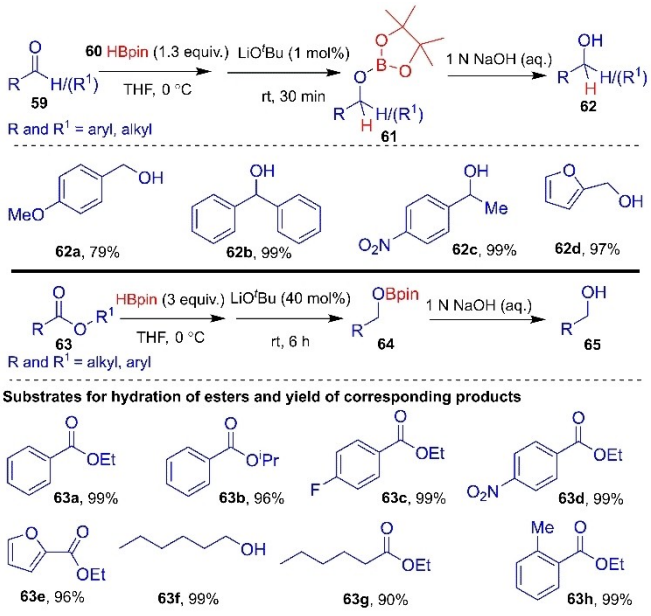

Scheme 42. Lithium *tert*-butoxide catalysed hydroboration.

using 1.0 mol% of lithium *tert*-butoxide, which added weightage to the effectiveness of this developed catalyst system.

The semi-reduction of alkynes into (*E*)-selective alkenes under transition metal-free conditions with pinacolborane and catalytic potassium tertiary butoxide were demonstrated by Grams and co-workers.[34] This protocol involves the reaction of primary and secondary propiolamide to provide the (*E*) isomer selectively and a broad range of substrate scope has been developed under the optimized reaction conditions. Instead of stoichiometric amounts, a catalytic amount of KO^{t}Bu produces the required molecules efficiently and in good yields. It was found that upon increasing the size of the counterion on tertiary butoxide from Li to K, reaction productivity increases amazingly (Scheme 43). The mechanistic investigations were carried out by employing deuterated propiolamide (Scheme 44).

Initially, the potassium *tert*-butoxide assists in the deprotonation of propiolamide **66** which is in equilibrium with ^{t}BuOD and the conjugate base of **66** i.e. **I**. In the next step, the Lewis basic oxygen from **I** forms a complex with pinacolborane **60** and activates the B–H bond, and also assists in the intramolecular pseudo-5-exo-dig hydride transfer to the α-carbon which is shown in TS-**II**. The *trans* alkene geometry in **III** is obtained due to the deuteration from the opposite side of the alkyne in TS-**II**. Upon workup of **III**, the compound **67** is generated.

A highly regioselective synthesis of polythiocarbonates from epoxides **68** and carbon disulfides can be achieved by the utilization of catalytic amounts of LiO^{t}Bu (Scheme 45), which is reported by Warner *et al.*[35] The investigation of the reaction has been started with 5 mol% of ^{t}BuOLi at ambient temperature, and the reaction was directed towards the formation of cyclic dithiocarbonates product **70**, while at lower catalyst loading with 0.25 mol% of ^{t}BuOLi, the reaction prefers the formation of **69**, a polymeric product over the cyclised product **70**.

Next, the effects of temperature and solvent have been observed on selectiveness. It was found that upon increasing the temperature, the reaction prefers the formation of product **70** with lower conversion and the same effect was observed in the case of solvent. The formation of polymeric product **69** *via* chain reaction growth has also been shown in Scheme 46 where both pathways of chain growth were exhibited.

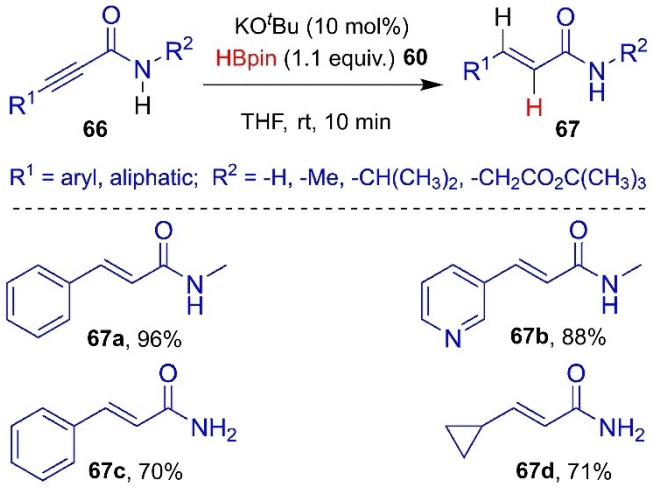

Scheme 43. Reduction of propiolamide into *E*-alkene.

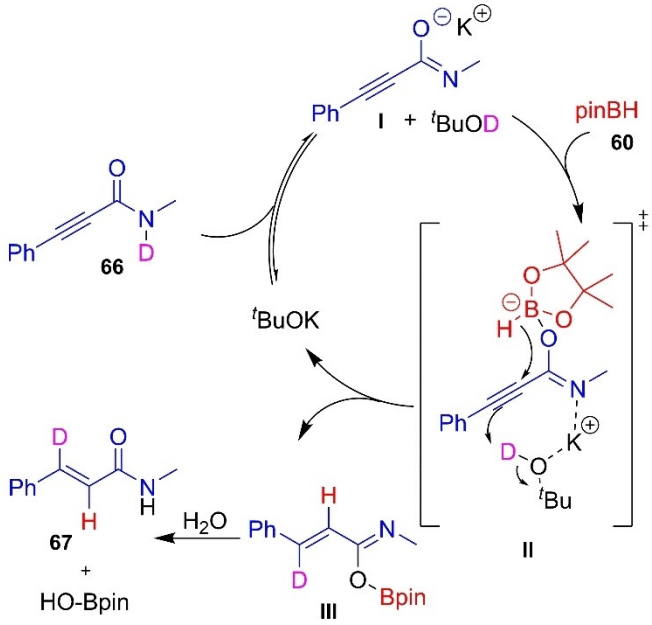

Scheme 44. Mechanism for the reduction of propiolamide.

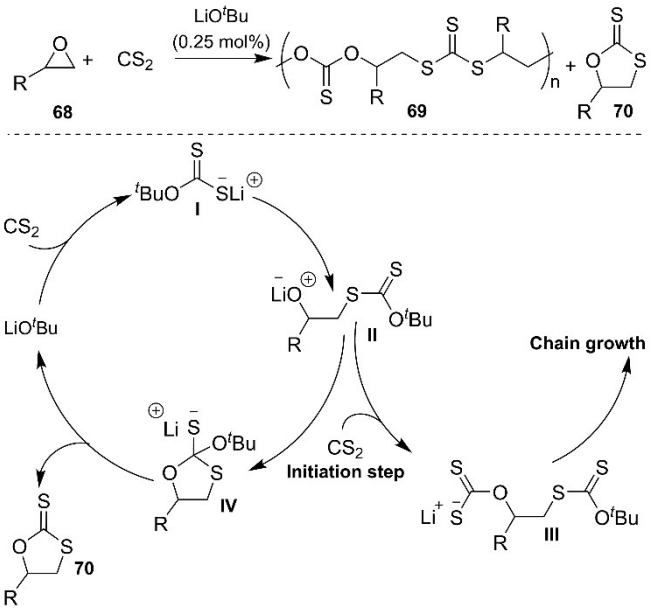

Scheme 45. Co-polymerization of epoxides with CS_2.

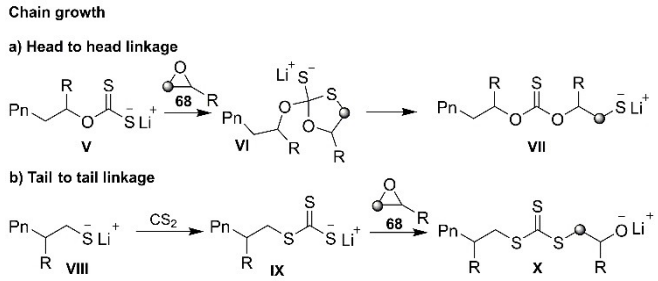

Scheme 46. Possible chain growth *via* different linkages.

3. Utilization of catalytic amounts of alkali-metal *tert*-butoxides with transition metals in organic transformations

3.1. Utilization with copper-complexes as catalysts

3.1.1. Kinetic resolution of oximes and alcohols

In 2018, Oestreich *et al.*[36] reported the kinetic resolution of oxime ethers having alpha-hydroxy substitution **71** using an enantioselective Cu-catalyzed dehydrogenative silylation method taking into consideration of catalyst system CuCl/NaO^{t}Bu/(R,R)-Ph-BPE. Good conversion rate and selectivity were observed in the presence of less bulky substituents on the hydrosilane keeping the catalyst system intact. On the other hand, more bulky substituted oxime ethers in the presence of Et_3SiH as a resolving agent using the same catalyst system show higher selectivity and a lesser conversion rate during the kinetic resolution. It was observed that the TIPS group substituted *Z*-isomer (*Z*-1b) of oxime ether shows remarkable selectivity and a good conversion rate as well (Scheme 47).

It is worth mentioning that to check the influence of oxime ether geometry on the selectivity and resolution processes, the *Z* and *E* isomers of TIPS substituted oxime ethers were employed with different substituted hydrosilanes in the presence of the same catalyst system. Based on the observed experimental results, it was concluded that the least bulky substituted hydrosilane (Me_2PhSiH) showed the highest selectivity and conversion rate. They also mentioned that the geometry of oxime ether is not very important to consider. Some differences were observed in the selectivity and conversion rate, which may be associated with steric reasons. The possibility of two-point binding of oxime nitrogen as a ligand with the copper catalyst in the resolution process was ruled out (Scheme 48).

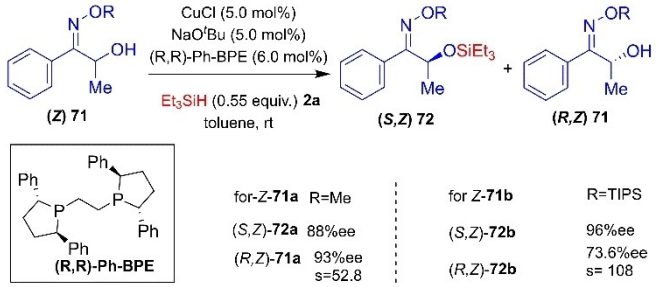

Scheme 47. Kinetic resolution of oxime ethers.

Also, the substrate scope for kinetic resolution involving the *E*-isomer of oxime ether with different electronically modified substituents was examined. The bulky substituents hampered the selectivity to a greater extent; whereas, the conversion rate was around 50% throughout. Branching in the substituted groups was not tolerated and hardly any conversion or selectivity were observed with aryl substitution. Despite these drawbacks, this method of kinetic resolution of oxime ether can be used over a broad range of substrates and different synthetically crucial conversions from highly enantiopure alcohol can be carried out with a negligible loss of enantiopurity in the product (Scheme 49).

Oestreich *et al.*[37] have published an article that presents a new method for the dynamic kinetic resolution of alcohols **75** using enantioselective silylation. The method utilizes two orthogonal transition metal catalysts, which allows for high yields and enantioselectivity. This nonenzymatic DKR process of acyclic and cyclic benzylic alcohols was innovative in the sense that the ruthenium and osmium pincer complexes were utilized as racemization catalysts with chiral copper catalysts to achieve the resolution in high yield and enantioselectivity instead of using the traditional ruthenium sandwich complex, which fails to fulfill the goal. The broad substrate scope and functional group tolerance represent this process as highly effective for the kinetic resolution of alcohols (Scheme 50).

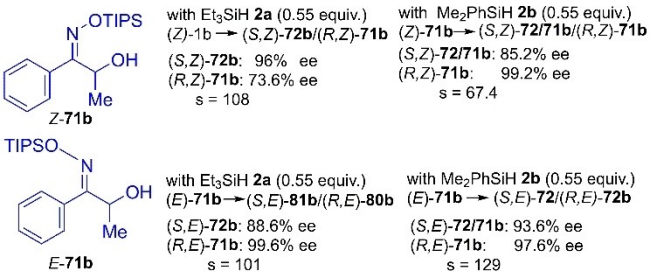

Scheme 48. Influence of the oxime ether geometry.

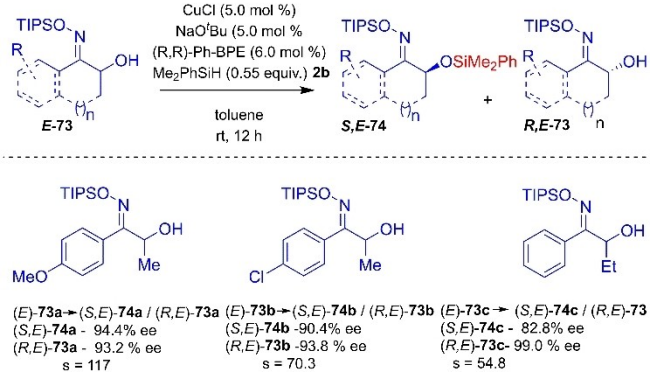

Scheme 49. Substrate scope of the kinetic resolution of α-hydroxy-substituted oxime silyl ethers.

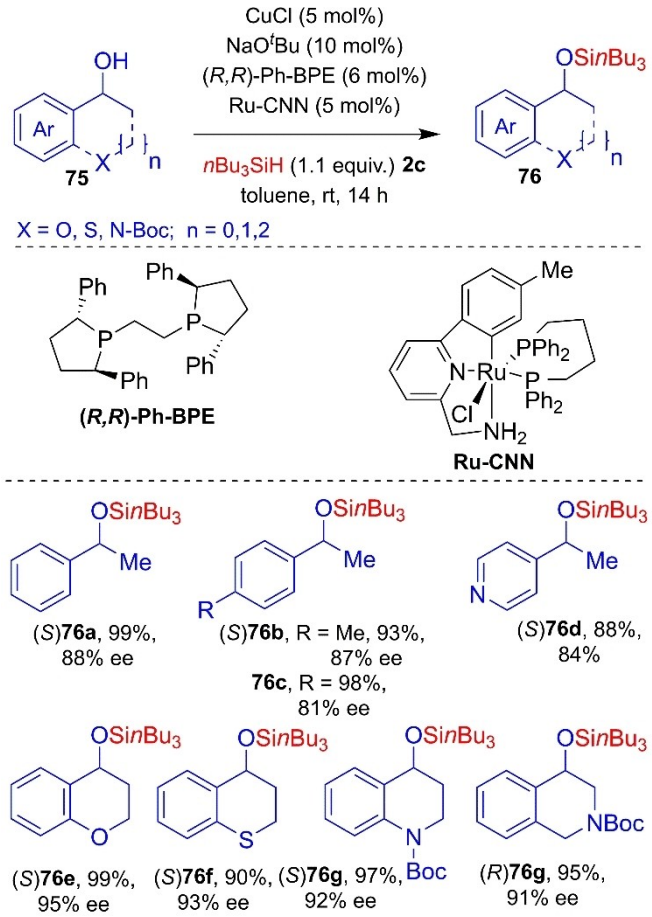

Scheme 50. Dynamic kinetic resolution of acyclic and cyclic benzylic alcohols by enantioselective silylation.

Oestreich *et al.*[38] in 2020, reported for the first time, how efficiently the enantioselective kinetic resolution of the secondary alcohols **77**, which are neopentyl substituted at the beta position and sterically congested is carried out in the presence of CuCl/NaO^{t}Bu/R,R-Ph-BPE catalyst system along with 3,5-xylyl-substituted tertiary hydrosilane as a resolving agent (Scheme 51). The observations they have drawn upon hydrosilane screening are that the hydrosilane is showing better selectivity and conversion rate with the substrate compared to other hydrosilane derivatives. Next, the substrate scope for this enantioselective kinetic resolution was examined in presence of the hydrosilane keeping the catalyst system intact. When the methyl group is attached to alpha carbon with reference to the OH group was replaced with ethyl substituent, and as a results both selectivity and conversion rate are tremendously hampered. Further, to check the effects of rigidity on the reaction rate, different cyclic and acyclic substituted substrates were subjected to the same reaction conditions.

It is worth mentioning that the spirocyclic compounds were found to be promising candidates in terms of reaction time and selectivity. To move on, further spirocyclic derivatives were tested and revealed great selectivity as well as reactivity. It was observed that cyclic alcohol structure is not required for excellent kinetic resolution, when an indane backbone is

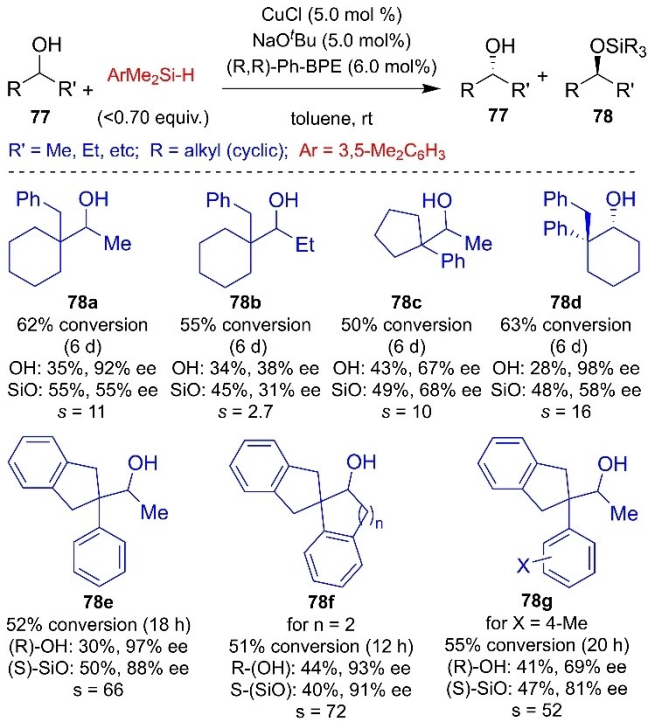

Scheme 51. Kinetic resolution of alcohols by copper-catalyzed enantioselective silylation with hydrosilanes.

present in the substrate. Furthermore, the functional group tolerance is high to achieve excellent selectivity and reaction rates. This method represents a unique approach to acquiring enantiomerically pure, sterically congested, all beta-carbon substituted alcohol.

3.1.2. Borylation reactions

Park and co-workers have demonstrated that the catalytic Cu(I)-NHC/NaO^{t}Bu system produces selective (α and β) vinylboronates with high conversion *via* hydroboration of propargyl alkynes **79** utilizing bis(pinacolato)diborane **80** compound as borylation reagent[39] (Scheme 52).

Two different copper-NHC complexes **A** and **B** have been investigated to find the selectivity pattern of the hydroboration adduct. In most of the conditions catalyst **A** preferred the hydroboration of propargyl species with high α-selectivity; whereas, the catalyst **B** preferred β-selectivity. It was also observed that the nitro-substituted phenyl ethers and the bulkier groups have been found to posses opposite selectivity. In the case of nitro-substituted phenyl ethers, the products were obtained with α-selectivity **81** in high yield in the presence of both catalysts **A** or **B** (Scheme 53).

Tsuji *et al.* have reported another regio-controlled (α-and β-selective) copper-catalyzed hydroboration reaction of alkynes using a copper/ligand/NaO^{t}Bu catalyst system *via* two different copper (Cu–H and Cu–B) species, and the regioselectivity was controlled by introducing the effects of directing group[40]

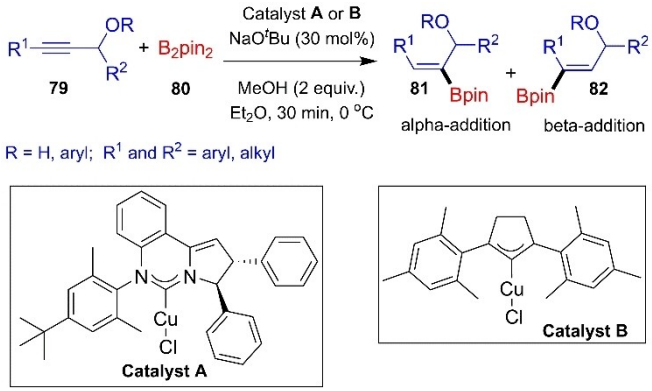

Scheme 52. Regioselective hydroboration of functionalized-propargylic alkynes.

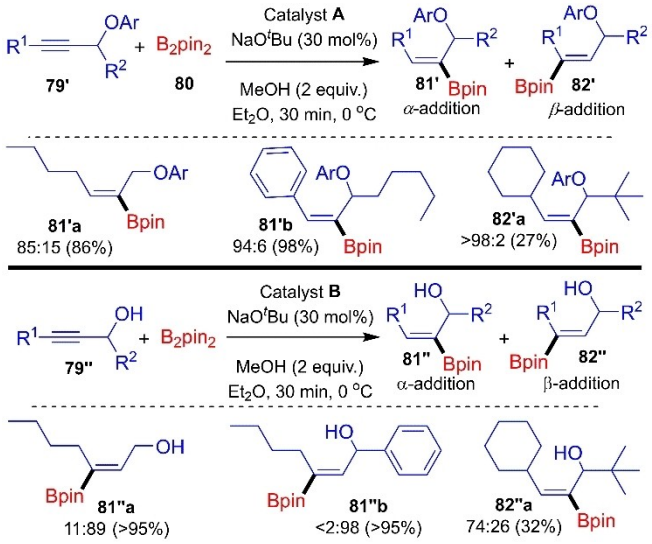

Scheme 53. Regioselectivity for catalysts **A** and **B**.

(Scheme 54). The α-selective boronates were synthesized with high regio-selectivity in good yields by utilizing Cu–H species, which were furnished by pinacolborane (HBpin) and MeAr-Xan as a ligands. When the HBpin was replaced with B_2pin_2/MeOH and CF_3Ar-Xan ligand, the Cu–B species were obtained, which resulted in the formation products with β-selectivity (Scheme 55).

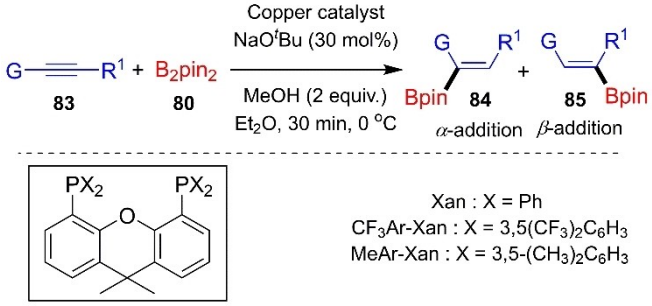

Scheme 54. Regio-controlled hydroboration of alkynes.

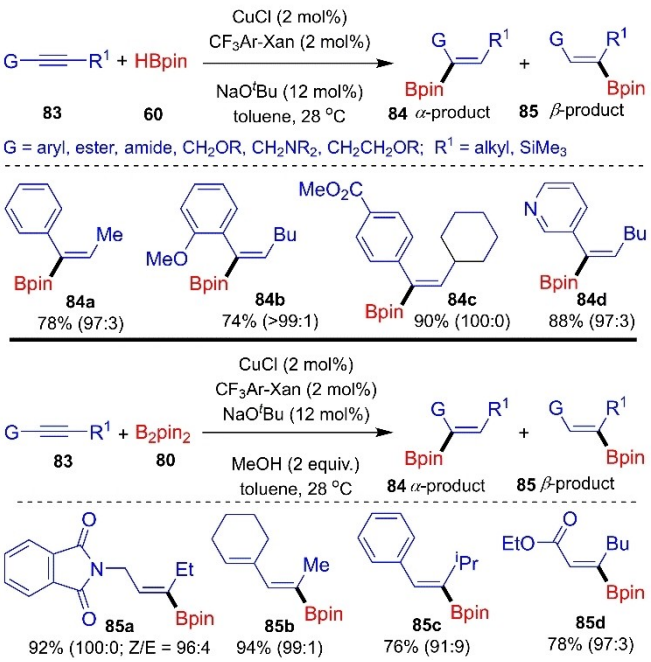

Scheme 55. Hydroboration of different alkynes for α-selective and β-selective product formation.

The catalytic cycle for the hydroboration reaction has been proposed by considering the experimental results. The species **II** LCu(O^{t}Bu) was obtained from LCuCl and NaO^{t}Bu, after the reaction with HBpin or B_2Pin_2, the active catalysts LCu–H or LCu–B **III** were formed. The *syn* addition of active catalyst **III** on **83** either by hydrocupration or borylcupration delivered the species **V**. Thus, the reaction with HBpin, the corresponding α-selective product **84**, and the reaction with B_2pin_2/MeOH, the β-selective product **85** were observed (Scheme 56).

Yun *et al.* have demonstrated the regio and stereo-selective monoboration of alkynes having electron-withdrawing groups by considering bis(pinacolato)diboron as borylating agent, and catalyzed by ligand-copper(I)/NaO^{t}Bu system in the presence of MeOH.[41] Further, one pot conjugate reduction of alkenyl boronates has been achieved for the synthetic application of alkenyl boronates to produce an important building block of chiral boron compounds. The reaction of alkynoates **86** with borane compound **80** and 1 equiv. of MeOH in the appearance of josiphos ligand completed in 7 hours and after insertion of 1.5 equiv. of PHMS and tertiary butanol to the reaction mixture, delivered the desired product **87** (Scheme 57).

Another ligand-copper(I)/NaO^{t}Bu catalyzed selective monoboration approach of conjugated diynes **89** has been reported by Yun *et al.*[42] in 2014 by employing bis-(pinacolato) diboron **80** as a borylation reagent. The optimized reaction conditions have been found with diynes in the presence of catalytic amounts of CuCl (5 mol%), NaO^{t}Bu (10 mol%), and P(*p*-tol)$_3$ (6 mol%) as monodentate ligand using 2 equiv. of MeOH in THF as solvent at 11 °C. It was found that the utilization of other bases or bidentate ligands was not helpful to the reaction. The reaction demonstrated good functional group tolerance with

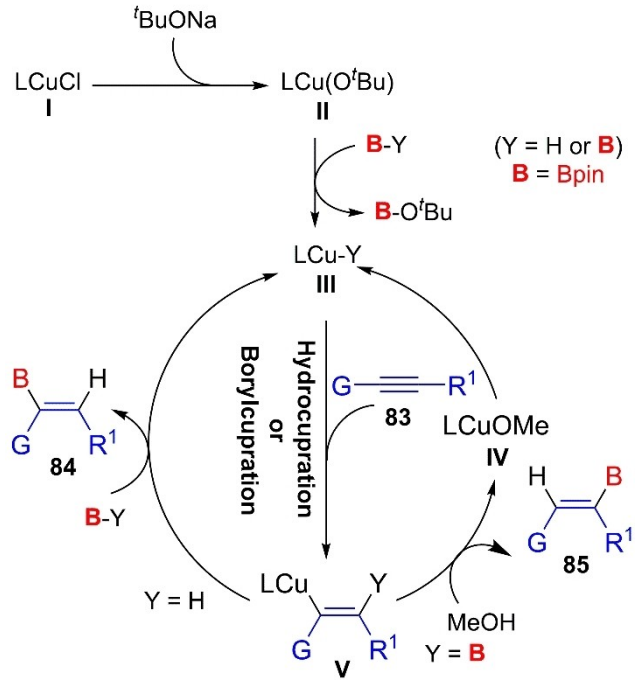

Scheme 56. Proposed mechanism of Hydroboration of alkynes.

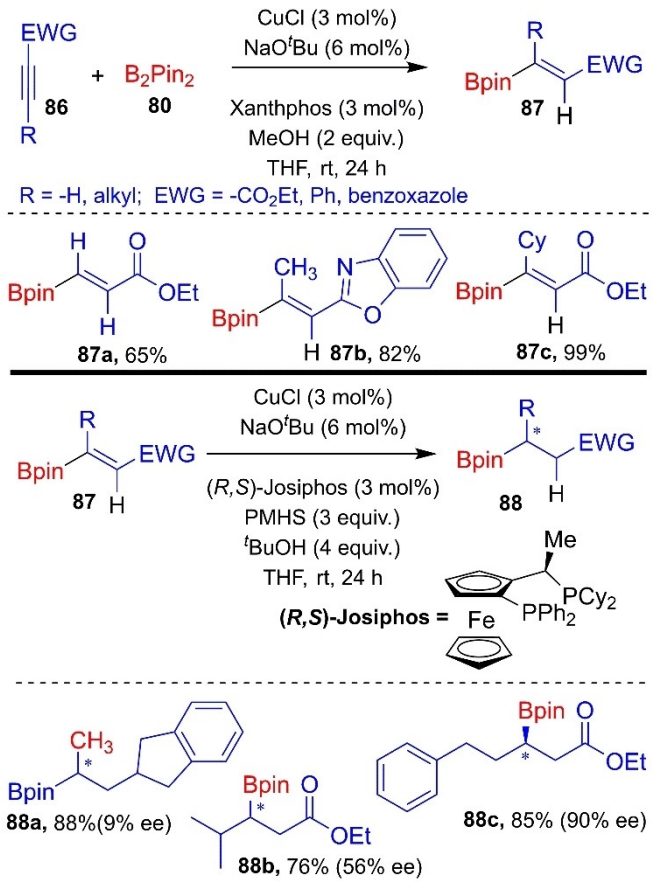

Scheme 57. Boration and reduction of activated alkyne.

high regio- and stereo-selectivity and good yields of the products. The symmetrical diynes produced product **90** without the formation of any other isomer and the effects of sterically hindered substitution on diynes and further transformation of borane-substituted enynes have been mentioned (Scheme 58).

Moure and co-workers[43] have demonstrated a regio-controlled borylation of various propargylic-functional groups containing internal alkynes **92** with bis(pinacolato)diboron **80** in the presence of a copper/ligand/NaO^{t}Bu catalytic system to deliver the product **93** in good yields and the further transformation of **93** has been achieved. The reaction was robustly based on the nature of the reactivity of the ligands and the ligands with a more donating tendency proceeded with complete conversion. The bidentate ligands showed poor reactivity for this reaction (Scheme 59).

Liu and co-workers[44] have described the copper-catalyzed and ligand/^{t}BuONa assisted regio and enantioselective cyclization and borylation of 1,6-enynes **94** to obtain the chiral hydrobenzofuron derivatives **95** *via* effective β-borylation and consequtive conjugate addition to cyclohexadienone (Scheme 60).

Zhu and co-workers have reported a brief study on the hydroboration reaction of thioacetylene to obtain the (*Z*)-α and (*Z*)-β-selective alkenyl boronates in moderate to good yields.[45] Based on the control experiments and DFT calculations, they have found that the selectivity of the reaction is not directed by the ligand, but it depends upon the sulfur atom of the –SR group. Concerning the selectivity of the reaction, a controlled experiment was performed by considering **96** and **80** as substrates without using the ligand DPEphos, although the β-selective product was observed with excellent selectivity. It was concluded that the selectivity was directed by the –SR group (Scheme 61).

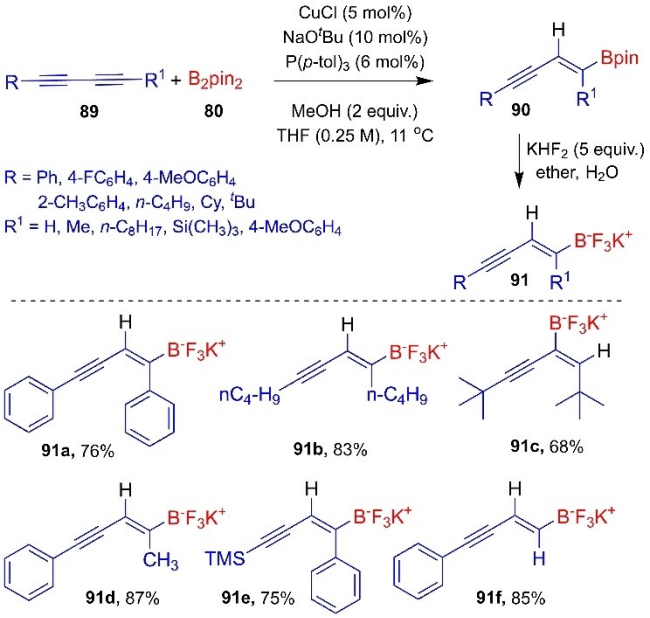

Scheme 58. Borylation of symmetrical and unsymmetrical diyenes.

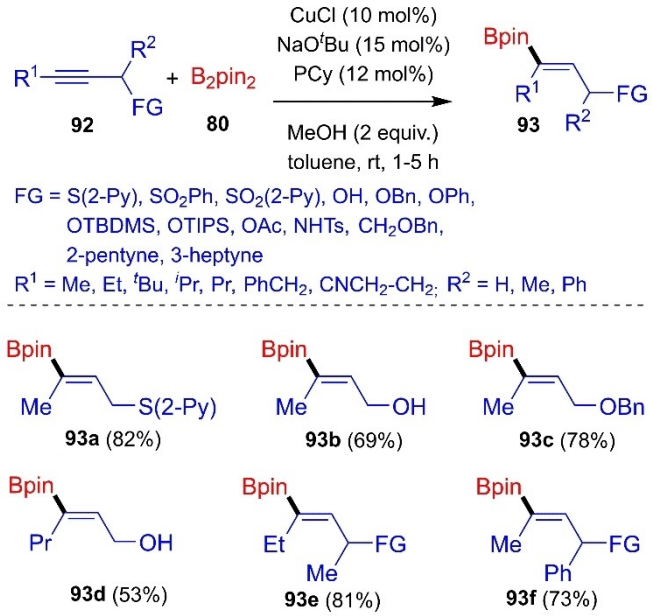

Scheme 59. The β-borylation of propargylic substituted different internal alkynes.

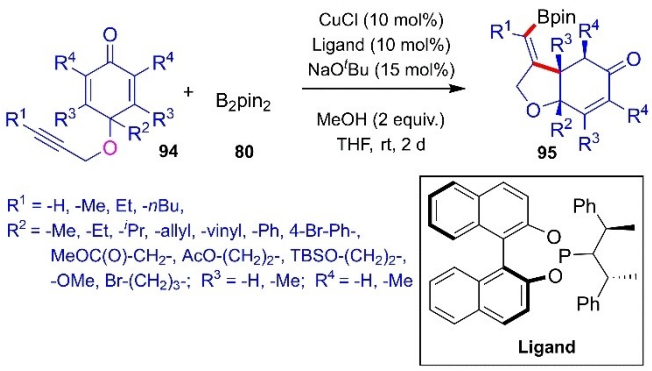

Scheme 60. Borylative cyclization of cyclohexadienone.

In 2014, Yoshida and co-workers[46] reported the α-selective hydroboration of various terminal alkynes with (pin)B–B(dan) as a borylating reagent in the presence of a copper-NHC/KO^{t}Bu catalyst system to deliver a variety of alkenyl boronates in excellent yields. By reducing the Lewis acid character of boron moieties using masked diboron compounds **98**, the regio-selectivity has been achieved successfully following Markovnikov selectivity and further transformation of delivered compounds has been mentioned to obtain bexarotene and LG100268 (Scheme 62).

In the proposed catalytic cycle of this hydroboration approach, the alkenyl copper species **V** was formed through the addition of alkynes **8** to active catalyst **III**. Afterwards, upon the protonation of **V** with MeOH, the desired product **99** was obtained and it was mentioned that the formation of Cu–B(dan) was controlled by the steric interaction between copper and substituent groups present on the alkynes (Scheme 63).

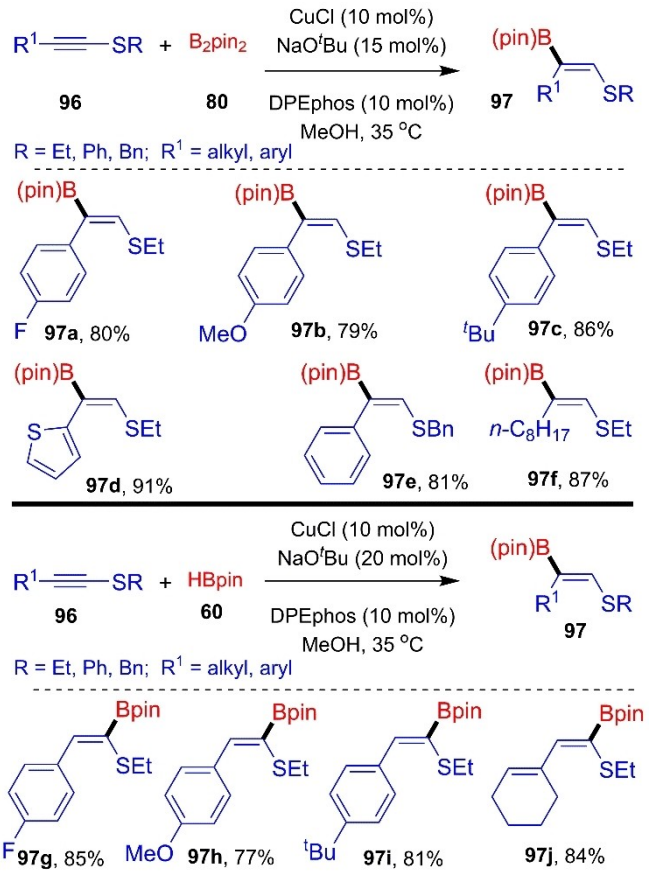

Scheme 61. The selective hydroboration of thioacetylenes.

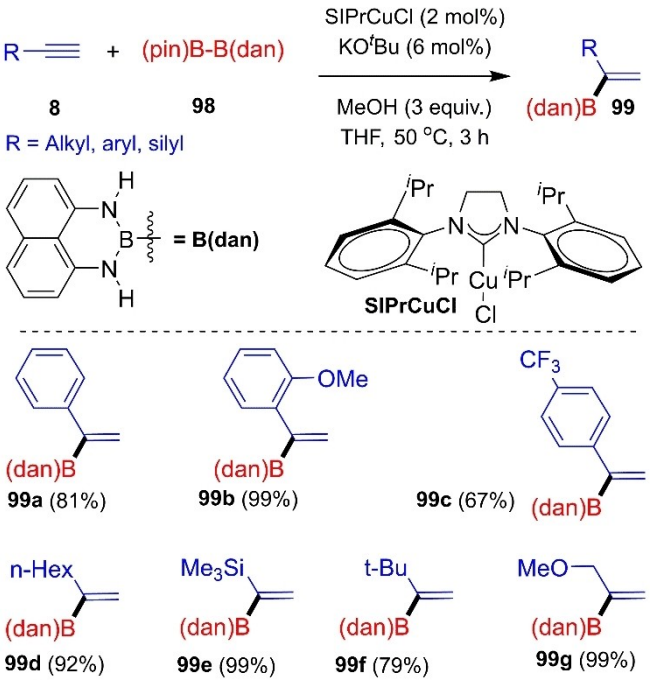

Scheme 62. The α-selective hydroboration of alkynes.

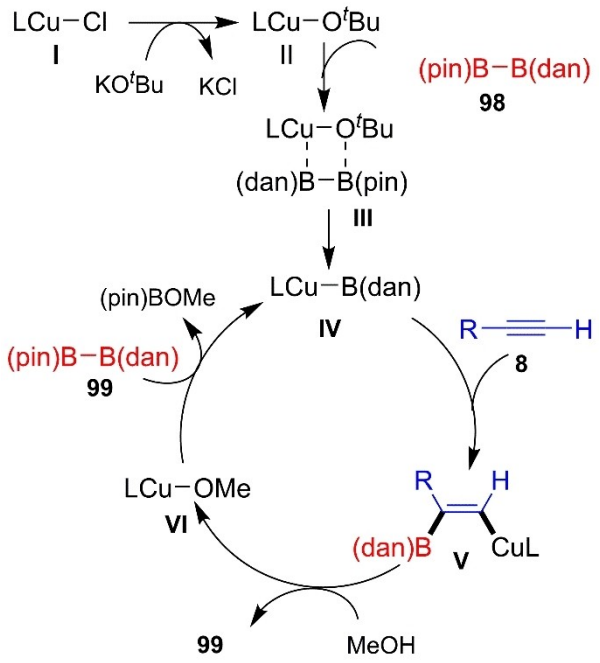

Scheme 63. The proposed catalytic cycle for hydroboration approach.

In 2014, Clark *et al.*[47] published an article demonstrating a novel method for the synthesis of 1,1-disubstituted and trisubstituted vinyl boronate ester **102** (Scheme 64). It is worth mentioning that previously in 2010, the same group reported the synthesis of alpha-hydroxy boronate ester **101** from ketone **100** using (ICy)CuCl (ICy = *N*,*N*-dicyclohexylimidazolyl) and NaO^{t}Bu as catalyst system and B_2pin_2[Bis(pinacolato)diboron] as a borating agent in toluene as solvent. Alpha hydroxy boronate ester was prepared by following the same strategy using ketones, but it was further subjected to *para*-toluene sulfonic acid (*p*-TsOH) in DCM solvent to obtain the desired product 1,1-disubstituted and trisubstituted vinyl boronate ester *via* E1 elimination reaction. The electron-poor groups attached to aryl substituents were found to particularly increase the rate of the borylation reaction, and better yields of desired products were observed with aryl-moieties attached to electron-donating groups. The stereochemistry in the vinyl boronate product was observed to favor *Z* over *E* to decrease the steric congestion caused by Bpin.

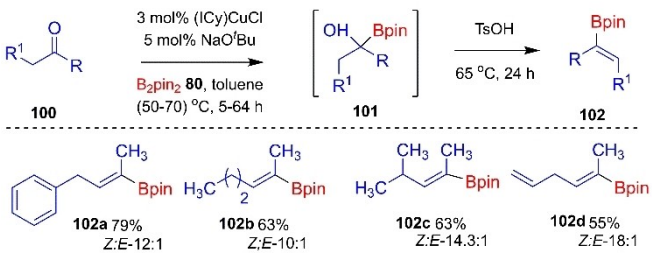

Scheme 64. Copper-catalyzed vinyl boronate ester formation.

Various ketones as substrates showed good selectivity of *Z* over *E*, except for the substrates having 2-degree alpha-carbon on either side of the carbonyl in the keto-substrates. The Suzuki-Miyaura coupling reaction was performed on the resulting vinyl boronate ester, which produces the corresponding *cis* alkene, and this indirectly proved *Z*-vinyl boronate ester formation. Overall, the described method to synthesize 1,1-disubstituted and trisubstituted vinyl boronate ester is important considering the crucial role of trisubstituted alkenes in natural products and pharmaceutically important candidates.

Chae and co-workers demonstrated the selective mono-borylation of silylalkynes using a copper/ligand/NaO^{t}Bu catalytic system and utilizing diborane compounds as borylating reagents in methanol to produce a diverse (*Z*)-*β*-(borylvinyl) silanes.[48] To understand the effects of ligands on regioselectivity, several bulky and robustly electron-rich NHC ligands were tested, and the SIMes·HCl NHC ligand was found to be the optimal ligand to carry out the reaction with great selectivity (Scheme 65).

Zhu *et al.* have witnessed copper/^{t}BuONa catalyzed stereoselective hydroboration of alkynamides to produce *Z*-alkenamides with quantitative yields.[49] Upon investigation of the reaction, it was observed that the product **107** was not observed with mono-dentate phosphine ligand, while the products **108** and **109** were observed. The reaction becomes stereospecific with the bidentate ligand xanthphos, which has produced the product **107** with high regio and stereoselectivity (Scheme 66).

Zhu *et al.* reported the hydroboration reaction of ynamides and bis(pinacolato)diboron under mild conditions to obtain the stereo-selective (*E*)-*β*-alkenylamide boronates in good yields using CuCl (10 mol%), ligand P(2-furyl)$_3$, and LiO^{t}Bu (15 mol%), and methanol (2 equiv.) in THF as solvent[50] (Scheme 67).

The possible catalytic cycle for the reaction mechanism has been discussed by considering *N*-butyl-*N*-(phenylethynyl) methanesulfonamide as a starting material (Scheme 68). Initially, upon trans-metalation between **I** and B_2pin_2, the complex **II** was formed, and then by the addition of starting material **110**, the intermediate **III** was formed in which S–O oxygen interacts with copper metal and causes the regioselectivity. Finally, the product **111** was formed as a result of protonation.

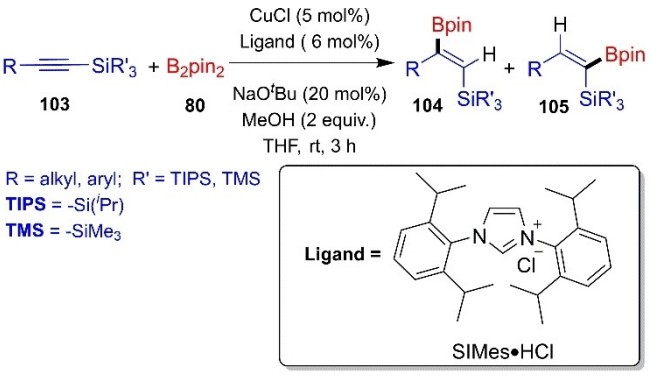

Scheme 65. The selective mono-borylation of silylalkynes.

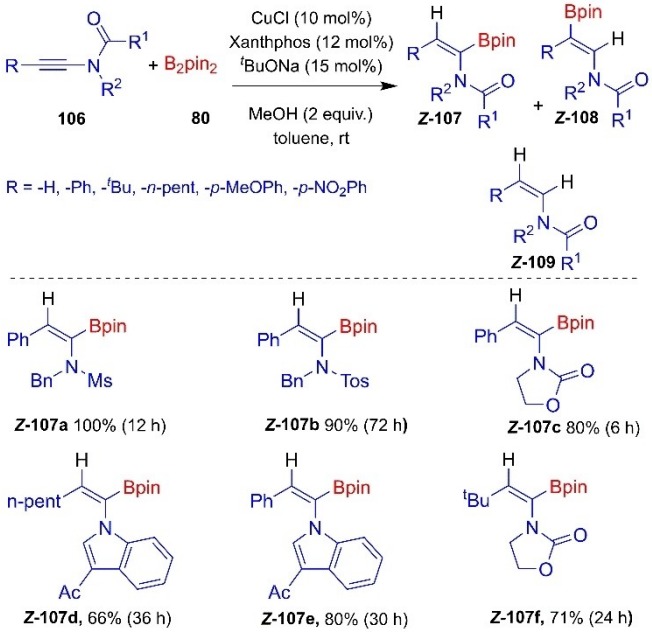

Scheme 66. Hydroboration of alkylnamide.

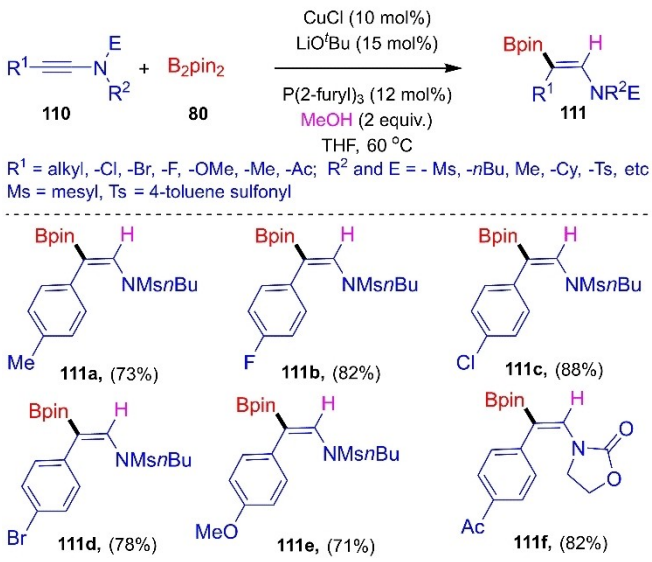

Scheme 67. Borylation of alkynes and substrate scopes.

3.1.3. Silylation reactions

He and co-workers[51] have developed a well-organized copper/ligand/^{t}BuONa catalyzed approach for the asymmetric silylative cyclization through the 1,4-addition of silylated allyl-copper intermediate towards the formation of bicyclo[4.3.0]nonanes. The optimized reaction conditions were obtained by considering 1,6-enalene **112** and $PhMe_2Si$-Bpin **113**, as model substrates in the presence of CuCl (10 mol%), ligand (12 mol%), ^{t}BuONa (15 mol%), and 2 equiv. of MeOH in THF as a solvent. Furthermore, by utilizing these reaction conditions, a diverse substrate scope was developed (Scheme 69).

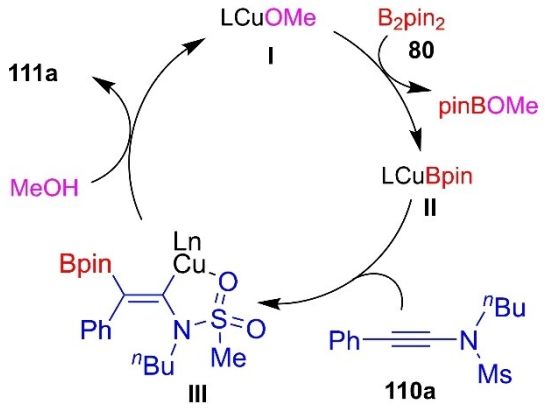

Scheme 68. Proposed mechanism for the borylation of alkynes.

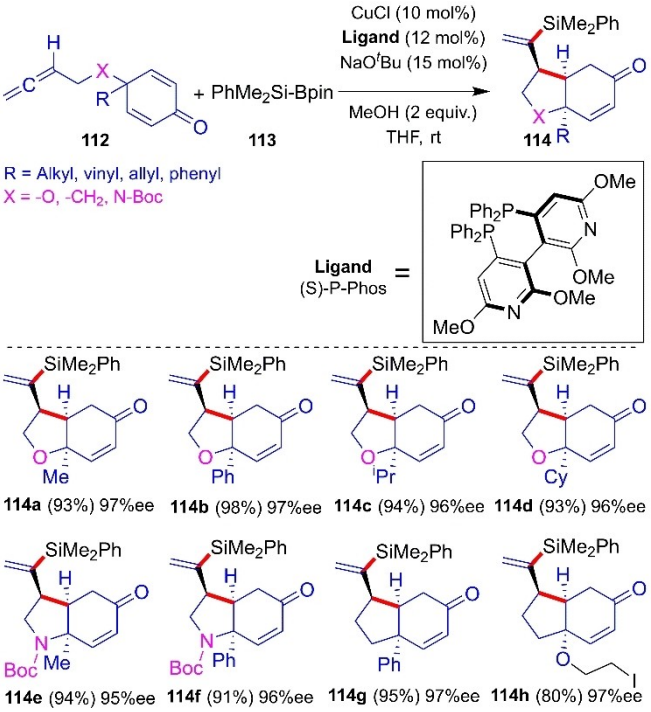

Scheme 69. The scope of various 1,6-enalenes as substrates.

Considering the immense importance of organosilanes particularly the α-aminosilanes in the pharmaceutical applications and as a precursor of important chemical transformations, Xu *et al.*[52] reported for the first time (in 2018) an asymmetric synthesis of cyclic alpha-aminosilanes **116** from 3-acylindole derivative **115** using a chiral (*N*-aryl-*N*'-alkoxy)-*N*-heterocyclic-carbene (NHC)-Copper(I) catalyst system in the presence of a catalytic amounts of NaO^{t}Bu and $PhMe_2Si$-Bpin as a silylating reagent. The role of solvents was examined, and CH_3CN was seen to increase the yield of the product and enantioselectivity. The enantioselectivity in this reaction was improved by the installation of a larger *N*-aryl group in NHC and the presence of a free hydroxyl group at the ligand side, which was also noted for a better conversion rate. Good to excellent enantiomeric excess (*ee*) was observed for 5/6-substituted indole substrates.

However, in some cases, THF was used as a solvent to increase the yield. Overall, the substrate scope for this dearomative silylation reaction was good, with moderate to good yields of the products and enantioselectivity. Regioselectivity was observed due to the addition of nucleophilic silicon at the 2-position of indole, which does not hamper the chirality of the products, and the isolation of single diastereomers was tactically possible due to epimerization, which is evident from the reaction mechanism established by proton NMR studies (Scheme 70).

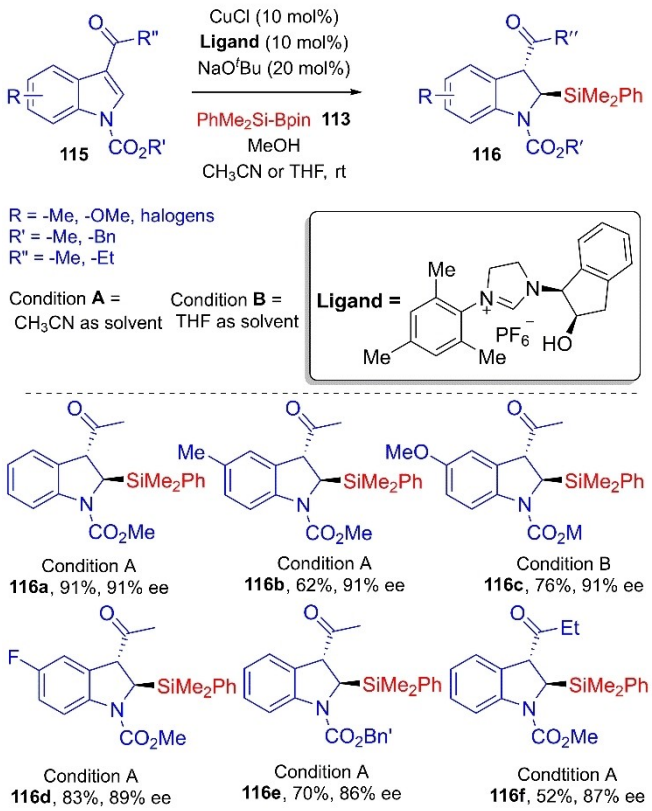

Scheme 70. NHC–Cu-Catalyzed asymmetric dearomative silylation.

From the proposed reaction mechanism (Scheme 71), it is evident that LCuOR **III** has generated the intermediate **IV** upon reaction with the borylsilane. The intermediate **IV** has given rise to the oxygen-bounded copper enolate **II** after coordinating with the C_2-C_3 double bond followed by the 1,4-addition reaction. Due to the presence of the silyl group in the enolate ion **II**, the protonation occurs from the opposite site selectively and results into *cis*-isomer as a major product **116b** and **116a** as a minor isomer. *In situ* active species **III** is regenerated in the previous step. The epimerization of **116b** during the course of the reaction gives rise to the diastereoisomer **116a**, which is thermodynamically more stable.

Oestreich *et al.*[53] in 2020 demonstrated the 1,4-conjugate addition of silylboronic esters to the enynoates, enynamides, and enynones with high enantioselectivity to form propargylic silane (Scheme 72) using copper/potassium *tert*-butoxide as a catalyst system. The screening reactions were performed with three different types of ligands, out of which the ligand **III** was found to be the propitious chiral ligand for 1,4-selectivity over 1,6-selectivity. The reactions were also tested with solvent THF and various bases/alcohols as additives, and it was found that KO^{t}Bu/MeOH was the most promising condition to afford 1,4-adduct with 74% yields in 70% *ee*. When the solvent was replaced with 2-Me THF, the yields of the products increased up to 85% with 91% *ee*. The reaction conditions were in accordance with good functional group compatibility with different δ-aryl-substitutions on **117** towards the formation of 1,4-adducts in high enantiomeric excess. The enantiomeric excess is slightly less in the case of **117** (having an alkyl or silyl group at δ-position) with good yields of 1,4-adducts. The chemoselectivity is directed towards 1,6-adducts and delivers allenes with 50% yields, when a methyl substituent is attached to β-carbon. The

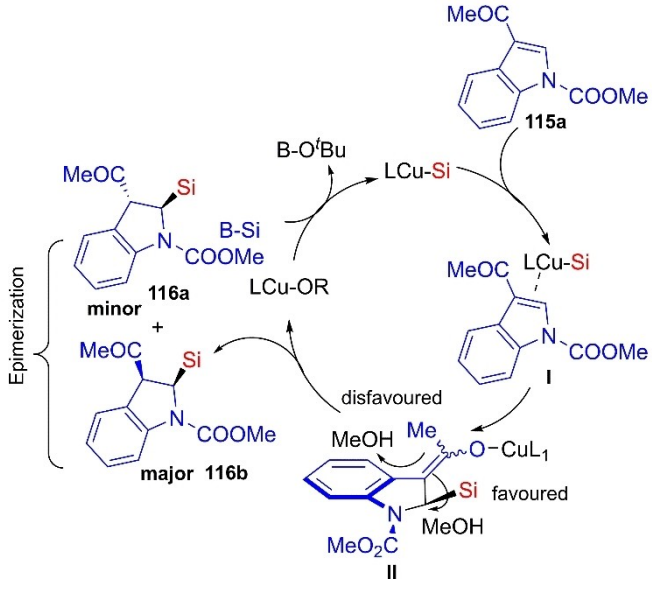

Scheme 71. Plausible reaction mechanism of asymmetric dearomative silylation.

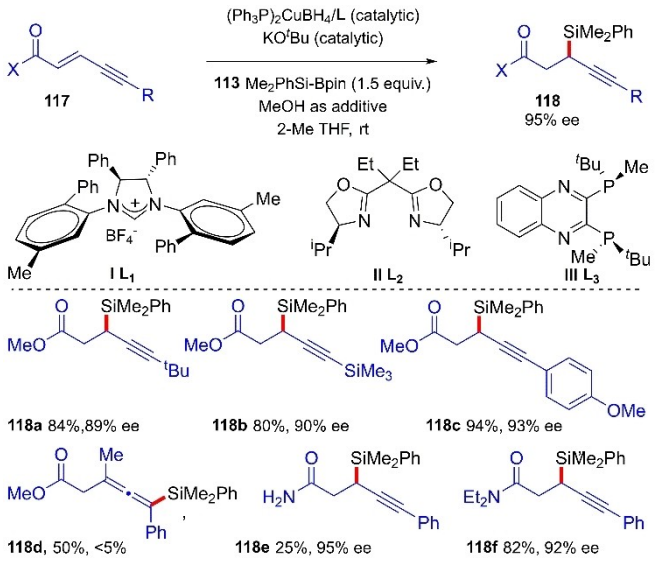

Scheme 72. Synthesis of α-chiral propargylic silanes.

same reaction conditions were applied to enynamides and enynones, which usually occurred over a longer period of time (60 hours).

3.1.4. Other reactions

Stahl *et al.*[54] in 2013 witnessed the mechanistic evaluation of aerobic oxidation of alcohols catalyzed by the copper/TEMPO/KO^{t}Bu catalytic system. The aerobic oxidation of alcohols into aldehydes or ketones using copper/TEMPO catalytic systems was developed by Semmelhack in 1984. In 2003, using catalytic $CuBr_2$, Sheldon and his group reported the same approach by considering bpy as a ligand and catalytic KO^{t}Bu as an additive.

Next, Koskinen has performed the reaction with $Cu^{II}(OTf)_2$/TEMPO by substituting KO^{t}Bu with NMI and/or DBU in acetonitrile. Finally, Stahl and coworkers (in 2011) have carried out the mechanistic evaluation using the Cu^{I}OTf/TEMPO/NMI catalytic system with an improvement in the performance of catalyst and substrate scope. The role of various bases such as NMI, DBU, and KO^{t}Bu has been discussed, and among these, NMI and DBU are beneficial as they can act as ligands. However, usage of a strong base such as KO^{t}Bu was not required; rather, it was mentioned that a strong base can result in epimerization of stereo-centers adjacent to the aldehyde in the product or isomerization of (*Z*)-enals to the thermodynamically favored (*E*) product.

They have investigated the mechanistic path of the Cu(I)-catalyzed system based on experimental observations. In the catalytic cycle (Scheme 73), the catalyst L_nCu^{I} as well as TEMPOH were oxidized in the presence of oxygen to generate complex **II**. After which the copper alkoxide intermediate **III** was obtained by the oxidation of alcohol **65**. The alkoxide may be generated without using any base and *via* hydrogen atom abstraction in the presence of TEMPO; the aldehyde **59** was delivered with the regeneration of the L_nCu^{I} catalyst.

The first site-selective allenylation of aldehydes and ketones **59** using propargylic boronates **119** in the presence of copper/ligand/LiO^{t}Bu catalytic system was reported by Frandrick and co-workers in 2013.[55] The site-selectiveness of the reaction depends on the nature of PBE ligand. The ligands MePBE and EtPBE provide the corresponding product **120** alone, and it was established that ^{i}PrPBE was not a good choice to deliver the product **120**; whereas, PhPBE ligand provides the product **121** with good selectivity (Scheme 74).

In this approach, it was assumed that the active intermediate **B**, the allenyl cuprate provides the product **120** and upon disturbing the intermediate **B**, it can be converted into intermediate **A** and thus, the product **121** can be obtained (Scheme 75).

O'Neil *et al.*[56] in 2013 published an article indicating the synthesis of 1,3-diols from alpha-beta unsaturated ketones, or terminal enones. The terminal enones were first converted into beta-hydroxy ketones using the beta-borylation/oxidation sequence in the presence of CuCl, B_2pin_2 [bis(pinacolato)diboron], catalytic NaO^{t}Bu, and $NaBO_3$ (Scheme 76). In the following step, the beta-hydroxy ketones were converted directly into cyclic

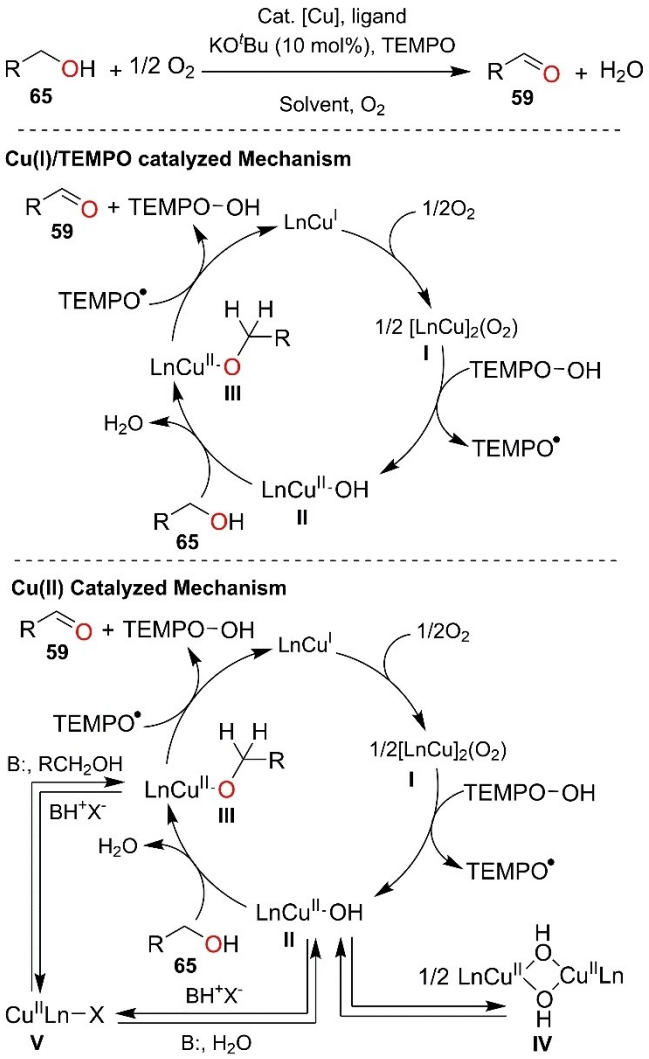

Scheme 73. Mechanistic evaluation of copper/TEMPO catalyzed oxidation of alcohols.

siloxane products (Scheme 77) by the use of diphenylchlorosilane (Ph_2SiHCl), imidazole, and triethylamine (Et_3N) as base *via* the co-operative Lewis base mediated intramolecular carbonyl hydro-silylation process.

The proposed mechanism indicates the formation of a six-membered chair-like transition state during the silylation of beta-hydroxy ketones, due to which the important diastereoselectivity was observed. This particular protocol has been found to produce *syn-syn* and *syn-anti* stereotriads in very good yields. These are the crucial precursors for the preparation of complicated polytide targets such as discodermolide (Scheme 77).

Pooi and co-workers[57] have demonstrated a method for the cyclization of two isocyanides **127** and **128** (Scheme 78) to furnish a range of cyclic products (1,4-diaryl imidazoles), using copper metal as a catalyst and catalytic amounts (50 mol%) of potassium tertiary butoxide as an additive. An activator IPrCl [1,3-bis(2,6-diisopropylphenyl)-1*H*-imidazol-3-ium chloride] has also been used to activate the C–H bond.

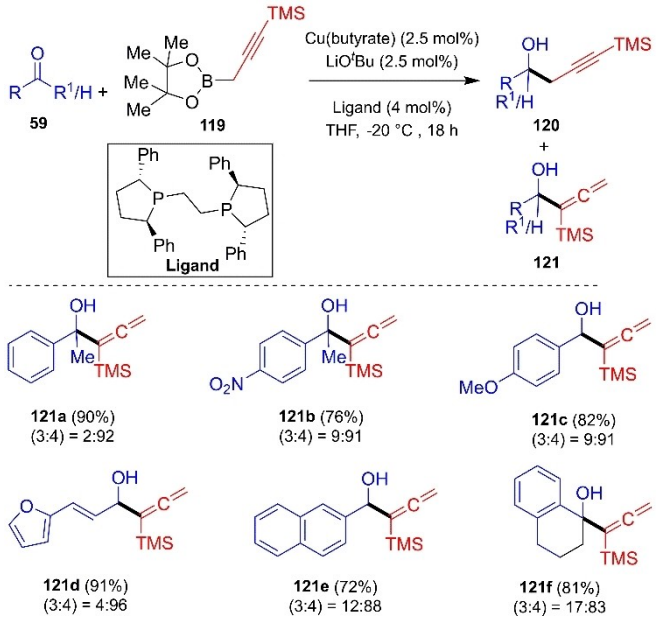

Scheme 74. Allenylation of various ketones and aldehydes with propargyl boronates.

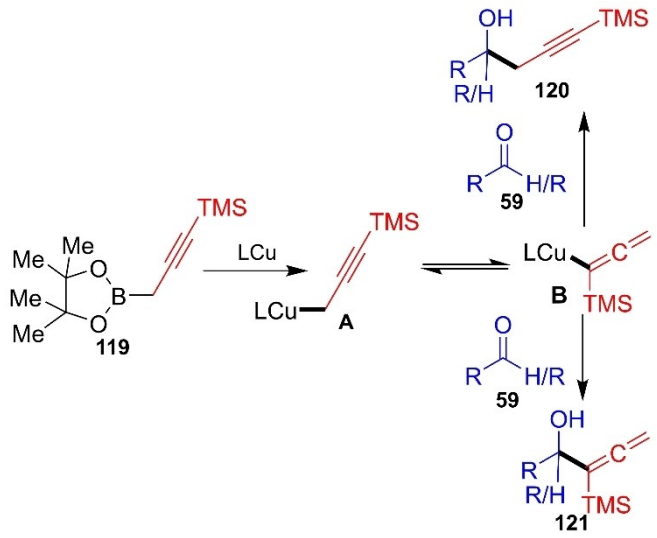

Scheme 75. Approaches for the propargylation and allenylation.

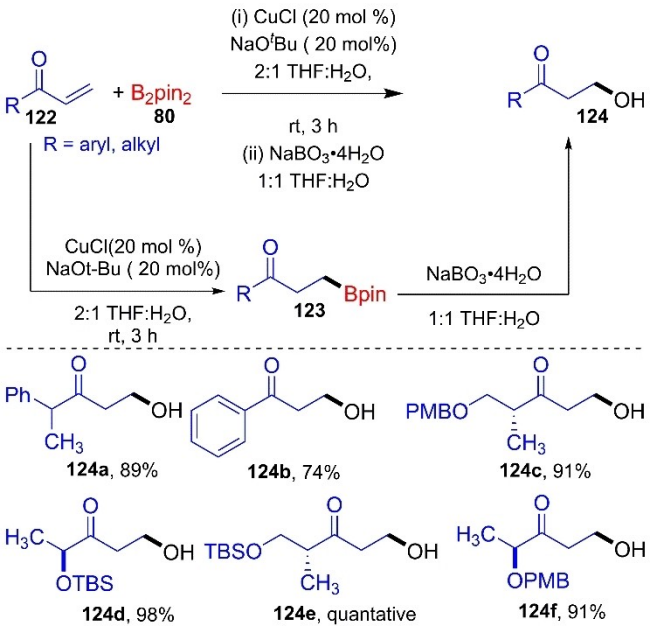

Scheme 76. Preparation of β-hydroxy ketones from terminal enones *via* beta-borylation/oxidation method.

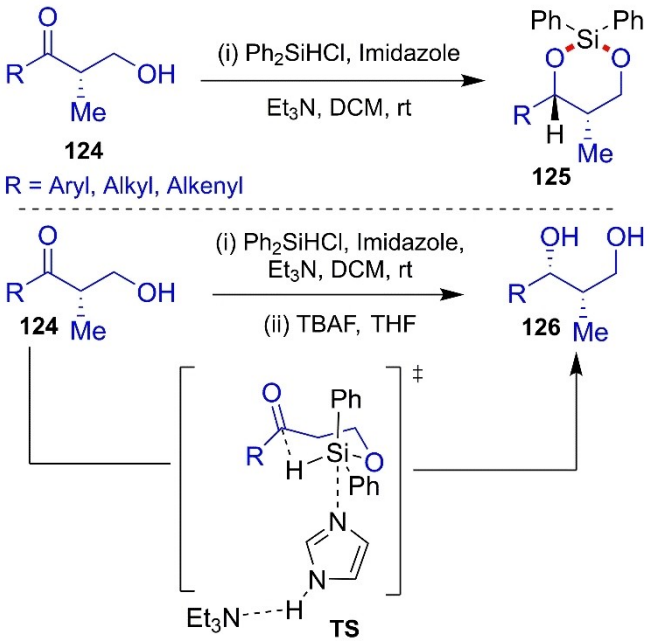

Scheme 77. Felkin-controlled intramolecular hydrosilylation.

During the optimization of the reaction, it was discovered that the reaction was functioning only with KO^{t}Bu as an additive in catalytic amounts, and when it was replaced by NaO^{t}Bu, the yield of the reaction decreased from 83% to 47%. It was also found that the yields of the product were much less with other alkali metal alkoxides and using other additives, the transformation was not realized. It is also perceived that the variation in product yields occurred due to the changes in the amounts of catalysts and additives; on decreasing the amounts of catalyst the yields of the product increased, while on decreasing the loading of additives the product yields decreased drastically. The scope of this reaction was analyzed over various substrates by applying the reaction conditions, which showed excellent yields. On application to the first component of the reaction, with the substrate **127** which has *para*-substitution on the phenyl ring, an excellent yield of product **129c** was seen, and the yields of the products with respect to the second component **128** were also excellent.

The mechanism is described in two cycles; the first cycle involves the formation of *N*-arylformimidate **E** as an intermediate, and the second cycle involves the product formation. As in the proposed mechanism (cycle **I**) the catalyst first interacts

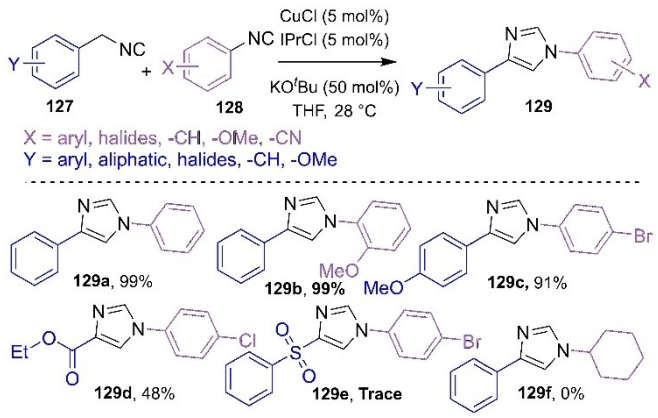

Scheme 78. The synthesis of 1,4-diaryl imidazoles.

with KO^{t}Bu to form active compound **A** in a very short time (within 5 min), after which **A** reacts with **128** and forms **B**. Upon an intramolecular rearrangement of **B** and introducing potassium *tert*-butoxide and *tert*-butyl alcohol compound **E** was obtained. Then, the (cycle **II**) intermediate **E** undergoes nucleophilic substitution with benzylic nitrile anion **F** to give **G**, which is stabilized by the coordination with potassium cation followed by the introduction of KO^{t}Bu, **G** converts into vinyl isocyanide **H** which makes the isocyanide carbon more electrophilic, and this causes cyclization to deliver the compound **129** (Scheme 79).

3.2. Utilization of *tert*-butoxides with Iron-complexs as catalysts

Asymmetric transfer hydrogenation of ketones has been disclosed by Bigler and coworkers (Scheme 80) in 2014 by the application of isonitrile iron(II) complex as a catalyst and a catalytic amount of sodium tertiary butoxide in isopropanol as solvent.[58] The reaction conditions were found by considering 1.0 mmol of **130** in ^{i}PrOH (0.25 M) to obtain the desired product **131** in excellent yield. Various isonitrile iron(II) complexes were synthesized and applied successfully for the asymmetric hydrogenation of ketones. The reaction was optimized by using

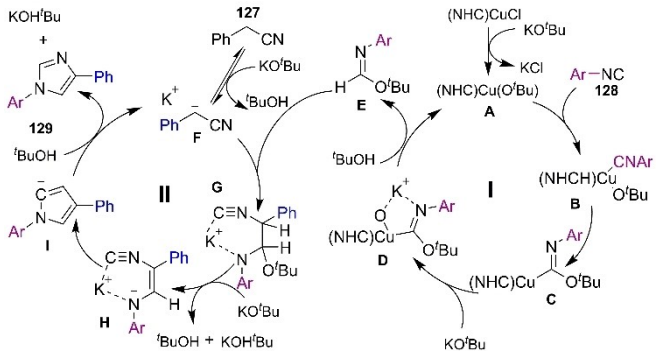

Scheme 79. The proposed mechanism for synthesis of 1,4-diaryl imidazole.

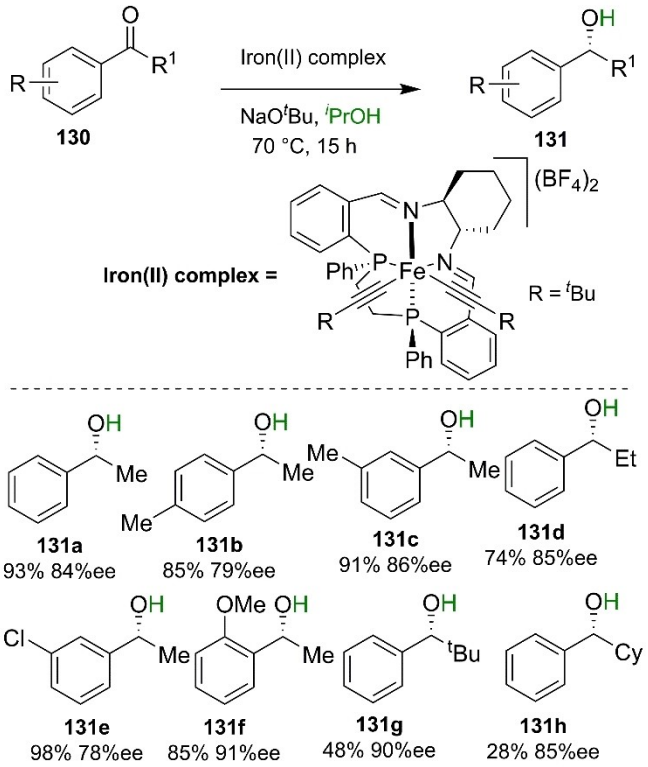

Scheme 80. Asymmetric transfer hydrogenation of acetophenones.

isonitrile iron(II) complex (1 mol%) in the presence of (4 mol%) NaO^{t}Bu. A broad range of substrate scope was developed with excellent enantioselectivity. *Ortho*-substituted acetophenones gave higher enantioselectivity of product **131 f** in 91% *ee*, with bulkier group substitutions **131 g** and **131 h** giving 90% *ee* and 85% *ee* respectively.

Thomas *et al.*[59] in 2016, discovered a new catalytic system for hydro-functionalization reactions by the activation of non-precious earth-abundant metals like iron, cobalt, and manganese in the low oxidation state using NaO^{t}Bu as a pre-catalysts activator. This approach is successfully applicable with air- and moisture-sensitive stable reagents and catalysts to carry out the hydroboration, hydrosilylation, hydrogenation, and $[2\pi + 2\pi]$ cycloaddition reactions of alkenes **132** and **135**. The NaO^{t}Bu was successfully applied for the activation of iron and cobalt pre-catalyst and the conditions were applied for the hydroboration and hydrosilylation of alkenes and alkynes (Scheme 81). It was observed that the reaction condition provides a *Z*-selective product with an iron catalyst and an *E*-selective product with a cobalt catalyst.

In 2018, Cheng and co-workers[60] developed a chiral oxazoline-iminopyridine (OIP) iron complex (OIP-$FeCl_2$) and using this metal-complex as a precatalyst in the presence of NaO^{t}Bu as an activator, an enantioselective, and highly Markovnikov selective hydrosilylation process of terminal aliphatic alkenes was accomplished to obtain the crucial chiral organosilane. The phenyl silane was used as a silylating agent. An increase in regio and enantioselectivity was noted, when more sterically hindered imines were introduced in the ligand backbone.

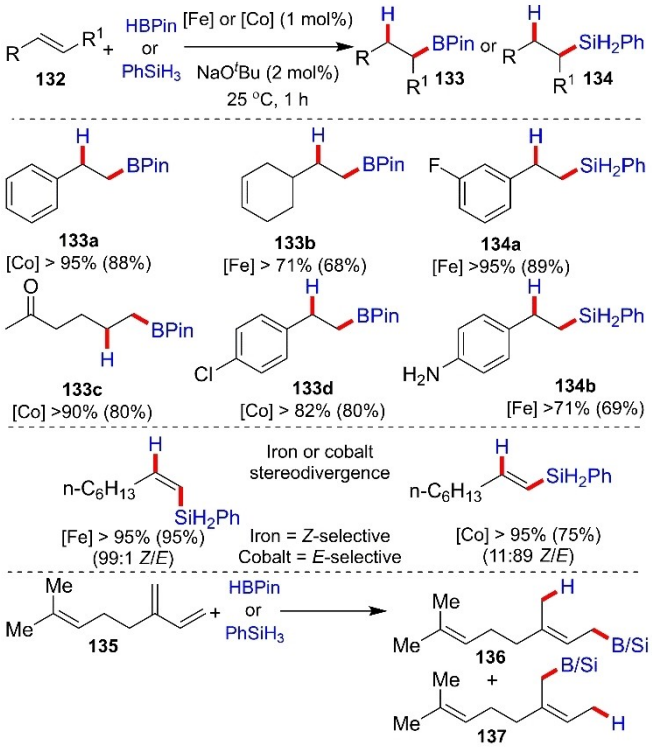

Scheme 81. The Iron and cobalt catalyzed hydrosilylation and hydroboration of alkenes and alkynes.

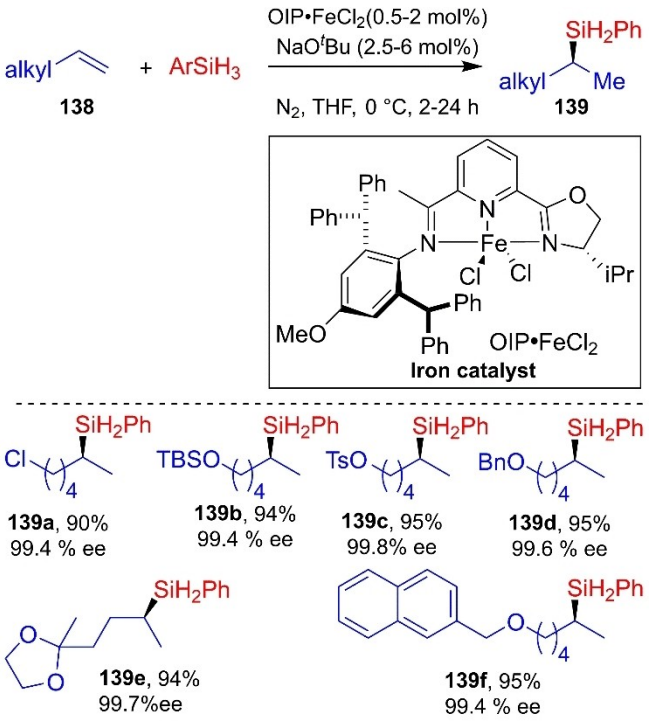

Scheme 82. Iron-catalyzed Markovnikov selective, enantioselective hydrosilylation of alkene.

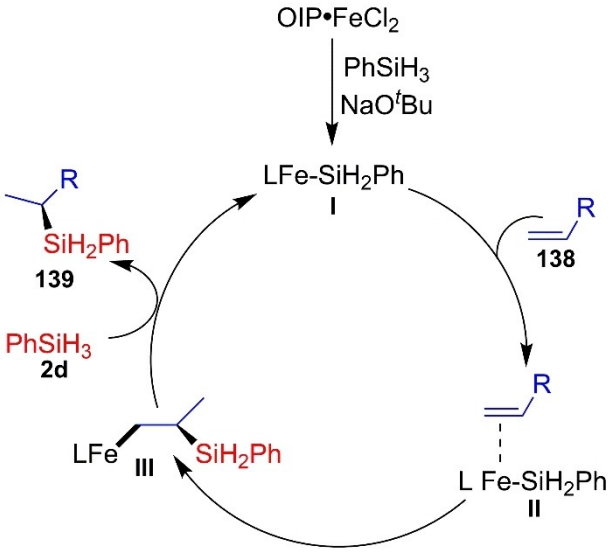

Scheme 83. Proposed reaction mechanism.

Whereas the oxazolone did not show any change in regio and enantioselectivity upon stereoelectronic modification. This catalytic hydrogenation process can tolerate large functional group variance and delivers high yield (up to 97%) with very good enantioselectivity (>97%) on various substrate scopes. Further derivatization of chiral organosilane was processed to synthesize important products (Scheme 82).

In the proposed reaction mechanism (Scheme 83), the iron-silyl moiety **I** is generated from the reduction of OIP·$FeCl_2$ in the presence of sodium *tert*-butoxide and $PhSiH_3$, and delivers the intermediate **II** after reacting with the alkene moiety **138**. Afterwards, the alkene moiety gets inserted into the iron-silicon bond and gives rise to an iron alkyl moiety **III**. In the next step, **III** reacts with $PhSiH_3$ to form hydrosilylation moiety **139**, which regenerates iron-silicon moiety **I**.

Transfer hydrogenation is a well-established method for the reduction of a wide variety of substrates including ketone, aldehyde, imine, etc. The iron-based complexes are known to be efficient catalysts for the transfer hydrogenation reactions, and NHC ligands are particularly effective in increasing the activity and selectivity of these catalysts. The use of donor-functionalized NHCs in this process is designed to improve the electronic properties of the catalyst leading to increased reactivity and selectivity. Additionally, donor-functionalized NHCs can lead to improved catalytic stability and catalyst recovery. Lopes and co-workers[61] published an article where they studied the catalytic activities of bifunctional iron(II) complexes bearing NHC ligands functionalized with acetamide, amine, and hydroxyl groups in transfer hydrogenation reactions. They have reported that the complex containing the acetamide group showed the best catalytic activity. In the NMR study, it was concluded that the use of the catalytic amounts of LiO^tBu assisted in the deprotonation of the acetamide group in the reaction mechanism, and ^{i}PrOH acted as the hydrogen source (Scheme 84). In addition, the authors prepared a Fe-NHC catalyst system for this reaction by utilizing glycerol as a

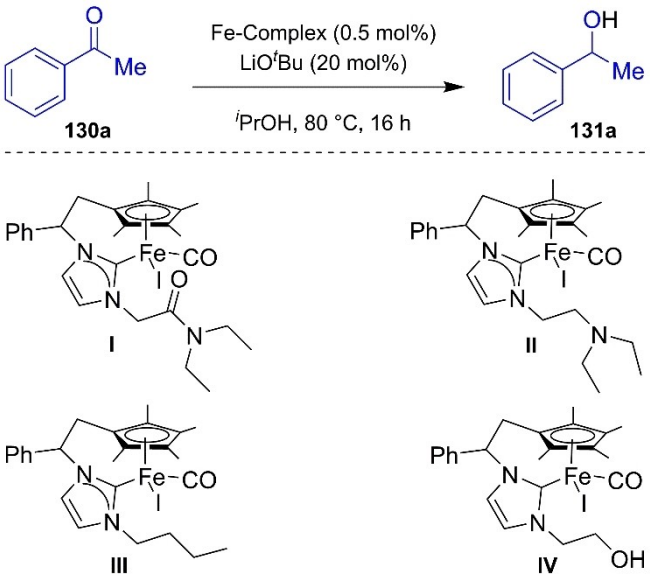

Scheme 84. Reaction scheme for Fe(II)-NHC catalyzed transfer hydrogenation reaction.

hydrogen source under microwave irradiation in the presence of catalytic amounts of an additive.

3.3. Utilization with cobalt-complexs as catalysts

3.3.1. Hydrogenation of nitriles

Adam and his co-workers devised the selective hydrogenation of nitriles using a catalytic tetra-dented phosphine ligand with a cobalt catalyst in the presence of 10 mol% of KO^{t}Bu (Scheme 85).[62] To understand the effects of base, solvent, and catalyst; several reactions were performed and it was observed that an appropriate amount of additive was required for the conversion into an amine. At low loading (less than 10 mol%) of KO^{t}Bu, a side product *N*-benzyl-1-phenylmethanimine was observed, and when the loading of the base was increased further, the formation of *N*-benzyl-1-phenylmethanimines was inhibited and the benzylamine derivative **141** was detected instead.

Aromatic nitriles were hydrogenated by using 4.0 mol% of cobalt catalyst and 10 mol% of potassium *tert*-butoxide at 80–120 °C in *tert*-butanol as solvent under 30 bar pressure of H_2; while, the same conditions were applied to aliphatic nitriles using 5 mol% catalysts under similar conditions as for aromatic nitriles at 140 °C for 24 hours. It was found that alkyl nitriles with bulkier substituents require either a higher amounts of catalyst loading or longer reaction time.

Fout *et al.*[63] in 2017 developed a method for the selective hydrogenation of nitriles into primary amines (Scheme 86) by the application of a cobalt precatalyst (^{Mes}CCC)Co(H_2)PPh_3 system in the presence of a catalytic amounts of potassium tertiary butoxide as an additive and a 4.0 atmosphere pressure of H_2. This reaction involved a Co(I/III)-catalyzed redox process,

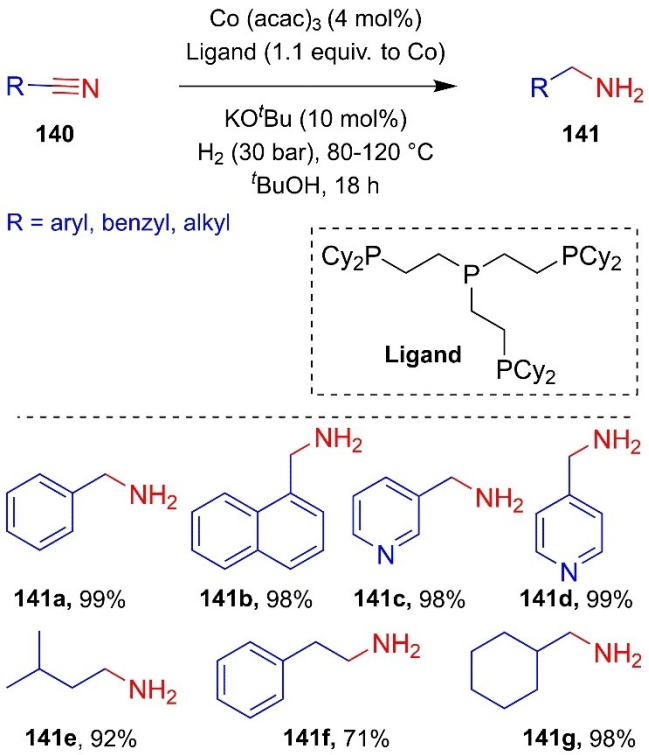

Scheme 85. Cobalt phosphine catalyzed selective hydrogenation of nitriles.

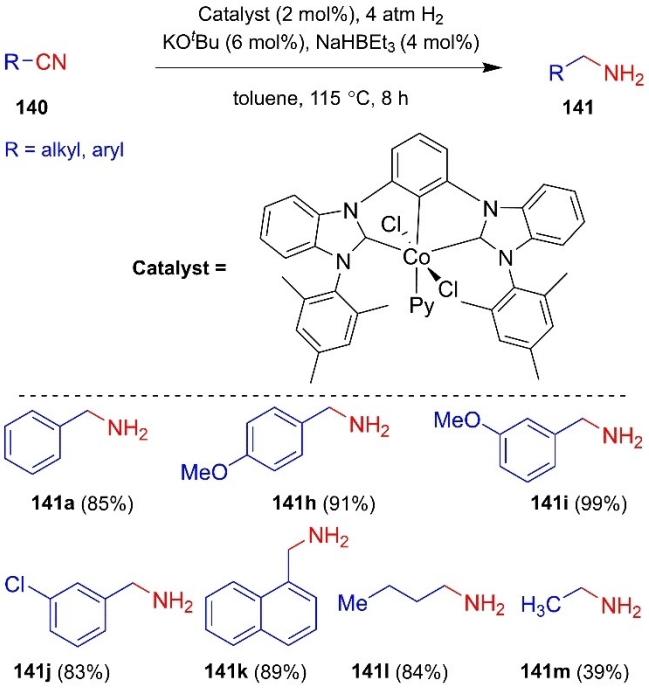

Scheme 86. Cobalt phosphine catalyzed selective hydrogenation of various nitriles.

which has been studied with *para*-hydrogen induced polarization (PHIP) transfer NMR.

The reaction was optimized by considering benzonitriles as starting materials, cobalt-complex as catalyst, and catalytic

amounts of KO^{t}Bu under a 4 atmosphere pressure of H_2. It was found that the reaction works best under the conditions of a 2 mol% catalyst, KO^{t}Bu (4 mol%) as an activator, and an additive $NaHBEt_3$ (6 mol%) in toluene as solvent at 115 °C. With these optimized conditions, various substrate scopes have been developed for aromatic and aliphatic nitriles. The hydrogenated product yields were high for aromatic nitriles having an electron-donating group (**141 h–i**) and slightly less for substrates having an electron-withdrawing group **141 j** (Scheme 86).

3.3.2. Hydroboration and silylation reactions

In 2017, Thomas *et al.*[64] developed a bipyridyl oxazoline ligand substituted cobalt catalyst (^{t}BuBPOCoCl$_2$), which was used for alkene hydroboration in the presence of NaO^{t}Bu as a co-catalyst to activate the catalyst *in situ*. The HBpin was used at room temperature as a boronating agent, and the addition was Markovnikov selective. This catalytic, Markovnikov selective alkene hydroboration was carried out on a variety of functional groups bearing electronically and sterically modified styrene derivatives to form corresponding boronic esters in high yields (up to 92% isolated yield) and excellent regioselectivity (98:2 branched to linear selectivity). This boronic ester is a powerful precursor for various carbon-carbon and carbon-heteroatom bond-forming reactions (Scheme 87).

In 2017, Cheng and co-workers[65] synthesized an oxazoline-iminopyridine backbone by utilizing a cobalt catalyst (OIP·CoCl$_2$). With the help of this co-catalyst, a very efficient enantioselective, Markovnikov selective hydrosilylation of aryl and aliphatic alkenes was achieved to afford highly enantioselective organosilanes. The higher yield (up to 97%) and better enantioselectivity (up to 99% *ee*) were achieved using Et_2O as a solvent, NaO^{t}Bu as an activator for the catalyst, and phenyl silane as a silylating agent. An increase in enantioselectivity was observed by introducing sterically hindered imine as the ligand, attached to the catalyst. The electron-poor ligands lead to low yields, but high regioselectivity in comparison to electron-donating moieties (Scheme 88). Additionally, better selectivity was noted in less sterically hindered oxazolines. This enantioselective hydrosilylation has a very good substrate scope and atom economy, with excellent functional group tolerance. The turnover frequency (TOF) and turnover number (TON) are up to 1800 and 860 respectively. This reaction can be easily processed for gram-scale synthesis with 0.1 mol% of Co-catalyst. From the proposed reaction mechanism (Scheme 89), it is evident that OIP·CoCl$_2$ gets reduced to cobalt-silicon moiety **I** in the presence of sodium *tert*-butoxide and $PhSiH_3$. In the next step, the intermediate **I** undergoes alkene insertion to generate intermediate **II**, which upon reaction with $PhSiH_3$ forms the corresponding hydrosilylation product **139** and regenerates cobalt-silicon species **I**.

Cobalt(II) coordination polymers have emerged as a promising class of pre-catalysts for the selective hydroboration of aldehydes, ketones, and imines. The use of these polymers allows for the efficient and selective formation of corresponding alcohols or amines, with high selectivity and low catalyst loading.

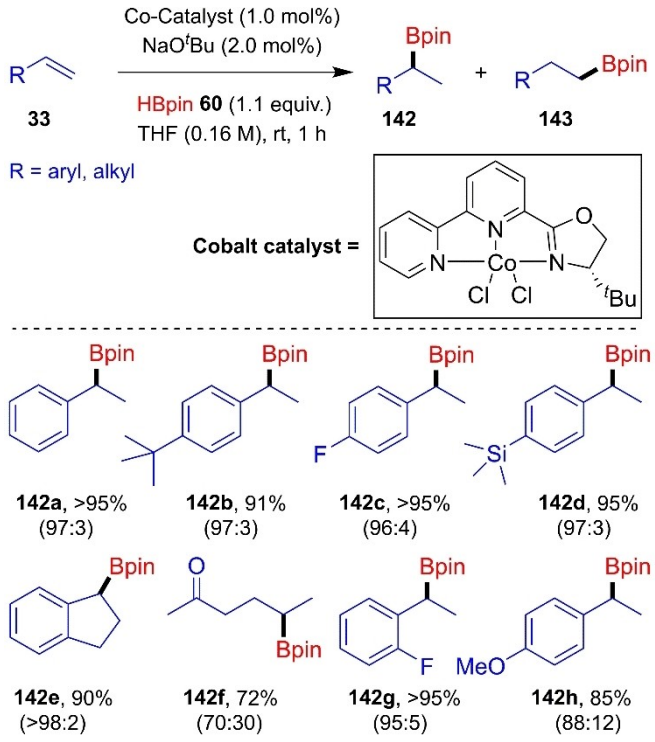

Scheme 87. Bipyridyl-oxazoline cobalt-catalyzed Markovnikov selective hydroboration of alkenes.

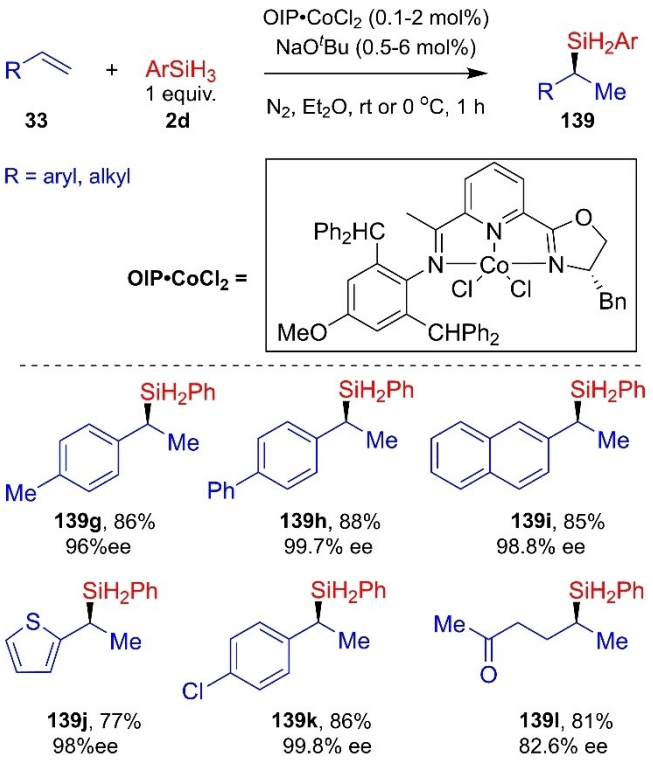

Scheme 88. Cobalt-catalyzed enantioselective Markovnikov selective hydrosilylation of alkenes.

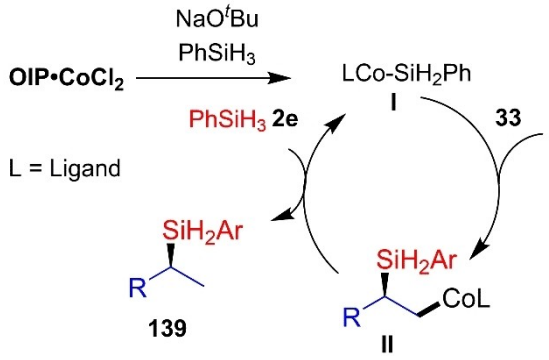

Scheme 89. Proposed reaction Mechanism.

In a recent study, Wu *et al.*[66] synthesized a series of cobalt(II) coordination polymers using different ligands and investigated their performance as pre-catalysts for the hydroboration of aldehydes, ketones, and imines. In one study, Wu *et al.* synthesized a cobalt(II) coordination polymer using a ligand containing both bidentate and tridentate binding sites. The polymer was found to have a high selectivity for the hydroboration of aldehydes over ketones and imines with low catalyst loading and shorter reaction times.

The hydroboration was carried out in the presence of cobalt(II) coordination polymers as the pre-catalyst and HBpin as the hydroborating agent, in THF at room temperature. It was found that the use of cobalt(II) coordination polymers resulted in the high conversion of the aldehydes and ketones and excellent selectivity for the formation of corresponding alcohols. The same ligand also showed good activity in the hydroboration reaction of imines, but the selectivity was not as high as that observed for aldehydes and ketones. The authors also performed a detailed characterization of cobalt(II) coordination polymers using various techniques such as powder X-ray diffraction, Fourier transform infrared spectroscopy, and thermogravimetric analysis. These studies revealed that the cobalt(II) coordination polymer had a highly porous structure, with a high surface area and a high number of active sites, which likely contributed to its high activity and selectivity in the hydroboration reaction (Scheme 90).

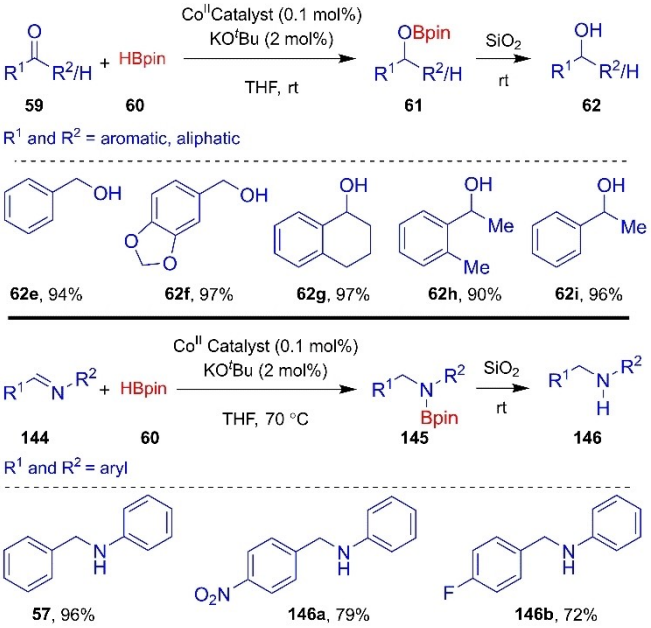

Scheme 90. Reaction scheme and substrate scope for Co(II) coordination polymer catalyzed hydroboration reaction.

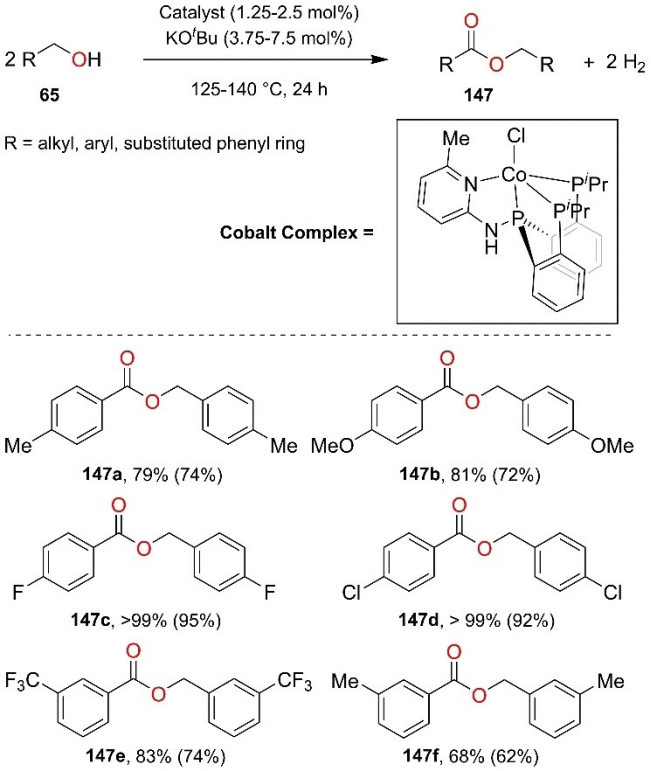

Scheme 91. Dehydrogenative homo-coupling of primary alcohols.

3.3.3. Dehydrogenative coupling reactions

Ding *et al.*[67] in 2018, developed a catalytic system of cobalt complexes for dehydrogenating homo-coupling of alcohols. Benzyl alcohols (0.5 mmol) **65** were successfully converted into benzyl benzoate **147** in the presence of cobalt catalyst (1.25 mol%) and catalytic KO^{t}Bu (3.75 mol%) in excellent yields. Using the optimized conditions of reaction, a broad range of substrate scope was developed (Scheme 91). The role of KO^{t}Bu was tested by loading it with benzyl alcohol in various amounts, and it was observed that the loading of 1.25 mol% of KO^{t}Bu was only enough to activate the catalyst, and the desired products were obtained with only a 4% yield. When the loading amount increased to 2.5 mol%, the product yield also increased to 88%.

Cobalt catalyzed formation of carbon-carbon bonds towards the selective synthesis of 1,5-diketones **148** using hydrogen borrowing strategies has been demonstrated in 2021 by

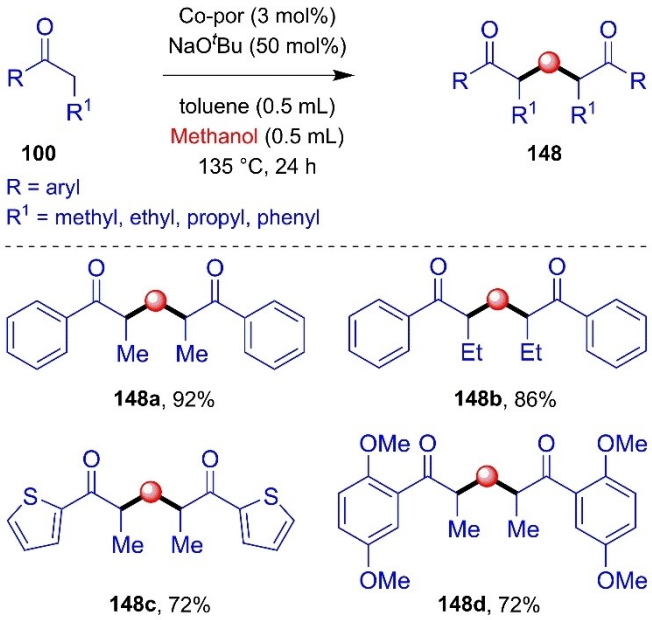

Scheme 92. Selective synthesis of 1,5-Diketones.

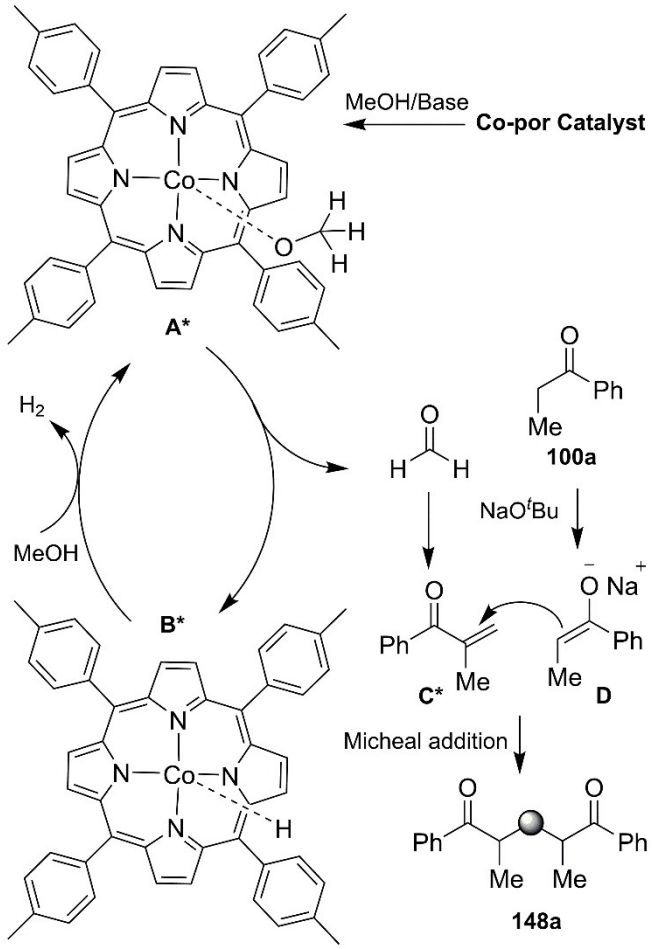

Scheme 93. Proposed reaction mechanism.

Chandrasekhar *et al.*[68] Propiophenone **100** and methanol (carbon source) were used as model substrates under the influence of the cobalt porphyrin complex and catalytic amounts of NaO^{t}Bu (Scheme 92). The reaction conditions were optimized, and it was found that the loading of 3.0 mol% catalyst and 50 mol% additive gave the best conditions for the reaction. Upon application of reaction conditions, a wide range of substrate scope was developed.

Based on the controlled experiments and literature support, a plausible mechanism for the reaction of propiophenone and methanol in the presence of catalyst Co-por was proposed (Scheme 93). According to the proposed mechanism, the catalytic cycle is initiated by the formation of a complex (A*) produced by MeOH in the presence of a catalyst and additive. The complex (A*) released formaldehyde and species (B*). Then the species (B*) reproduced the complex (A*). The transient formaldehyde generates the intermediate (C*) in the reaction with propiophenone. Upon Michael's addition reaction between the intermediate (C*) and propiophenone, the desired product 1,5-diketone **148** was obtained.

3.3.4. Reductive C–O bond cleavage of lignin β-O-4 ketones

Xia *et al.* developed the reductive C–O bond cleavage of lignin β-O-4 ketone substrates to give corresponding ketones and phenols using a pyridine diimine cobalt-catalyst system and diboron as a reducing agent.[69] The use of NaO^{t}Bu in catalytic amounts with cobalt-catalyst and additive helps towards the complete conversion of lignin β-O-4 ketone. A broad substrate scope was developed employing the lignin β-O-4 ketone derivatives (Scheme 94). The described synthetic method was applied for the depolymerization of polymeric lignin β-O-4 ketone compounds. The plausible catalytic cycle was proposed based on quantitative kinetic studies and literature reports involving the 1,2-Brook type rearrangement reaction (Scheme 95).

3.4. Utilization with manganese-complexes as catalysts

Manganese pincer complex and catalytic ^{t}BuONa were found to be an effective catalytic system for the selective hydrogenation of various aldehydes, ketones, and nitriles into corresponding alcohols (Scheme 96) and amines (Scheme 97).[70] In this methodology of hydrogenation, four different types of catalysts were prepared and applied for the investigation of reaction parameters, and the optimal conditions were found at 50 bar pressure of H_2 in toluene solvent and catalytic amounts of ^{t}BuONa to activate the manganese complex. The reaction reveals good functional tolerance and was employed successfully for the hydrogenation of aliphatic and aromatic nitriles and various aldehydes and ketones to deliver the desired products in excellent yields.

An outer sphere mechanism was proposed (Scheme 98) with the understanding of controlled experiments and previous literature. According to the mechanism, the transfer of hydride

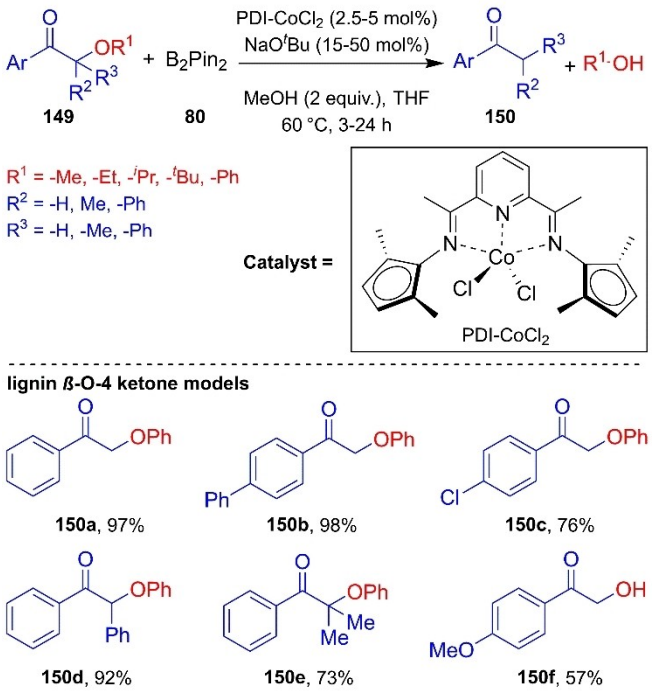

Scheme 94. Reductive C–O bond cleavage of lignin β-O-4 ketone compounds.

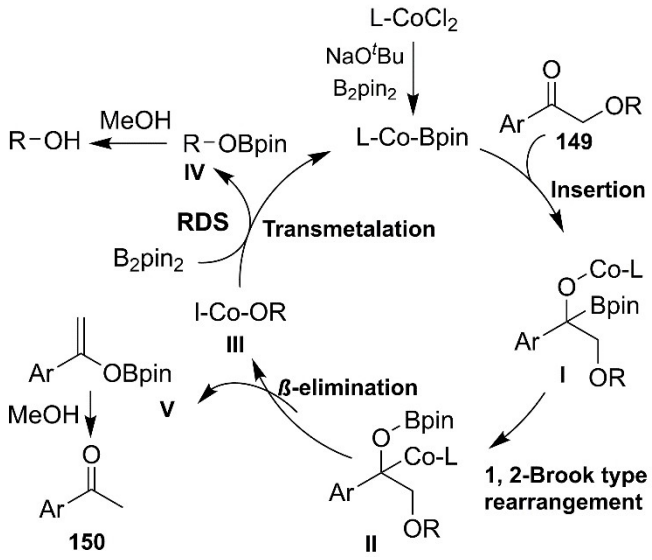

Scheme 95. Proposed mechanism of reductive C–O bond cleavage of lignin β-O-4 ketone.

and proton takes place between Mn–H and N–H. As a result, the formation of imine **45** and complex **II** would occur. The catalyst was regenerated by the addition of molecular hydrogen, and in the further cycle of the mechanism, the imine **45** was converted into amine **141**.

Rueping *et al.*[71] have successfully introduced the very first, catalytic hydrogenation of carbonates and polycarbonates into alcohols under mild conditions by employing the base-metal catalysis approach. To investigate the methodology, a precise

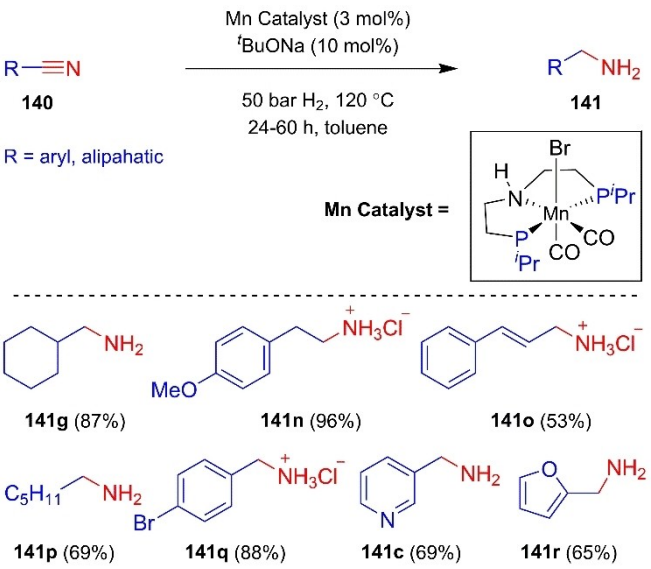

Scheme 96. Hydrogenation of various nitriles.

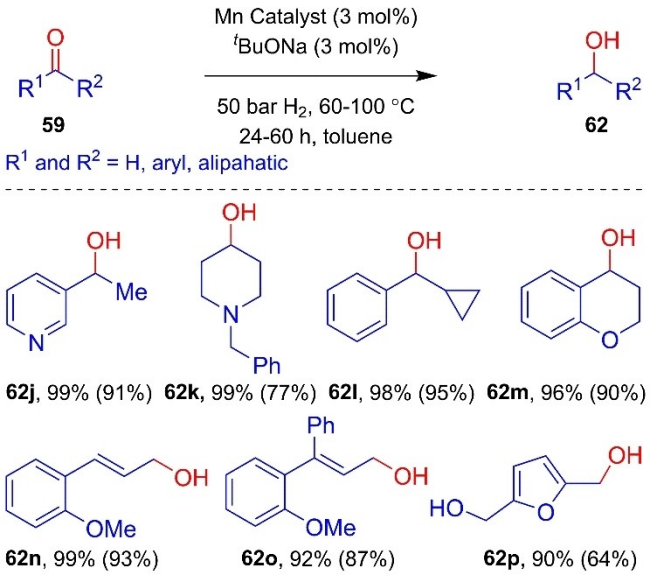

Scheme 97. Catalytic hydrogenation of aldehydes and ketones.

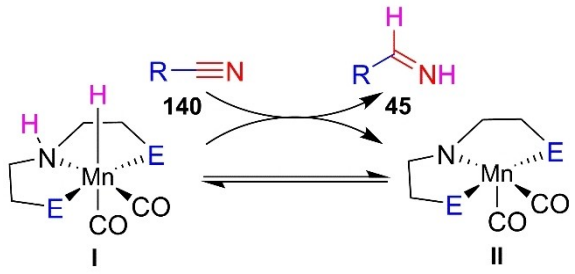

Scheme 98. Proposed outer sphere mechanism.

Mn-pincer complex has been synthesized and investigated with a very small loading of catalyst and base to establish the

reaction conditions. Upon applying the optimized conditions to various carbonates and polycarbonates, they have been converted into the corresponding diols and methanols (Scheme 99).

The reaction mechanism has been proposed in three catalytic cycles; among which the first cycle involves the hydrogenation of **151a** into **153**, the second involves the hydrogenation of **153** into **152a** and formaldehyde; and the third cycle involves the hydrogenation of formaldehyde into methanol. The catalytic cycle **1** was initiated by the addition of H_2 with Mn-complex *via* a non-spontaneous process to provide (Mn-H_2) complex **I**. Thereafter, upon hydride transfer *via* species **II**, the species **III** was obtained. Again, in the presence of excess methanol which was produced in the reaction mixture, the metathesis of **III** occurs and species **IV** is produced. The species **V** was then directed by the addition of an H_2 molecule, prompt rehydration of active spots of manganese, and proton transfer to metholates leading to the regeneration of MeOH and Mn-H_2 species. Following the similar steps in cycles **2** and **3**, the final products **152a** and MeOH can be delivered (Scheme 100).

Balaraman *et al.* have reported the utilization of a base/metal catalysis hydrogen borrowing approach for the selective C_3-alkylation of oxindoles **154** using secondary alcohols **155** as an alkylating reagent to produce various 2-oxindole derivatives **156** in excellent yields by developing a manganese(II) complex in the presence of catalytic ^{t}BuOK and THF as solvent (Scheme 101).[72] The reaction was not effective in the absence of either Mn(II) catalyst or co-catalyst ^{t}BuOK.

Based on several controlled experiments, the reaction mechanism was postulated, and according to the proposal, the dehydrogenation of secondary alcohols through the catalytic

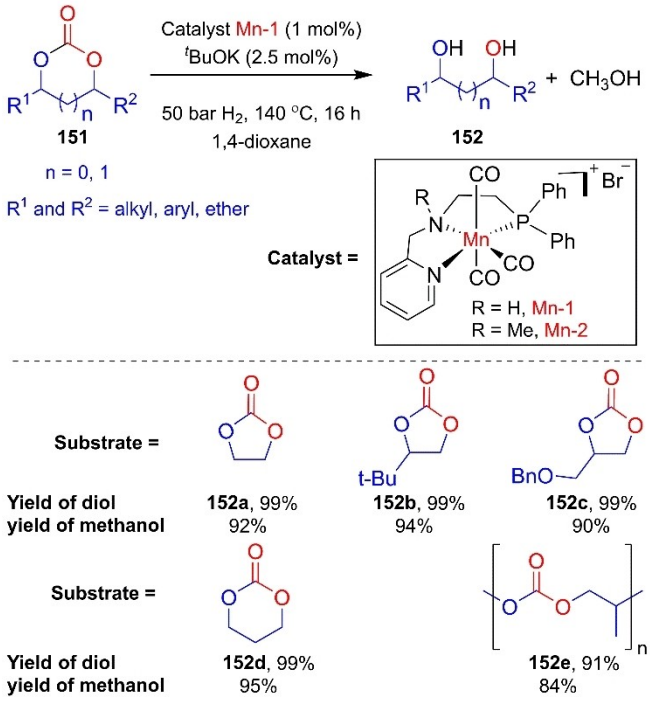

Scheme 99. Mn-Catalyzed hydrogenation of ethylene carbonates.

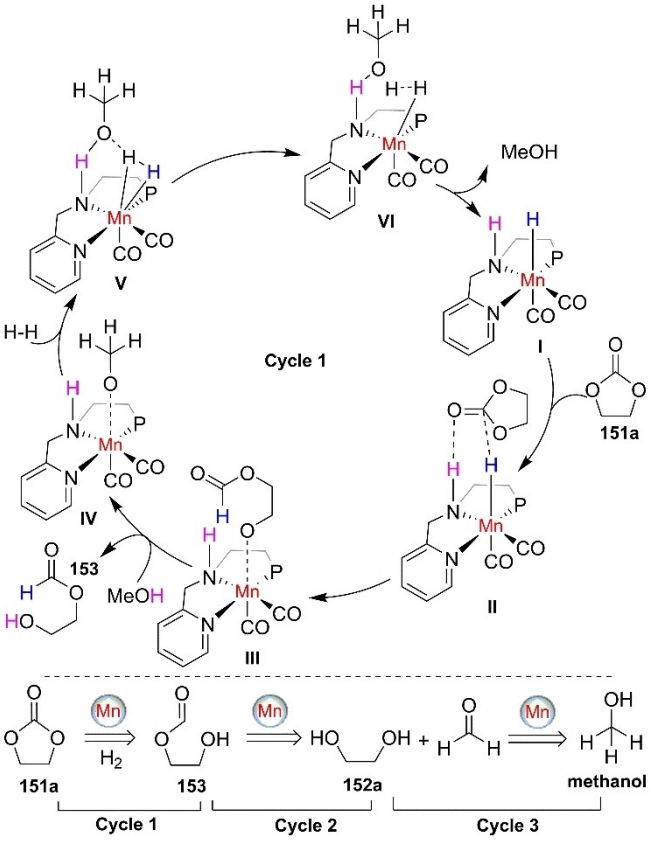

Scheme 100. Proposed mechanism for hydrogenation of ethylene carbonates.

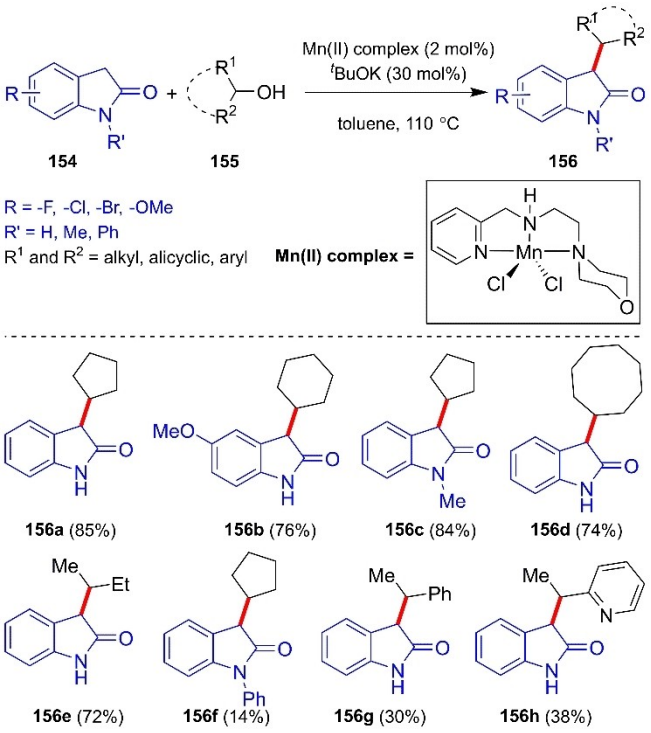

Scheme 101. C_3-Alkylation of oxindoles.

cycle occurs to produce compound **V**, and then condensation of **V** and **154** gives the condensation product **VI**. On catalytic hydrogenation of **VI** final product **156** was formed (Scheme 102).

Kempe *et al.*[73] in 2019 reported the hydrogenation of substituted imines using an Mn-based catalytic system in the presence of potassium *tert*-butoxide in a catalytic amount. This catalyst system can tolerate a variety of functional groups including the hydrogenation of olefins, nitriles, ketones, nitro groups, iodoarenes, benzyl ethers, etc. The X-ray findings suggested that the K–Mn bimetallic species was the main catalyst for hydrogenation. Consecutive two times deprotonations are required from the ligands, and large amounts of base do not accelerate the rate of this transformation. From the NMR studies, the reaction kinetics were observed to be first order with respect to imine, K–Mn-bimetallic moiety, and independent of potassium *tert*-butoxide concentration. The experimental studies, including the Hammett study, were performed to conclude that the hydrogenation step goes *via* the outer sphere mechanism, and proton transfer was not seen to be a part of the rate-determining step. The hydrogenation reaction of aldimines and ketimines occurs in the presence of a K–Mn bimetallic complex as a major catalyst, which was prepared from $[Mn–H]H_2$ and 2 equivalents of potassium *tert*-butoxide has been found to be very chemoselective. The proposed catalytic cycle was based on the NMR studies. This synthetic transformation only requires 4 mol% of potassium *tert*-butoxide as co-catalyst loading, and gram-scale synthesis has been achieved successfully (Scheme 103).

Scheme 104 represents the catalytic cycle for the hydrogenation of imines. It is assumed that the complex $[Mn–H]H_2$ is first activated in the presence of potassium *tert*-butoxide and produces $[Mn–H]K_2$ by reacting with H_2 and potassium *tert*-butoxide. Amine **146** and [Mn]K are produced when hydride

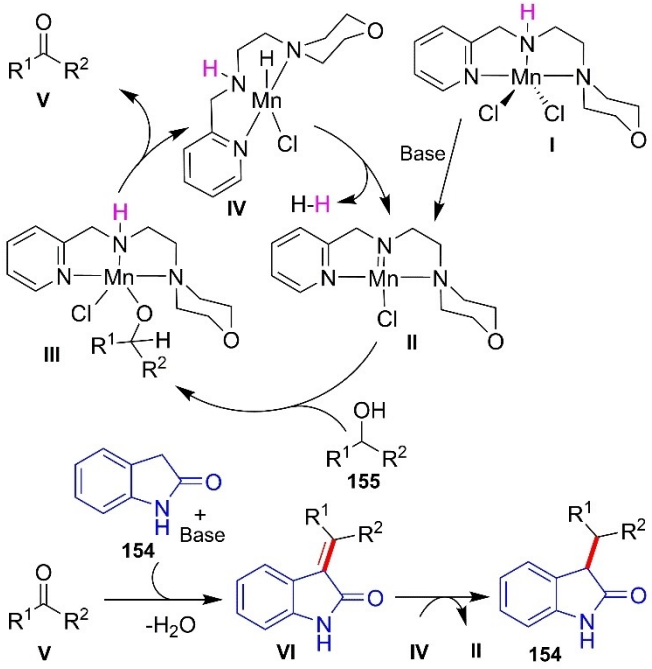

Scheme 102. Plausible mechanism for C_3-alkylation.

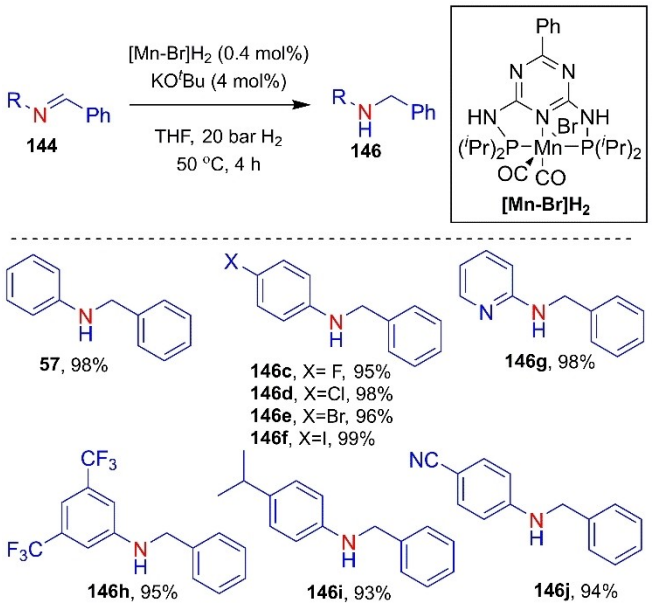

Scheme 103. Substrate scope for hydrogenation of imines.

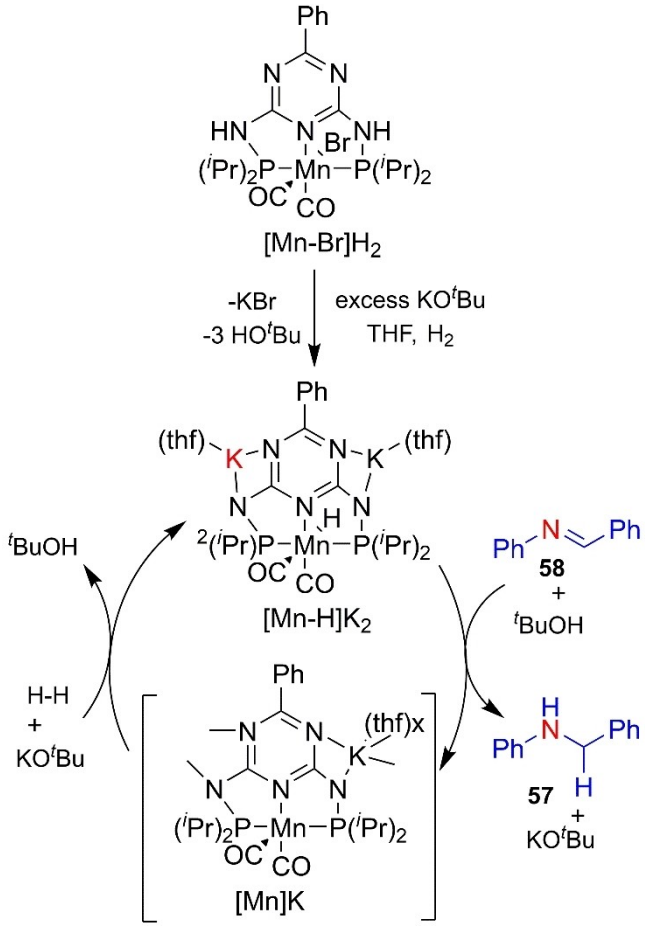

Scheme 104. Proposed reaction mechanism for the hydrogenation of imines.

transfer occured from [Mn–H]K_2 to imine **144** in the presence of *tert*-butanol and potassium *tert*-butoxide is reproduced. The complex [Mn]K further reacts with potassium *tert*-butoxide and H_2 to reproduce complex [Mn–H]K_2 and 1 equivalent of *tert*-butanol which closes the catalytic cycle.

3.5. Utilization with nickel-complexes as catalysts

Buslov and co-workers have demonstrated a silylation reaction of alkenes **138**, catalyzed by a nickel complex using sodium *tert*-butoxide in catalytic amounts as a co-catalyst.[74] The reaction conditions worked well only with catalytic NaO^{t}Bu, which was proven by performing a reaction with the 1.0 equivalent of NaO^{t}Bu. No product was observed for the reaction, while using 5–10 mol% of NaO^{t}Bu with a nickel catalyst. These were considered the ideal conditions for the reaction. These results were similar, when NaO^{t}Bu was replaced by KO^{t}Bu. The reaction conditions were applied for the number of substrates and resulted in good yields by using Me_2(OMe)SiH with various terminal alkenes (Scheme 105).

In the proposed mechanism, NaO^{t}Bu initiated the disproportionation reaction. Initially, the reaction starts with a nucleophilic attack of the anion ($^-$O^{t}Bu) on **2** generating a pentacoordinated species **I** and that reacts with compound **2** to form hydrosilane compounds **2 g** and **2 f** with the regeneration of NaO^{t}Bu (Scheme 106) and then, by applying nickel pincer complex with **2** and **2 g** alkylhydrosilane **157** was obtained.

Zhang *et al.*[75] in 2021 reported the hydrosilylation of terminal alkenes using the $NiCl_2 \cdot 6H_2O$ catalyst system in the presence of potassium *tert*-butoxide as an activator in catalytic amounts and primary silanes as a silylating agent. The secondary and tertiary silanes are found to not be suitable for the reported transformation. The mild reaction conditions, large substrate scopes, and favorable turnover numbers are the important features of this reported transformation. The experimental studies revealed that this anti-Markovnikov selective transformation occurs *via* an electrophilically active Si–H bond and does not generate metal hydrides (Scheme 107).

Scheme 108, represents the proposed reaction mechanism for the electrophilically activated hydrosilylation of terminal alkenes. The catalytic cycle starts with the reduction of Ni(II) to Ni(0) in the presence of primary silane **2 h**. In the presence of potassium *tert*-butoxide as an activator, the silane forms a pentacoordinated complex. In step **I**, which is basically the rate-determining step, the Si–H bond of pentacoordinate complex displaces the solvent molecule to form active Ni(0)-complex **B** *via* the electrophilic activation of the Si–H bond. In step **II**, the electrophilic attack from the Si–H bond to alkene *via* intermolecular or intramolecular pathway happens, which completes the addition reaction. In step **III**, activator and secondary silane products **158** are generated.

Obata and co-workers[76] contributed an innovative work, which was published in 2017 indicating the use of nickel complex as a catalyst in the presence of potassium *tert*-

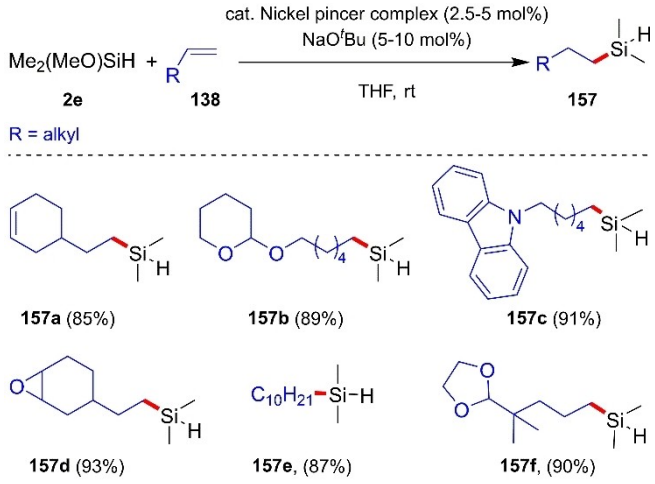

Scheme 105. Hydrosilylation of alkenes using sodium *tert*-butoxide as a co-catalyst.

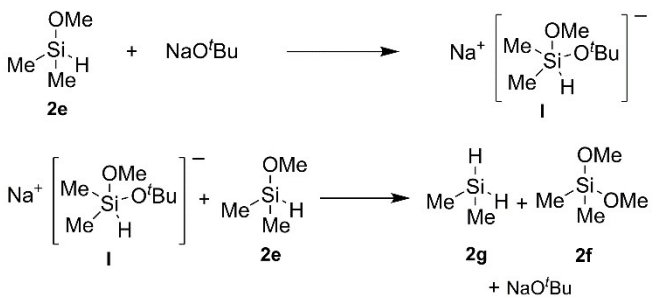

Scheme 106. Mechanism of hydrosilylation initiated by NaO^{t}Bu.

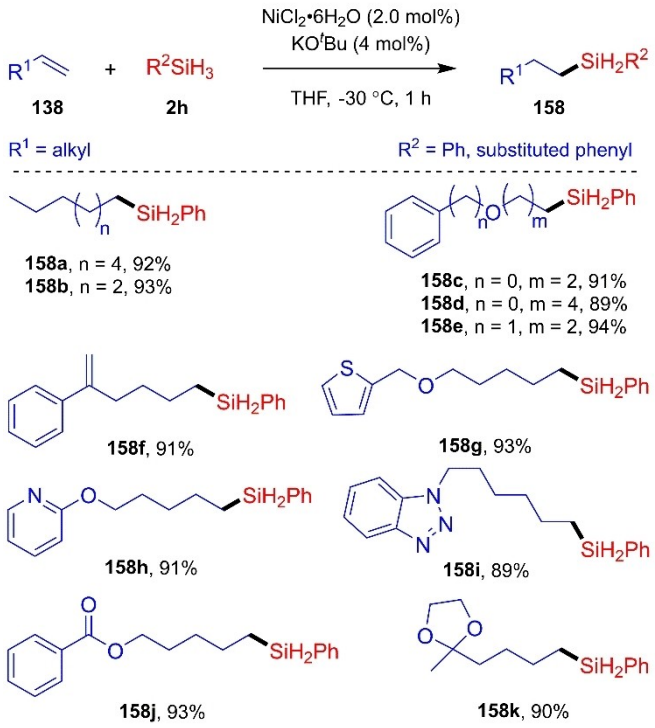

Scheme 107. Substrate scope for terminal alkene hydrosilylation.

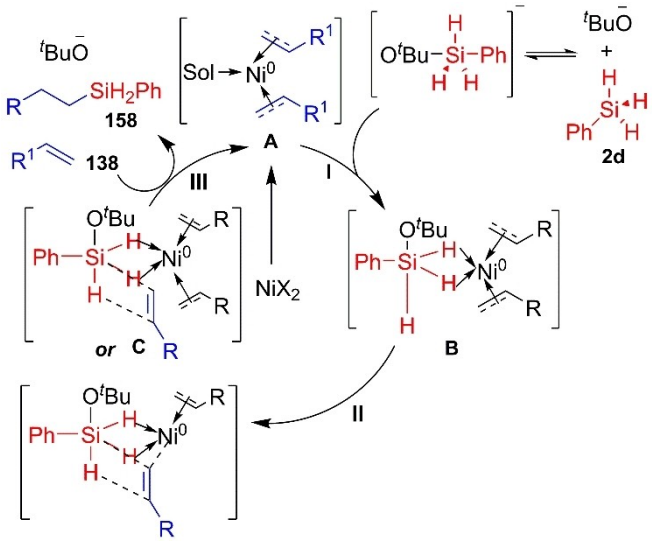

Scheme 108. Proposed mechanism for the hydrosilylation of terminal alkenes.

butoxide in catalytic amounts for selective C–H activation starting from aromatic moieties and alkynes. The interesting fact is that many 3d-metal catalysts (Pd, Rh, Ir based) are present for the same purpose, but the use of nickel is cost-effective and the complexes are readily available. Recently, the same group shared a report with nickel catalyst [Ni(0), Ni(II)], but the limitation of this method was that only a few aromatic moieties possessing directing groups showed considerable conversion. The use of potassium *tert*-butoxide, high substrate scope, functional group tolerance, and regioselectivity are noteworthy to mention for this method. The use of potassium *tert*-butoxide facilitates the formation of nickel-nitrogen bonds for the C–H activation process (Scheme 109).

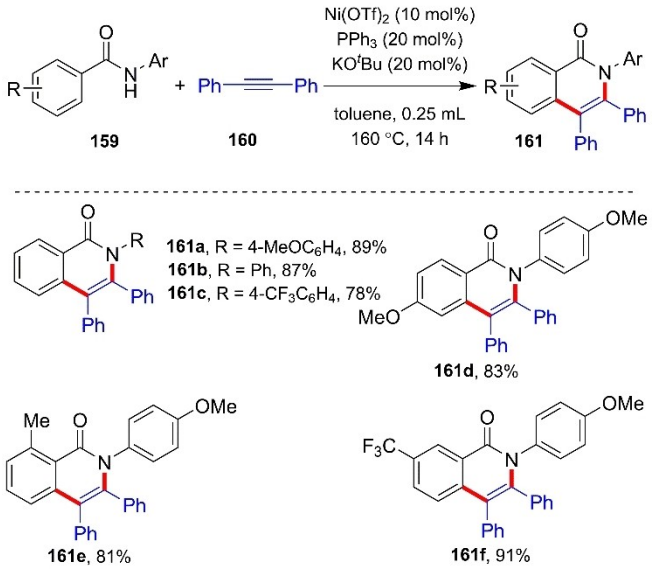

Scheme 109. Nickel catalyzed annulation of aromatic amides with alkynes.

In the main catalytic cycle (Scheme 113), where the Ni(0) is the main catalytic moiety that initiates the reaction. The amidate anion **159′** in the presence of Ni(0) gives complex **I**, which undergoes an oxidative addition reaction to generate the nickel-hydride species **II**. The complex **IV** is generated after successive insertions of an alkyne into H–Ni and C–Ni bonds. Afterwards, the reductive elimination and protonation by *tert*-butanol generate the isoquinolinone **161** with the regeneration of Ni(0) and potassium tert-butoxide with the formation of an alkene (Scheme 110).

In Scheme 111, the potassium *tert*-butoxide captures a proton from amide to generate the amidate anion **159′**, which in the presence of Ni(II) forms complex **I**. The breaking of *ortho* C–H bonds produces complex **II**, which undergoes an insertion reaction with an alkyne into an N–Ni bond, followed by the reductive elimination reaction to generate complex **IV** and regenerate Ni(0).

Obata and co-workers[77] in 2019 reported the development of a new catalytic system based on nickel catalyst for the first time, which can perform C–H activation and N–H annulation in *N*-heteroarene moieties without the use of noble transition metal as a catalytic system. The interesting fact in this case is that there is no need of *N*,*N*′-bidentate directing group for the successful transformation, which was reported by this group in 2011, rather an earth-abundant cost-friendly potassium *tert*-butoxide has been found to play a crucial role in the reaction mechanism, albeit in catalytic amounts. Experimental studies supported by DFT calculations have been pivotal in proposing two pathways for the above-said transformation. One pathway requires a Ni(II) system in presence of a catalytic amount of potassium *tert*-butoxide; whereas, the second pathway utilizes a

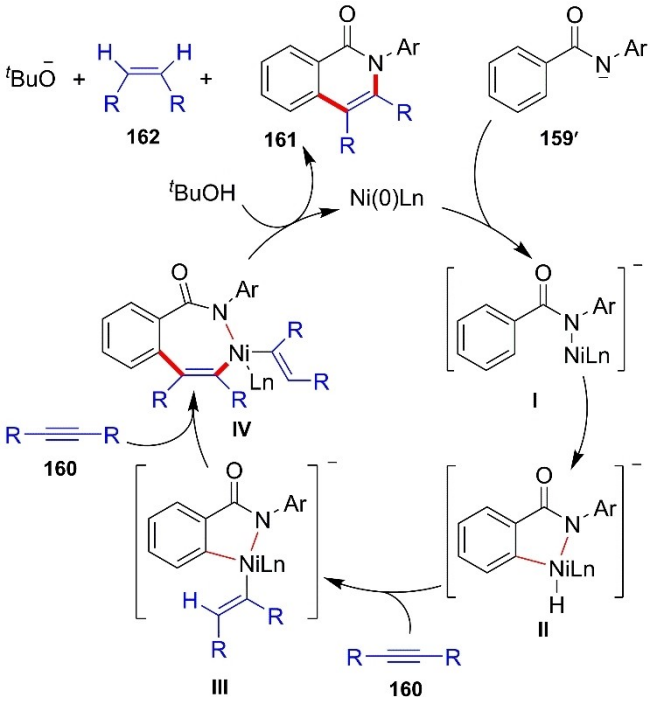

Scheme 110. Proposed mechanism *via* path A.

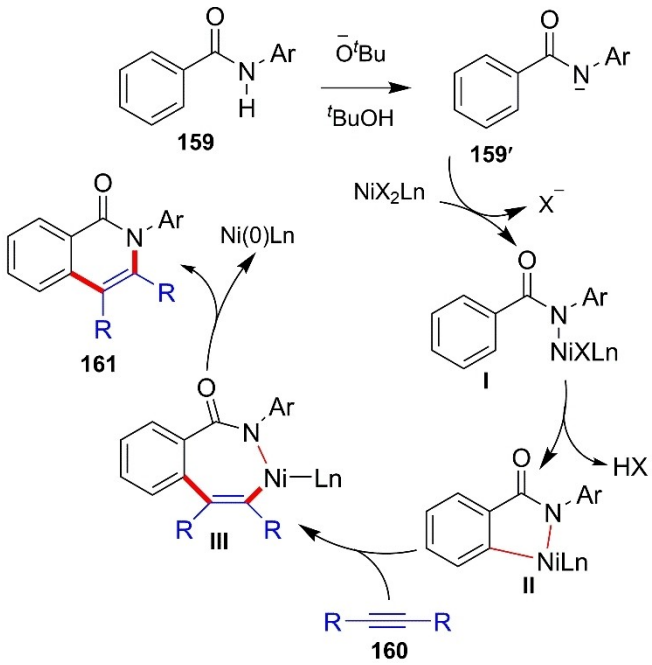

Scheme 111. Proposed mechanism *via* path B.

Ni(0) system in the absence of any co-catalyst, and the transformation proceeds successfully. The Ni(0) catalytic system in the absence of a base has been found to be the major catalytic system for this transformation, which has a vital role in the pharmaceutical industry as most of the drugs contain *N*-heteroaromatic scaffolds. High functional group tolerance has been observed (Scheme 112). The major catalytic cycle has been found to proceed through the ligand-to-ligand hydrogen transfer mechanism.

Scheme 113 represents the proposed reaction mechanism of C–H/N–H annulation of *N*-heteroaromatic arenes where potassium *tert* butoxide abstracts protons from **163 a** to generate **163′a**, which in the presence of Ni(II) produces complex **I**. Complex **III** was generated when the *ortho* C–H bond brokes, followed by the insertion of an alkyne into a C–Ni bond in complex **II**. Then, reductive elimination generates product **164** and Ni(0) species. It is noteworthy to mention that here Ni(0) does not undergo oxidation to Ni(II), rather initiates another catalytic cycle. In the presence of Ni(0) the sp^2 N-atom of **163 a** gives complex **IV**, which further produces complex **V** *via* the ligand-to-ligand hydrogen transfer mechanism, where the *ortho* hydrogen atom is directly transferred to alkyne carbon. The generation of complex **VI** happens by successive insertions of an alkyne into C–Ni bonds. The compound **164** was generated after reductive elimination followed by deprotonation, which also regenerates Ni(0) and alkene.

Very recently, Panigrahi and co-workers[78] have developed diphosphine-phosphonite as well as triphosphine-phosphite ligands having tridentate and tetra-dentate capacities respectively, and their corresponding complexes built upon 3d metal Nickel (II) core. The structure and flexibility of the complexes bearing the above-mentioned ligands have been determined by single-crystal XRD. It is noteworthy to mention that the 2.5 mol% of Ni(II) complexes with the phosphonite ligand $PhP(OCH_2PPh_2)_2$ have been found promising in *N*- alkylation reaction of primary aryl amines **165** (0.5 mmol), 4-methoxy benzyl alcohols **65** (1 mmol) with the catalytic presence of potassium *tert*-butoxide (0.4 mmol). The substrate scopes include challenging environments and the carbon-nitrogen coupled products were isolated in good yield in Scheme 114.

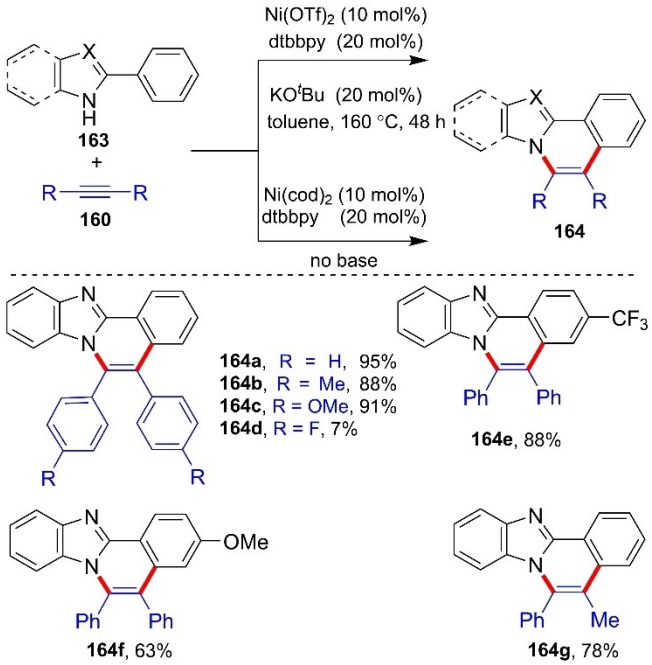

Scheme 112. Ni-Catalysed C–H/N–H annulation of *N*-heteroaromatic arenes.

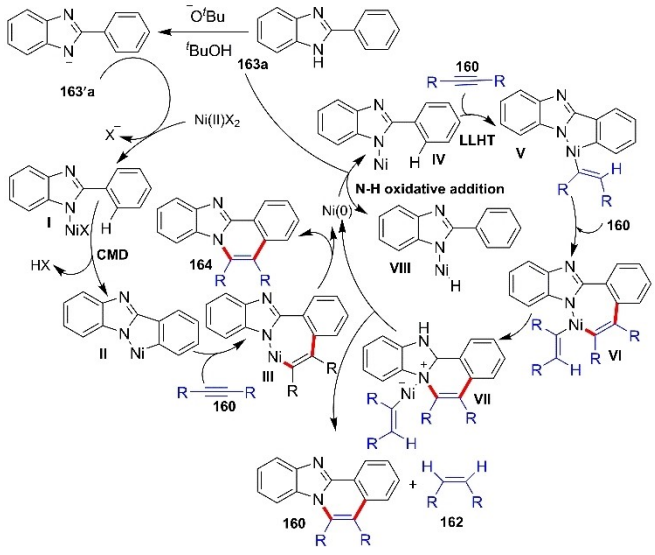

Scheme 113. Proposed mechanism for Ni-catalysed C–H/N–H annulation of *N*-heteroaromatic arenes.

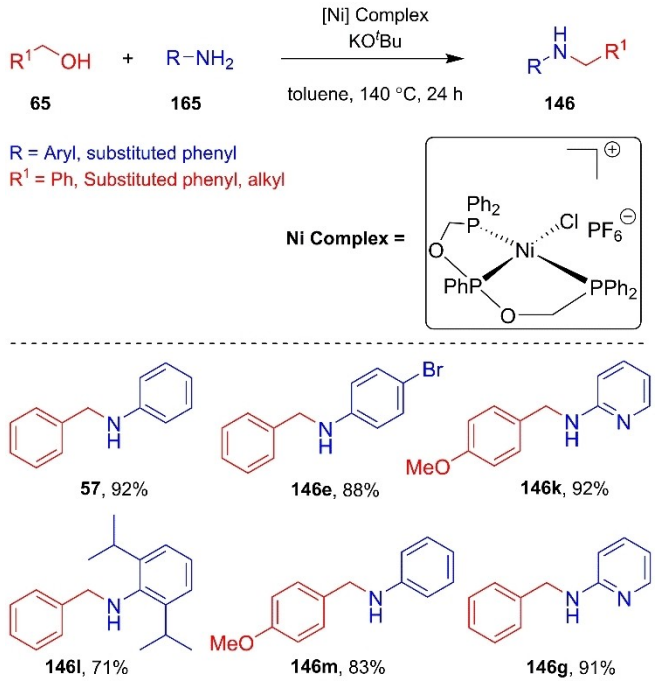

Scheme 114. Substrate scope for *N*-alkylation reaction.

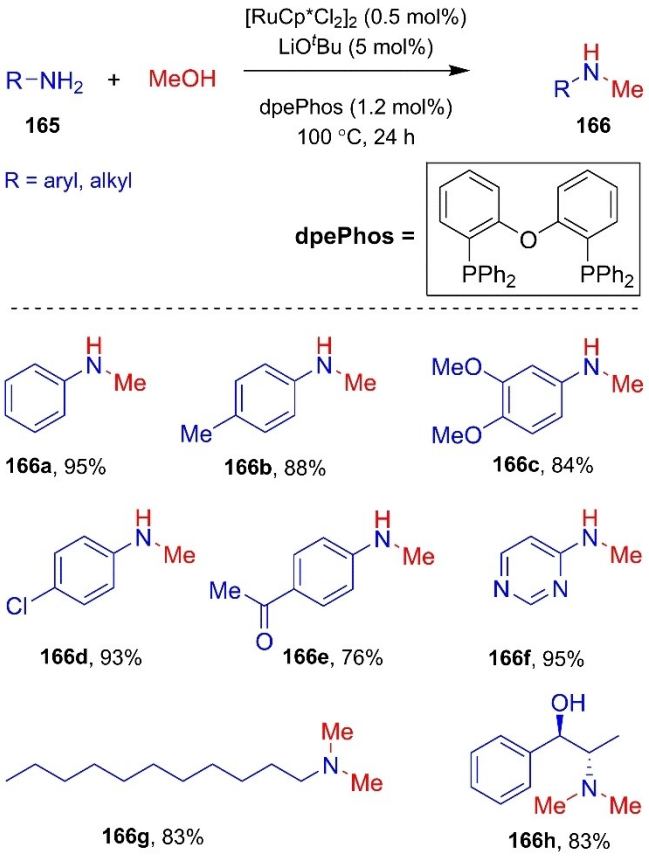

Scheme 115. *N*-methylation of amines.

3.6. Utilisation with ruthenium-complexes as catalysts

A ruthenium-catalyzed hydrogen borrowing approach was reported by Seayad *et al.* for selective *N*-methylation and dimethylation of primary amines **165**.[79] The strategy proceeds through *in situ* production of a ruthenium complex from [RuCp*Cl$_2$]$_2$ and ligand dpePhos in the presence of catalytic lithium-*tert*-butoxides and MeOH as a methylation reagent. The potential of this method was expressed by developing the substrate scope and applying the reaction conditions to a diversity of primary amines. The reaction conditions can tolerate a series of both electron-rich and electron-poor functional groups (Scheme 115).

The reaction mechanism has been proposed based on experimental results and literature reports. According to the mechanism, the reaction might be initiated with the formation of active catalyst **II** *via* ruthenium complex **I**, which was produced *in situ*. Thereafter, upon the β-hydride abstraction, complex **III** was formed with formaldehyde. Next, the catalytic cycle is undergone upon insertion of imine that generates complex **IV**, and finally the hydrogen transfer may take place with the formation of compound **166** in the presence of methanol (Scheme 116).

In another, the ruthenium-catalyzed *N*-methylation approach is witnessed by the *N*-alkylation of aromatic amines (Scheme 117) by applying a catalytic amounts of KO^{t}Bu as a co-catalyst.[80] To better understand this transformation, the authors performed the isotope-labeling experiments and it was revealed that the formation of *N*-methylaniline-d_3 took place in the presence of CD_3OD. The examination of the reaction was carried out by considering aniline as a standard substrate with methanol, using various ruthenium catalysts and a catalytic amount of co-catalyst to obtain the exact methylated products over the dehydrogenating coupling products.

Using the optimized conditions, various scopes of substrates has been developed; methylated products **166 b** and **166 i** having *o/p*- methyl substituted anilines were produced with excellent yield, while on the contrary sterically crowded **166 j** was obtained with 13% yield. The compounds with halogen substituents at *para* position **166 k**, **166 d**, and **166 l** were also obtained with 97%, 86%, and 97% yields respectively. It has been mentioned that for mono-methylation of 3-aminopyridine 60 mol% of KO^{t}Bu was required; whereas, for 2-aminopyridine 100 mol% of KO^{t}Bu was required. It was also investigated that at low loadings of ruthenium catalyst, more amounts of KO^{t}Bu is needed to complete the reaction, and when the amount of catalyst loading is reduced, yield is also decreased. It was also found that at 0.005 mol% catalyst loading, the yield was reduced to 80% and at 0.002 mol% the yield changed to 43%.

Saito *et al.* have demonstrated the synthesis of multi-substituted pyrrole derivatives **169** from *in situ* generated α-amino aldehydes by considering ruthenium catalysts in the presence of catalytic KO^{t}Bu as catalyst systems.[81] For preliminary investigation, the authors have performed the reaction by considering valinol **167 a** and propiophenone **168 a** as starting model substrates in a (1:2 molar) ratio in the presence of ruthenium catalyst (1 mol%) and KO^{t}Bu (10 mol%) to obtain the desired product **169 a** in 77% yields (Scheme 118).

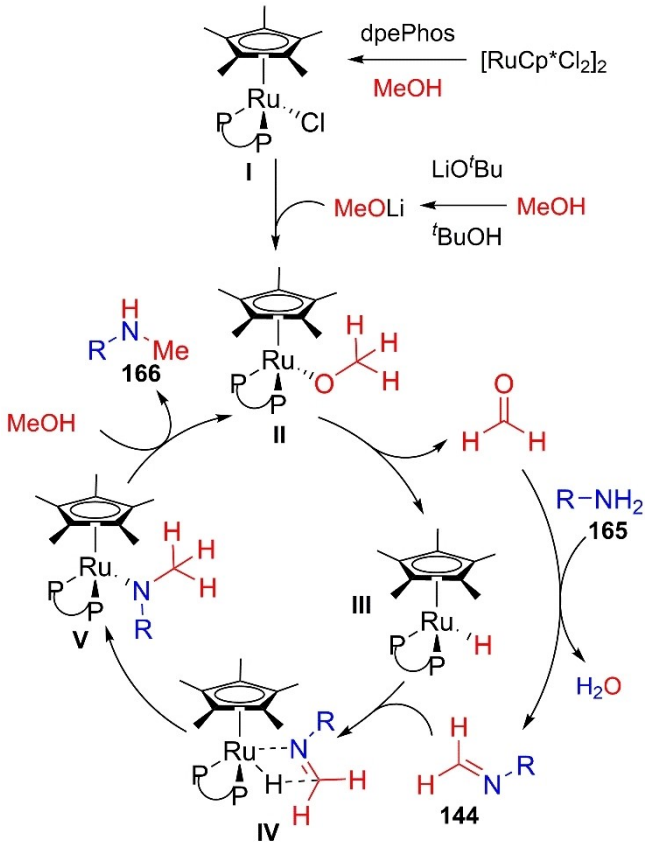

Scheme 116. Proposed mechanism for *N*-methylation of primary amines.

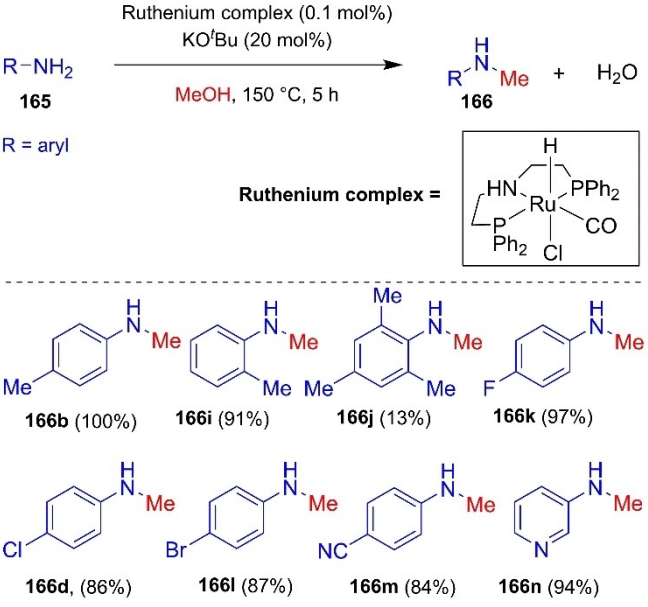

Scheme 117. *N*-monomethylation of aromatic amine.

To illustrate the possible pathways of reaction, several controlled experiments were conducted and it was proven that path **3** is the more suitable reaction path. According to the mechanistic path for **169**, the intermediate **III** which was formed

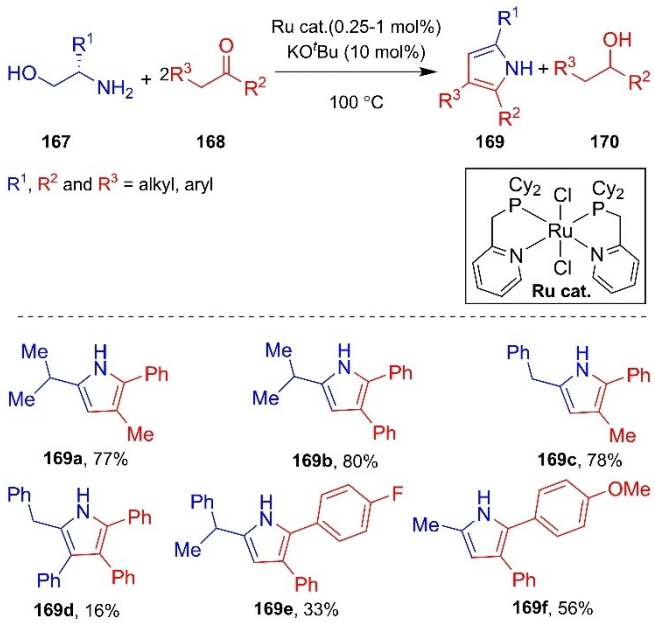

Scheme 118. Synthesis of substituted pyrroles.

via the dehydrogenation and nucleophilic addition process of **167 a** and **168 a**, underwent intramolecular condensation by the loss of water molecule to generate the intermediate **IV**, which again lost water molecule to form the intermediate species **V**. As a result of the rearrangement of intermediate **V**, the final product **169 a** was formed (Scheme 119).

Jiang *et al.*[82] have reported an easy and straightforward synthesis of various substituted quinazoline derivatives **172** (Scheme 120) from 2-aminobenzyl alcohols **171** and various nitriles **140** by the utilization of the ruthenium/ligand/KO^{t}Bu catalytic system. In this methodology, various ruthenium catalysts and ligands were investigated to establish the reaction conditions, and the obtained reaction conditions proceeded with good functional group tolerance over the substrates **171** and **140** in moderate to good yields.

A mechanistic strategy has been proposed for this approach, which may involve the nucleophilic addition of the

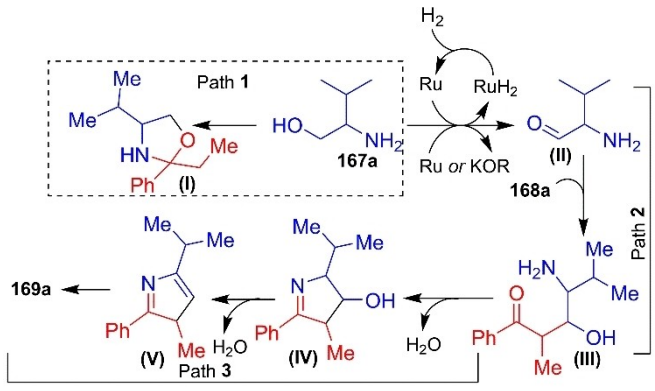

Scheme 119. Mechanistic path for the synthesis of pyrroles.

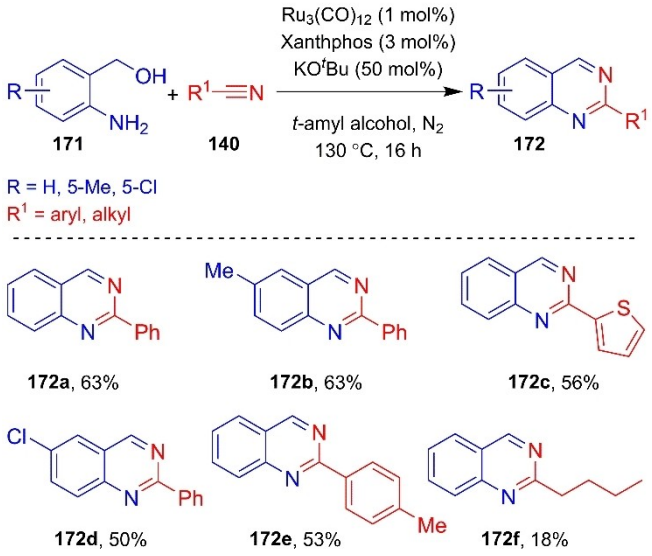

Scheme 120. Ruthenium catalyzed synthesis of substituted quinazolines derivatives.

amine group of compound **171** over nitrile **140** to generate intermediates **I** or **II**. After which, in the presence of a ruthenium catalyst intermediate **III** will be formed as a result of dehydrogenation of the alcohol group and then, through intramolecular condensation the final product **172** can be generated (Scheme 121).

Nakamura and co-workers have demonstrated the hydrogen borrowing strategy for the hydro-amination of allyl alcohols **173** by using a ruthenium/ligand/KO^{t}Bu catalytic system (Scheme 122).[83] A hypothetical mechanism has been provided (Scheme 123) in which the allyl alcohol undergoes an oxidation process through β-hydride elimination to provide conjugated ketone **122** and then hydro-amination can occur *via* 1,4-addition, which generates the intermediate **176** that can undergo hydrogenation in the presence of metal hydride species to obtain the final product **175**.

In 2016, Chianese *et al.*[84] contributed a Ruthenium-based CNN-Pincer complex (Scheme 124) having no methylene linker in between the pyridine and imidazole rings, which is a modified version of the Ru-based complex reported by Song *et al.* in 2011. This Ru-CNN-Pincer complex acts as a homogeneous catalyst. For ester hydrogenation and the reversible

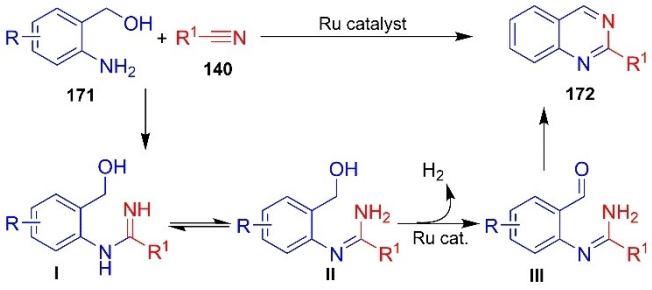

Scheme 121. Mechanistic strategy for the synthesis of quinazoline.

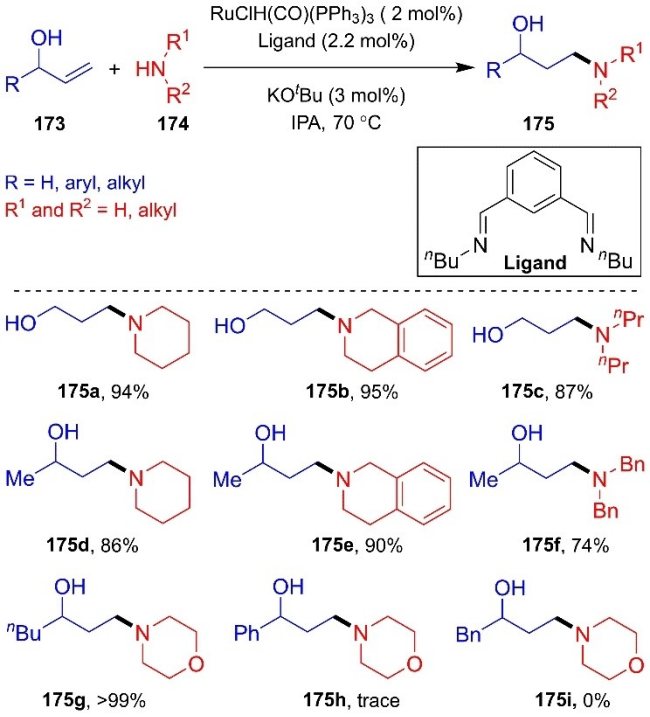

Scheme 122. Ruthenium catalyzed hydroamination of allyl.

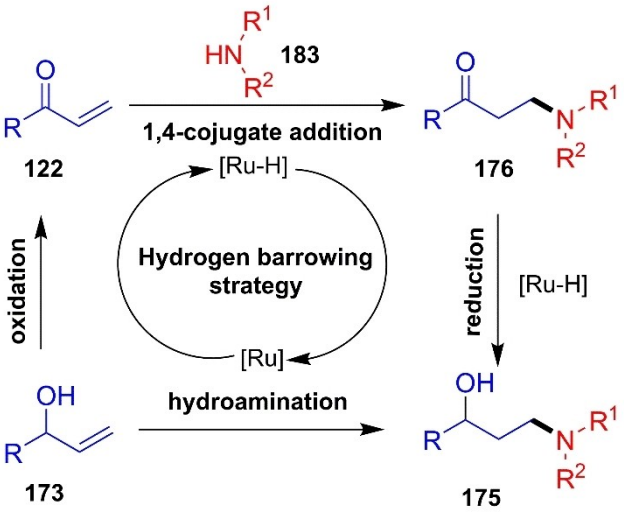

Scheme 123. Hypothetically proposed mechanism.

dehydrogenation process was described under milder reaction conditions (105 °C, 6 bar H_2 pressure) using sodium tertiary butoxide as a co-catalyst in the presence of the Ru-CNN complex. When NaO^{t}Bu was used in larger equivalents, more reproducible yields were observed. Diethylamino substituted ligand was seen to increase the catalytic activity of the catalyst to a very significant value (turnover number 420) compared to dimethylamino substituted ligand (turnover number 33) for the production of benzyl alcohol from ethyl benzoate at 6:1 ratio of NaO^{t}Bu to Ru-CNN-complex. The transformation was carried out at 105 °C temperature, 6 bar H_2 pressure in toluene as

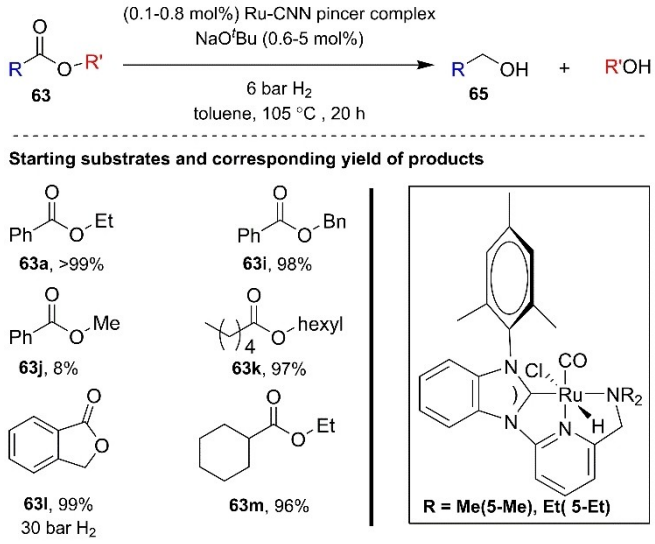

Scheme 124. Ester Hydrogenation using 5-Et catalyst.

solvent. For benzyl benzoate TON is up to 980 for the NEt_2 variant. The substrate scope for ester hydrogenation using this Ru-CNN complex system in presence of NaO^{t}Bu is high as expected, because it converts methyl ester to corresponding alcohol to a negligible extent. Also, the diethylamino ligand substituted Ru-CNN-Pincer complex was seen to be a promising catalyst for the reversible dehydrogenation process for primary alcohols.

Le and co-workers[85] in 2018, revealed the preparation of the CNN-pincer-ruthenium complex and applied it for the hydrogenation of esters to observe their activity using sodium tertiary butoxide in catalytic amounts as a co-catalyst under 6 bar H_2 pressure. To observe the catalytic activity of the CNN-pincer-ruthenium complex a variety of substrates were used (Scheme 125).

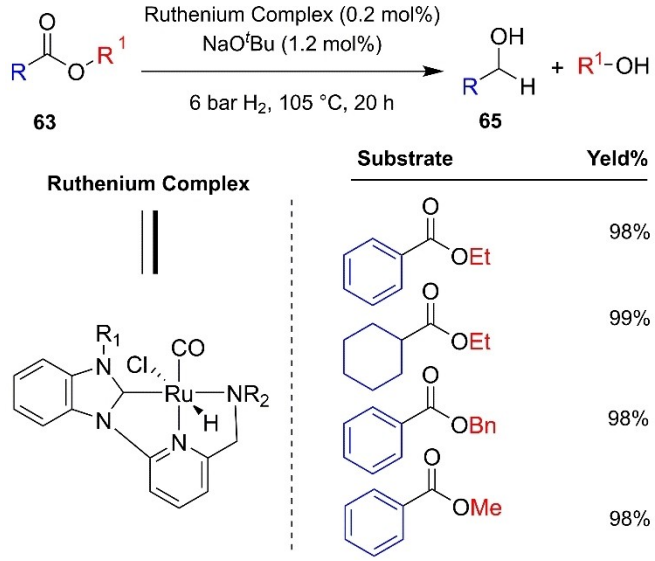

Scheme 125. Ester hydrogenation catalyzed by ruthenium complex.

Many experiments were performed to observe the activity of the complex. The experiments were started by changing the substitution on NHC substituents, and it was observed that the NHC substituents with more bulky groups, such as dipp showed more activity and for the smaller groups like mesityl substituents the activity was reduced. Thus, it was found that the catalytic system Ru-dipp-Et was the most active catalyst system for the hydrogenation of esters.

In 2020, Thiyagarajan and co-workers have developed a ruthenium-catalyzed α-alkylation of ketones (Scheme 126) applying a hydrogen-borrowing strategy *via* the C–N and C–C bond formation reactions.[86] Aromatic ketones were treated with secondary alcohols to provide the alkylated products of ketones in excellent yields. The potassium tertiary butoxide plays an important role in increasing the product yields of the reaction. While decreasing the amounts of KO^{t}Bu from 2 equiv. to 5 mol%, the product yield changes from 75% to 59%, and with 2 mol% of the co-catalyst, the yield is only 40%. An important observation was noticed that with NaO^{t}Bu the yield was almost similar, but there was no product formation with Cs_2CO_3.

The mechanistic investigation was done by using secondary alcohols. The plausible reaction mechanism illustrated in Scheme 127 indicates that in the presence of potassium *tert*-butoxide, the unsaturated intermediate **I** is formed from ruthenium catalyst, followed by the reaction of **I** with secondary alcohol **155** to generate intermediate **II**. In the next step, ruthenium dihydride intermediate **III** is formed due to the β-hydride elimination from **II** and ketone **59** is generated. This *in situ* generated ketone **59** undergoes a condensation reaction with aromatic ketone **130** under basic conditions to generate α,β-unsaturated **IV** which further gets hydrogenated by the

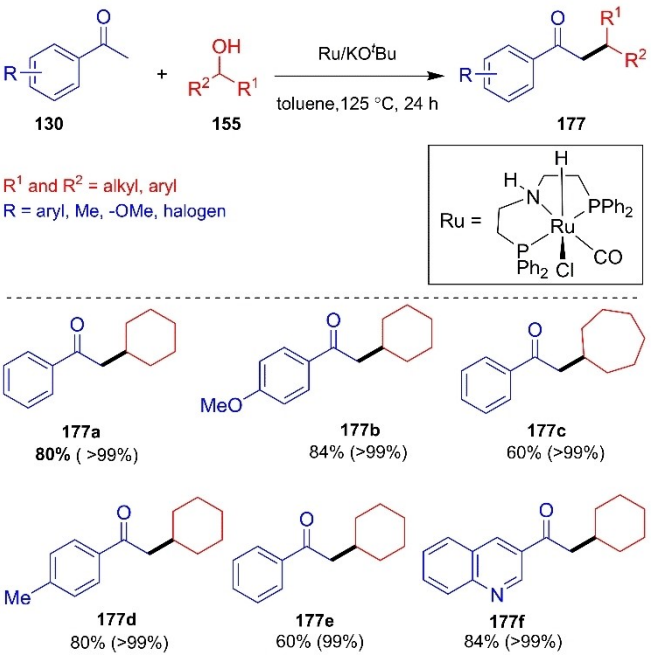

Scheme 126. α-Alkylation of ketones using secondary alcohols.

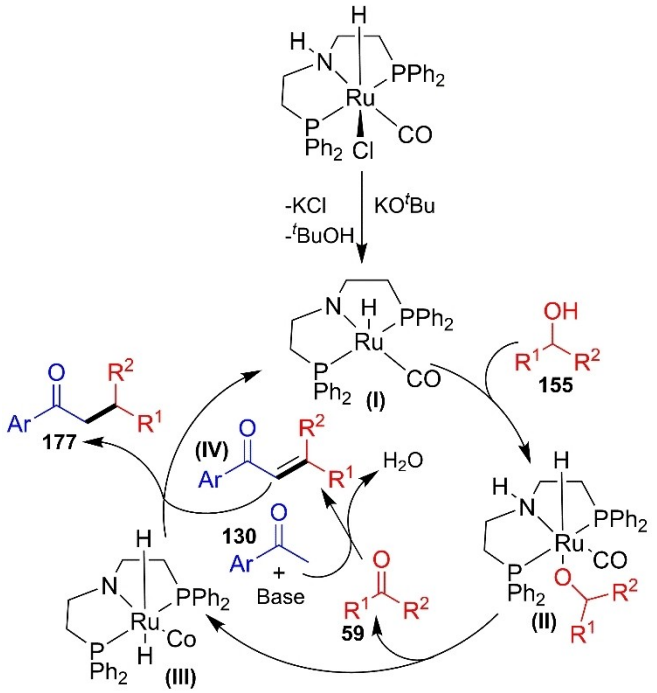

Scheme 127. Reaction mechanism for alkylation of ketones with secondary alcohols.

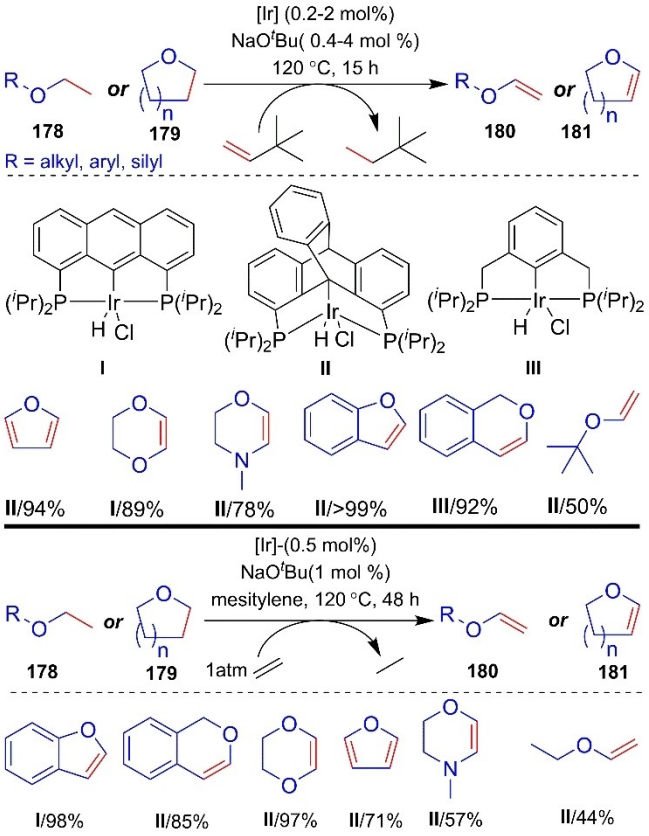

Scheme 128. Dehydrogenation of cyclic and acyclic ethers with TBE and ethylene as hydrogen acceptors.

intermediate **III** to regenerate active intermediate **I** and alkylated product **177**.

3.7. Utilization with rhodium and Iridium-complexes as catalysts

Brookhart *et al.*[87] in 2015, published an article introducing the concept of functionalized cyclic and acyclic ethers **178** or **179** dehydrogenations using diisopropyl substituted Ir-pincer complexes **I**, **II**, and **III** having anthrophos, triptycene moieties as catalysts in the presence of NaO^{t}Bu as co-catalyst to form useful alkenes. TBE (*tert*-butyl ethylene) was used as a hydrogen acceptor as well as ethylene which was reported for the first time. Using TBE, the turnover numbers was observed to reach 660, when **I** was used as a catalyst for the conversion of tetrahydrofuran to furan. Higher yield and turnover number (over 400 in most cases, for acyclic diethyl ether up to 90) were obtained for ethylene as a hydrogen acceptor in the presence of a catalyst **II**. The substrate scopes for cyclic and acyclic ethers were very good (Scheme 128).

Wang *et al.*[88] described a new method for transfer hydrogenation of alkenes **132** using ethanol as a hydrogen source catalyzed by a NCP pincer iridium complex. The authors demonstrated the efficiency of the catalyst system in reducing a wide variety of alkenes including both symmetrical and unsymmetrical compounds. They have also provided a detailed insight into the mechanism of the reaction, including the role of the NCP pincer complex in promoting the transfer of hydrogen from ethanol to the alkene substrate. One of the key findings of the study is the high efficiency of the NCP pincer iridium complex as a catalyst for the transfer hydrogenation of alkenes using ethanol. The authors described that the complex can catalyze the reaction at low temperatures and pressures with high selectivity for the desired products (Scheme 129).

The reaction mechanism for the transfer hydrogenation reaction in the presence of an iridium catalyst is mentioned in Scheme 130. At first the precatalyst **G** reacts with sodium *tert*-butoxide to form the 14-electron moiety [Ir], which upon reaction with EtOH generates **C** *via* oxidative addition. The intermediate **C** is proposed to bind with **B** in the presence of two molecules of EtOH and **B** is a resting state. In the rate-determining step, **C** generates **D** *via* β-hydride elimination with the formation of CH_3CHO which is converted into hemiacetal in the presence of EtOH and thereafter generates ethyl acetate by dehydrogenation. The coordination of dihydride complex **D** with alkene moiety **132** generates **E** followed by hydride migratory insertion to form **F**. Reductive elimination of **F** generates hydrogenated product **182** and [Ir] is regenerated.

Tang and co-workers[89] in 2018, introduced a dual-catalyst system consisting of pincer ligated iridium complexes (^{i}Pr-substituted phosphinothious-phosphinite iridium complexes) [(PSCOP)IrHCl] responsible for transfer dehydrogenation of normal alkane to form internal olefins using tertiary butylethylene (TBE) as a hydrogen acceptor in the presence of NaO^{t}Bu followed by the olefin isomerization-hydroformylation

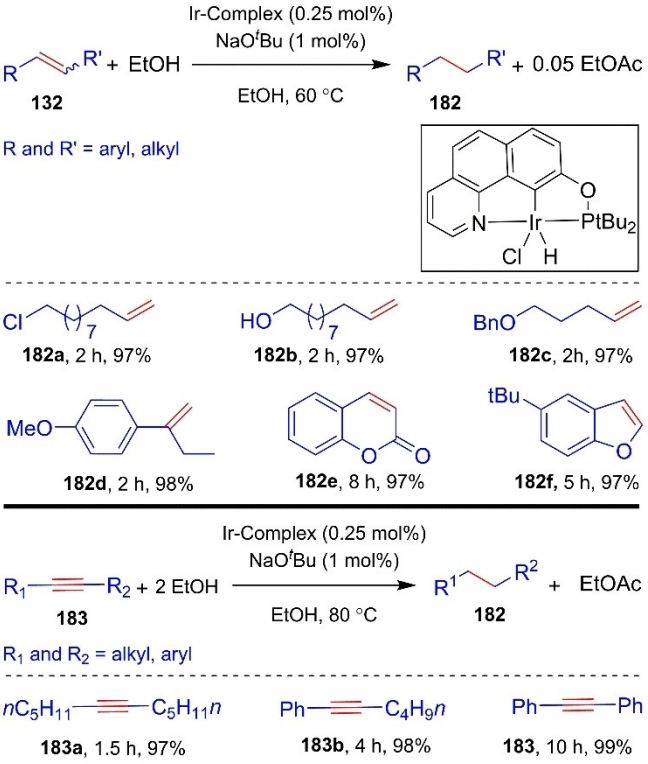

Scheme 129. Ir-Catalyzed transfer hydrogenation of alkenes and alkynes.

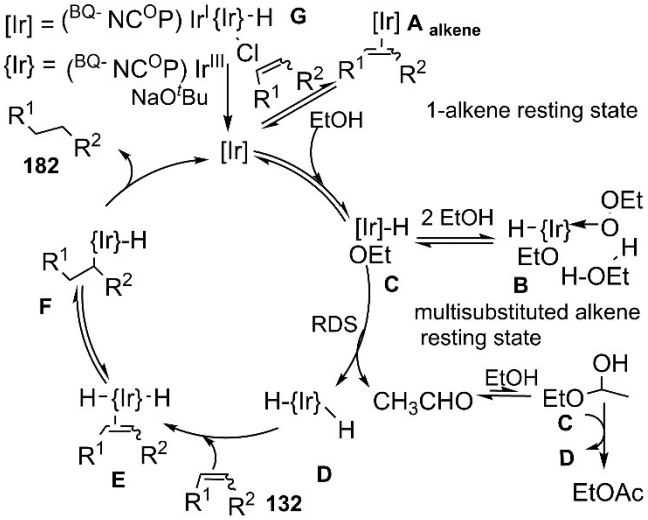

Scheme 130. Proposed reaction mechanism for transfer.

with a combination of rhodium catalyst [Rh(acac)CO5] and Co/H_2. This catalyst system has shown higher regioselectivity for *n*-alkane to *n*-aldehyde formation and a high turnover number (TON) in the presence of ethylene. In addition to this, the Ir/Rh catalyst has been found to effectively form linear alkyl amines from *n*-alkanes with very good regioselectivity (Schemes 131 and 132).

A consecutive alkane silylation by an Ir/Fe catalyst followed by alkane carbonylation using Ir/Rh catalyst has been effective

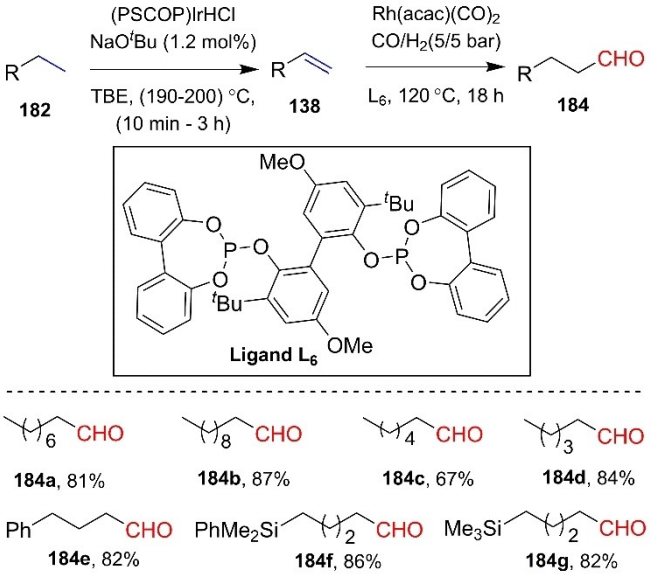

Scheme 131. Catalytic dehydrogenation and olefin-isomerization-hydroformylation of various alkanes.

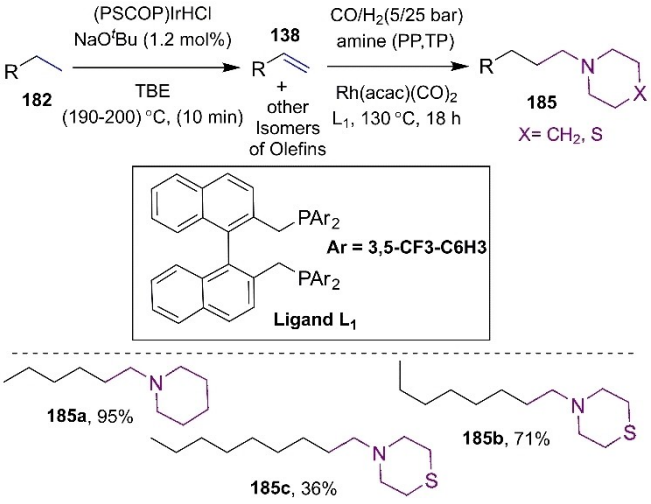

Scheme 132. Catalytic aminomethylation of alkanes and substrate scope.

in producing siloxy-terminated alkyl aldehydes from *n*-pentane Catalytic dehydrogenation and olefin-isomerization-hydroformylation of various alkanes.and *n*-hexane, which is a crucial precursor for silicone surfactants. This process is advantageous as it directly converts low-value, highly accessible, and diverse *n*-alkanes to industrially important linear aldehydes and amines in a very selective way. The TON's for the Ir/Rh catalyst for carbonylation is up to 571/1100 using ethylene as the hydrogen acceptor. Broad substrate scope and good site selectivity are particularly observed in this process.

3.8. Utilization with zinc-complexes as catalysts

Recently, Paul *et al.* demonstrated the dehydrogenation of *N*-heterocycles and dehydrogenative cross-coupling by introducing the concept of ligand accelerated redox-control method.[90] The dehydrogenation reaction has been catalyzed by the Zn(II) complex in the presence of a catalytic amounts of KO^{t}Bu as a co-catalyst. The proposed methodology has been achieved through the involvement of a single electron transfer process from aryl-azo scaffolds of stabled azo-anion radical Zn(II) complexes (Scheme 133 and 134). Furthermore, the authors also explored the synthesis of various substituted quinazolines, quinazolin-4(3*H*)-ones and quinolines derivatives *via* dehydrogenative coupling using the Zn(II) complex (Scheme 135).

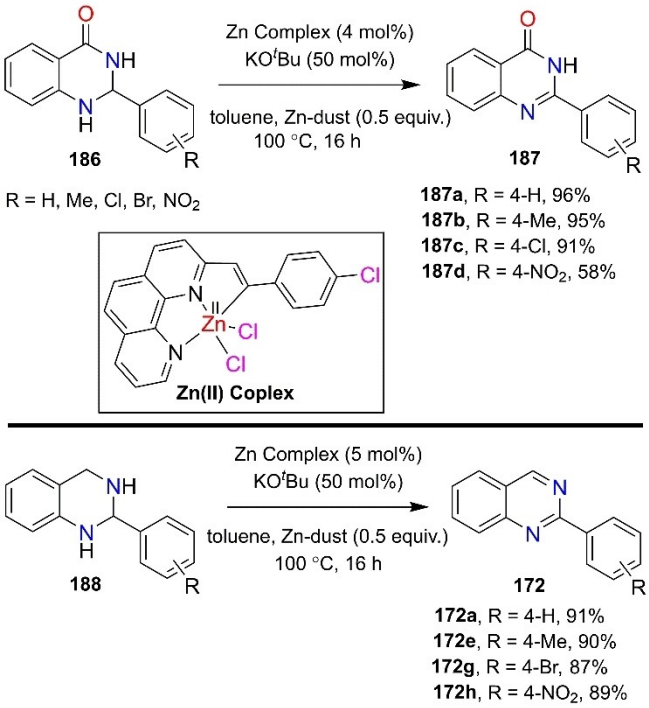

Scheme 133. Dehydrogenation of 2,3-dihydroquinazolinone and 2,3-dihydroquinazoline.

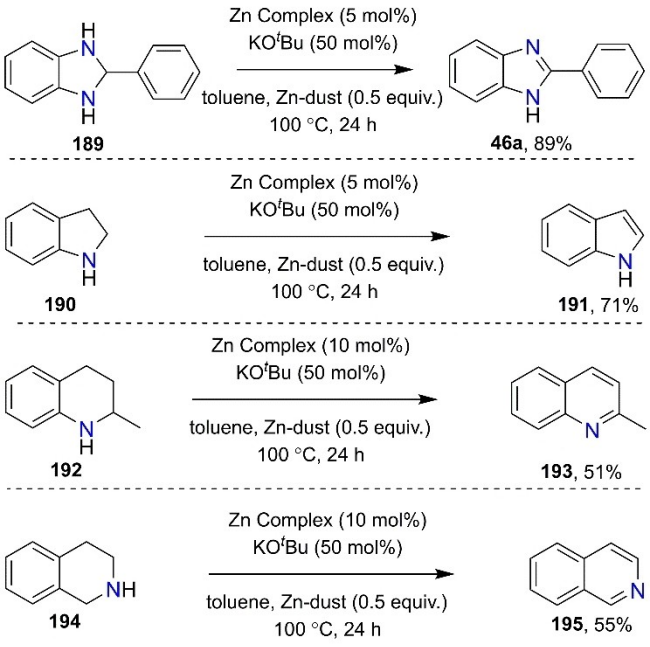

Scheme 134. Dehydrogenation of different *N*-heterocycles using Zn-complex.

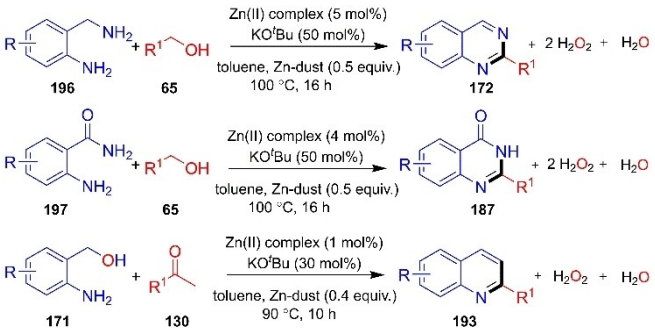

Scheme 135. Dehydrogenative coupling for synthesizing various substituted quinazolines, quinazolin-4(3*H*)-ones and quinolines derivatives using Zn-complex.

4. Conclusions

In conclusion, we have attempted to discuss the versatile catalytic roles of alkali metal *tert*-butoxides in organic transformations developed during the past decade (2012-2022). As discussed above, alkali metal *tert*-butoxides (NaO^{t}Bu, KO^{t}Bu, LiO^{t}Bu) have been found very useful in catalytic amounts for a broad range of organic transformations, which includes metal-free as well as metal-based reaction conditions. The atom-economical, environmentally benign, and easily available alkali metal *tert*-butoxides have been found as useful reagents towards the carbon-carbon, carbon-heteroatom, and heteroatom-heteroatom bond forming reactions. This review summarizes the versatile roles played by alkali metal *tert*-butoxides as a reagent in the synthesis of various kinds of transformations including silylation reactions, hydrogenation reactions, hydroboration reactions, kinetic resolution of oximes and alcohols, C–H activation reactions. The crucial reaction mechanisms are also discussed to understand the reaction mechanisms involved in these transformations.

Acknowledgements

C.C.M. appreciates the Science and Engineering Research Board (SERB), New Delhi, and NIT Manipur for financial support in the form of research grant (CRG/2020/004509 and ECR/2016/000337). We sincerely thank all the chemists who contributed towards the wellbeing of scientific community. C.K.P and K.K. are grateful to the Ministry of Education (MoE), New Delhi, for fellowship support.

Conflict of Interests

The authors declare no conflict of interest, financial or otherwise.

Data Availability Statement

Data sharing is not applicable to this article as no new data were created or analyzed in this study.

Keywords: Alkali metals *tert*-butoxides · C–C and C-heteroatom bond formation · Metal catalysis · Metal-free catalysis · Single-electron transfer (SET)

[1] a) C. C. Malakar, D. Schmidt, J. Conrad, U. Beifuss, *Org. Lett.* **2011**, *13*, 1972–1975; b) C. C. Malakar, D. Schmidt, J. Conrad, U. Beifuss, *Org. Lett.* **2011**, *13*, 1378–1381; c) C. C. Malakar, A. Baskakova, J. Conrad, U. Beifuss, *Chem. Eur. J.* **2012**, *18*, 8882–8885; d) N. Aljaar, C. C. Malakar, J. Conrad, S. Strobel, T. Schleid, U. Beifuss, *J. Org. Chem.* **2012**, *77*, 7793–7803; e) D. Singh, V. Kumar, N. Devi, C. C. Malakar, R. Shankar, V. Singh, *Adv. Synth. Catal.* **2017**, *239*, 1213–1226; f) D. Singh, N. Devi, V. Kumar, C. C. Malakar, S. Mehra, S. Rattan, R. K. Rawal, V. Singh, *Org. Biomol. Chem.* **2016**, *14*, 8154–8166; g) N. Devi, D. Singh, G. Kaur, S. Mor, V. P. R. K. Putta, S. Polina, C. C. Malakar, V. Singh, *New J. Chem.* **2017**, *41*, 1082–1093; h) D. Schmidt, C. C. Malakar, U. Beifuss, *Org. Lett.* **2014**, *18*, 4862–4865; i) K. Sudheendran, C. C. Malakar, J. Conrad, U. Beifuss, *J. Org. Chem.* **2012**, *77*, 10194–10210; j) D. Kaldhi, N. Vodnala, R. Gujjarappa, C. C. Malakar, S. Nayak, V. Ravichandiran, S. Gupta, C. K. Hazra, *Tetrahedron Lett.* **2019**, *60*, 223–229; k) D. Singh, P. Sharma, R. Kumar, S. K. Pandey, C. C. Malakar, V. Singh, *Asian J. Org. Chem.* **2018**, *7*, 383–394; l) N. Aljaar, C. C. Malakar, J. Conrad, W. Frey, U. Beifuss, *J. Org. Chem.* **2013**, *78*, 154–166; m) K. Kushwaha, B. Pinter, S. A. Shehzadi, C. C. Malakar, C. M. Vande, F. D. Proft, K. A. Tehrani, *Adv. Synth. Catal.* **2016**, *358*, 41–49; n) D. Singh, C. K. Hazra, C. C. Malakar, S. K. Pandey, B. S. Kaith, V. Singh, *ChemistrySelect* **2018**, *3*, 4859–4864; o) N. Devi, D. Singh, R. K. Sunkaria, C. C. Malakar, S. Mehra, R. K. Rawal, V. Singh, *ChemistrySelect* **2016**, *1*, 4696–4703; p) R. Gujjarappa, S. K. Maity, C. K. Hazra, N. Vodnala, S. Dhiman, A. Kumar, U. Beifuss, C. C. Malakar, *Eur. J. Org. Chem.* **2018**, *33*, 4628–4638; q) R. Gujjarappa, N. Vodnala, M. Kumar, C. C. Malakar, *J. Org. Chem.* **2019**, *84*, 5005–5020; r) V. P. R. K. Putta, N. Vodnala, R. Gujjarappa, U. Tyagi, A. Garg, S. Gupta, P. P. Pujar, C. C. Malakar, *J. Org. Chem.* **2020**, *85*, 380–396; s) R. Gujjarappa, N. Vodnala, V. G. Reddy, C. C. Malakar, *Eur. J. Org. Chem.* **2020**, *7*, 803–814; t) C. C. Malakar, K. Sudheendran, H. Imrich, S. Mika, U. Beifuss, *Org. Biomol. Chem.* **2012**, *10*, 3899–3905; u) V. P. R. K. Putta, R. Gujjarappa, U. Tyagi, P. P. Pujar, C. C. Malakar, *Org. Biomol. Chem.* **2019**, *17*, 2516–2528; v) V. P. R. K. Putta, R. Gujjarappa, N. Vodnala, R. Gupta, P. P. Pujar, C. C. Malakar, *Tetrahedron Lett.* **2018**, *59*, 904–908.

[2] a) A. K. Kabi, R. Gujjarappa, N. Vodnala, D. Kaldhi, U. Tyagi, K. Mukherjee, C. C. Malakar, *Tetrahedron Lett.* **2020**, *61*, 152535; b) C. C. Malakar, G. Helmchen, *Chem. Eur. J.* **2015**, *21*, 7127–7134; c) N. Vodnala, D. Kaldhi, S. Polina, V. P. R. K. Putta, R. Gupta, S. C. P. Promily, R. K. Linthoinganbi, V. Singh, C. C. Malakar, *Tetrahedron Lett.* **2016**, *57*, 5695–5699; d) N. Vodnala, R. Gujjarappa, V. Satheesh, R. Gupta, D. Kaldhi, A. K. Kabi, C. C. Malakar, *ChemistrySelect* **2020**, *5*, 10144–10148; e) N. Vodnala, R. Gujjarappa, S. Polina, V. Satheesh, D. Kaldhi, A. K. Kabi, C. C. Malakar, *New J. Chem.* **2020**, *44*, 20940–20944; f) C. C. Malakar, E. Merisor, J. Conrad, U. Beifuss, *Synlett* **2010**, *2010*, 1766–1770; g) R. Gujjarappa, N. Vodnala, A. Garg, C. K. Hazra, S. Gupta, C. C. Malakar, *ChemistrySelect* **2020**, *5*, 2419–2423; h) S. Polina, V. P. R. K. Putta, R. Gujjarappa, V. Singh, P. P. Pujar, C. C. Malakar, *Adv. Synth. Catal.* **2021**, *363*, 431–445; i) R. Gujjarappa, N. Vodnala, V. G. Reddy, C. C. Malakar, *Asian J. Org. Chem.* **2020**, *9*, 1793–1797; j) D. Kaldhi, R. Gujjarappa, N. Vodnala, A. K. Kabi, N. Aljaar, C. C. Malakar, *Chem. Lett.* **2019**, *48*, 1258–1261; k) R. Gujjarappa, N. Vodnala, A. K. Kabi, D. Kaldhi, M. Kumar, U. Beifuss, C. C. Malakar, *SynOpen* **2018**, *2*, 0138–0144; l) C. C. Malakar, L. Dell'Amico, W. Zhang, *Eur. J. Org. Chem.* **2023**, e202201114; m) R. Gujjarappa, N. Vodnala, C. C. Malakar, *Tetrahedron Lett.* **2020**, *61*, 151495; n) P. S. Kishore, R. Gujjarappa, V. R. K. Putta, S. Polina, V. Singh, C. C. Malakar, P. P. Pujar, *ChemistrySelect* **2022**, *7*, e202204238; o) R. Gujjarappa, N. Vodnala, D. Musib, C. C. Malakar, *Asian J. Org. Chem.* **2022**, *11*, e202100627; p) V. P. R. K. Putta, S. Polina, R. Gujjarappa, P. S. Kishore, C. C. Malakar, P. P. Pujar, *Polycyclic Aromat. Compd.* **2022**, 1–10; q) C. C. Malakar, V. Singh, *New J. Chem.* **2023**, *47*, 1186–1196; r) N. Aljaar, R. Gujjarappa, M. Al-Refai, M. Shtaiwi, C. C. Malakar, *Heterocycl. Chem.* **2019**, *56*, 2730–2743; s) D. Schmidt, C. C. Malakar, J. Conrad, U. Beifuss, *Org. Lett.* **2014**, *16*, 4862–4865.

[3] a) R. Gujjarappa, N. Vodnala, C. C. Malakar, *Adv. Synth. Catal.* **2020**, *362*, 4896–4990; b) R. Gujjarappa, N. Vodnala, C. C. Malakar, *ChemistrySelect* **2020**, *5*, 8745–8758; c) A. Garg, K. Kant, K. K. Roy, A. Sahoo, C. C. Malakar, S. Gupta, *Mater. Today: Proc.* **2022**, *57*, 300–306; d) N. Aljaar, M. M. Ibrahim, E. A. Younes, M. Al-Noaimi, K. A. Abu-Safieh, B. F. Ali, K. Kant, N. Al-Zaqri, R. Sengupta, C. C. Malakar, *Asian J. Org. Chem.* **2023**, *12*, e202300036; e) R. Reetu, A. Garg, K. K. Roy, A. Roy, S. Gupta, C. C. Malakar, *Mater. Today: Proc.* **2022**, *57*, 44–48; f) A. K. Kabi, M. Pal, R. Gujjarappa, C. C. Malakar, M. Roy, *Heterocycl. Chem.* **2023**, *60*, 165–182; g) R. K. Devappa, C. C. Malakar, H. P. S. Makkar, K. Becker, *Nat. Prod. Res.* **2013**, *27*, 1459–1462; h) M. Shtaiwi, N. Aljaar, L. Al-Najjar, C. C. Malakar, A. Shtaiwi, M. Abu-Sini, M. Al-Refai, *Polycyclic Aromat. Compd.* **2022**, 1–14; i) R. Reetu, R. Gujjarappa, C. C. Malakar, *Asian J. Org. Chem.* **2022**, *11*, e202200163; j) I. Muthukrishnan, V. Sridharan, J. C. Menéndez, *Chem. Rev.* **2019**, *119*, 5057–5191; k) V. Sridharan, P. A. Suryavanshi, J. C. Menéndez, *Chem. Rev.* **2011**, *111*, 7157–7259.

[4] F. G. Bordwell, *Acc. Chem. Res.* **1988**, *21*, 456–463.

[5] W. Liu, H. Cao, H. Zhang, H. Zhang, K. H. Chung, C. He, H. Wang, F. Y. Kwong, A. Lei, *J. Am. Chem.* **2010**, *132*, 16737–16740.

[6] E. Shirakawa, K. Itoh, T. Higashino, T. Hayashi, *J. Am. Chem. Soc.* **2010**, *132*, 15537–15539.

[7] S. Yanagisawa, K. Itami, *ChemCatChem* **2011**, *3*, 827–829.

[8] E. Shirakawa, T. Hayashi, *Chem. Lett.* **2012**, *41*, 130134.

[9] J. Madasu, S. Shinde, R. Das, S. Patel, A. Shard, *Org. Biomol. Chem.* **2020**, *18*, 8346–8365.

[10] D. E. Pearson, C. A. Buehler, *Chem. Rev.* **1974**, *74*, 45–86.

[11] I. D. Jenkins, E. H. Krenske, *ACS Omega* **2020**, *5*, 7053–7058.

[12] H. Yoshida, *ACS Catal.* **2016**, *6*, 1799–1811.

[13] A. A. Toutov, W. Liu, K. N. Betz, A. Fedorov, B. M. Stoltz, R. H. Grubbs, *Nature* **2016**, *518*, 80–84.

[14] W. Liu, D. P. Schuman, Y. Yang, A. A. Toutov, Y. Liang, H. F. T. Klare, N. Nesnas, M. Oestreich, D. G. Blackmond, S. C. Virgil, S. Banerjee, R. N. Zare, R. H. Grubbs, K. N. Houk, B. M. Stoltz, *J. Am. Chem. Soc.* **2017**, *139*, 6867–6879.

[15] S. Banerjee, Y. Yang, I. D. Jenkins, Y. Liang, A. A. Toutov, W. Liu, D. P. Schuman, R. H. Grubbs, B. M. Stoltz, E. H. Krenske, K. N. Houk, R. N. Zare, *J. Am. Chem. Soc.* **2017**, *139*, 6880–6887.

[16] H. Lee, C. Kwak, D. Kim, H. Kim, *Green Chem.* **2021**, *23*, 1193–1199.

[17] I. A. Bidusenko, E. Yu. Schmidt, I. A. Ushakov, B. A. Trofimov, *Eur. J. Org. Chem.* **2018**, *2018*, 4845–4849.

[18] A. R. Claus, T. A. C. Goulart, D. F. Back, G. Zeni, *Eur. J. Org. Chem.* **2021**, *2021*, 2180–2187.

[19] A. Kumar, T. Janes, S. Chakraborty, P. Daw, N. V. Wolff, R. Carmieli, Y. -Posner, D. Milstein, *Angew. Chem. Int. Ed.* **2019**, *58*, 3373–3377.

[20] L. Chen, J. Zhang, W.-W. Yang, J.-Y. Fu, J.-Y. Zhu, Y.-B. Wang, *J. Org. Chem.* **2019**, *84*, 8090–8099.

[21] S. Wang, Y. Xiang, T. Chen, X. Wua, D. Xing, *Org. Chem. Front.* **2022**, *9*, 1642–1648.

[22] Y. Xiang, R. Du, S. Wang, X. Wu, J. Tang, F. Yang, D. Xing, *Mol. Diversity* **2022**. https://doi.org/10.1007/s11030-022-10503-8.

[23] D. Y. Li, K. J. Shi, X. F. Mao, Z. L. Zhao, X. Y. Wu, P. N. Liu, *Tetrahedron Lett.* **2014**, *70*, 7022–7031.

[24] R. Gai, D. F. Back, G. Zeni, *J. Org. Chem.* **2015**, *80*, 10278–10287.

[25] Z. Chen, L. Wu, H. Fang, T. Zhang, Z. Mao, Y. Zou, X. Zhang, M. Yan, *Adv. Synth. Catal.* **2017**, *359*, 3894–3899.

[26] T. P. Reddy, A. V. Krishna, D. B. Ramachary, *Org. Lett.* **2018**, *20*, 6979–6983.

[27] R. Govindarajan, J. Ahmed, A. K. Swain, S. K. Mandal, *J. Org. Chem.* **2019**, *84*, 13490–13502.

[28] S. Thiyagarajan, V. Krishnakumar, C. Gunanathan, *Asian Chem. Ed. Soc.* **2020**, *15*, 518–523.

[29] M. Shigeno, Y. Shishido, K. Hayashi, K. -Kumada, Y. Kondo, *Eur. J. Org. Chem.* **2021**, *2021*, 3932–3935.

[30] A. K. Kabi, R. Gujjarappa, A. Roy, A. Sahoo, D. Musib, N. Vodnala, V. Singh, C. C. Malakar, *J. Org. Chem.* **2021**, *86*, 14597–14607.

[31] L. Wang, A. Ishida, Y. Hashidoko, M. Hashimoto, *Angew. Chem. Int. Ed.* **2016**, *56*, 870–873.
[32] Y. Xu, X. Shi, L. Wu, *RSC Adv.* **2019**, *9*, 24025.
[33] J. H. Kim, A. K. Jaladi, H. T. Kim, D. K. An, *Bull. Korean Chem. Soc.* **2019**, *40*, 971–975.
[34] R. J. Grams, C. J. Garcia, C. Szwetkowski, W. L. Santos, *Org. Lett.* **2020**, *22*, 7013–7018.
[35] J. Diebler, H. Komber, L. Häußler, A. Lederer, T. Werner, *Macromolecules* **2016**, *49*, 4723–4731.
[36] X. Dong, Y. Kita, M. Oestreich, *Angew. Chem. Int. Ed.* **2018**, *57*, 10728–10731.
[37] J. Seliger, M. Oestreich, *Angew. Chem. Int. Ed.* **2020**, *60*, 247–251.
[38] Z. Papadopulu, M. Oestreich, *Org. Lett.* **2021**, *23*, 438–441.
[39] J. K. Park, B. A. Ondrusek, D. T. McQuade, *Org. Lett.* **2012**, *14*, 4790–4793.
[40] K. Semba, T. Fujihara, J. Terao, Y. Tsuji, *Chem. Eur. J.* **2012**, *18*, 4179–4184.
[41] H. Jung, X. Feng, H. Kim, J. Yun, *Tetrahedron Lett.* **2012**, *68*, 3444–3449.
[42] D. Li, Y. E. Kim, J. Yun, *Org. Lett.* **2015**, *17*, 860–863.
[43] A. L. Moure, R. G. Arrayás, D. J. Cárdenas, I. Alonso, J. C. Carretero, *Am. Chem. Commun.* **2012**, *134*, 7219–7222.
[44] P. Liu, Y. Fukui, P. Tian, Z. He, C. Sun, N. Wu, G. Lin, *J. Am. Chem.* **2013**, *135*, 11700–11703.
[45] G. Zhu, W. Kong, H. Feng, Z. Qian, *J. Org. Chem.* **2014**, *79*, 1786–1795.
[46] H. Yoshida, Y. Takemotoa, K. Takakia, *Chem. Commun.* **2014**, *50*, 8299.
[47] W. Guan, A. K. Michael, M. L. McIntosh, L. K. Selfridge, J. P. Scott, T. B. Clark, *J. Org. Chem.* **2014**, *79*, 7199–7204.
[48] Y. M. Chae, J. S. Bae, J. H. Moon, J. Y. Lee, J. Yuna, *Adv. Synth. Catal.* **2014**, *356*, 843–849.
[49] G. He, S. Chen, Q. Wang, H. Huang, Q. Zhang, D. Zhang, R. Zhang, H. Zhu, *Org. Biomol. Chem.* **2014**, *12*, 5945–5953.
[50] Y. Bai, F. Zhang, J. Shen, F. Luo, G. Zhu, *Asian J. Org. Chem.* **2015**, *4*, 626–629.
[51] Z. He, X. Tang, L. Xie, M. Cheng, P. Tian, G. Lin, *Angew. Chem. Int. Ed.* **2015**, *54*, 14815–14818.
[52] Y. Shi, Q. Gao, S. Xu, *J. Org. Chem.* **2018**, *83*, 14758–14767.
[53] W. Mao, M. Oestreich, *Org. Lett.* **2020**, *22*, 8096–8100.
[54] J. M. Hoover, B. L. Ryland, S. S. Stahl, *ACS Catal.* **2013**, *3*, 2599–2605.
[55] K. R. Fandrick, J. Ogikubo, D. R. Fandrick, N. D. Patel, J. Saha, H. Lee, S. Ma, N. Grinberg, C. A. Busacca, C. H. Senanayake, *Org. Lett.* **2013**, *15*, 1214–1217.
[56] C. Medina, K. P. Carter, M. Miller, T. B. Clark, G. W. O'Neil, *J. Org. Chem.* **2013**, *78*, 9093–9101.
[57] B. Pooi, J. Lee, K. Choi, H. Hirao, S. H. Hong, *J. Org. Chem.* **2014**, *79*, 9231–9245.
[58] R. Bigler, A. Mezzetti, *Org. Lett.* **2014**, *16*, 6460–6463.
[59] J. H. Docherty, J. Peng, A. P. Dominey, S. P. Thomas, *Nat. Chem.* **2017**, *9*, 595–600.
[60] B. Cheng, W. Liu, Z. Lu, *J. Am. Chem. Soc.* **2018**, *140*, 5014–5017.
[61] R. Lopes, Á. Raya-Barón, M. P. Robalo, C. Vinagreiro, S. Barroso, M. J. Romão, I. Fernández, M. M. Pereira, B. Royo, *Eur. J. Inorg. Chem.* **2021**, *2021*, 22–29.
[62] R. Adam, C. Bheeter, J. C. Antonino, K. Junge, R. Jackstell, M. Beller, *ChemSusChem* **2017**, *10*, 842–846.
[63] K. Tokmic, B. J. Jackson, A. Salazar, T. J. Woods, A. R. Fout, *J. Am. Chem.* **2017**, *139*, 13554–13561.
[64] J. Peng, J. H. Docherty, A. P. Dominey, S. P. Thomas, *Chem. Commun.* **2017**, *53*, 4726–4729.
[65] B. Cheng, P. Lu, H. Zhang, X. Cheng, Z. Lu, *J. Am. Chem.* **2017**, *139*, 9439–9442.
[66] J. Wu, H. Zeng, J. Cheng, S. Zheng, J. A. Golen, D. R. Manke, G. Zhang, *J. Org. Chem.* **2018**, *83*, 9442–9448.
[67] K. Paudel, B. Pandey, S. Xu, D. K. Taylor, D. L. Tyer, C. L. Torres, S. Gallagher, L. Kong, K. Ding, *Org. Lett.* **2018**, *20*, 4478–4481.
[68] P. Biswal, S. Samser, P. Nayak, V. Chandrasekhar, K. Venkatasubbaiah, *J. Org. Chem.* **2021**, *86*, 6744–6754.
[69] K. Gao, M. Xu, C. Cai, Y. Ding, J. Chen, B. Liu, Y. Xia, *Org. Lett.* **2020**, *22*, 6055–6060.
[70] S. Elangovan, C. Topf, S. Fischer, H. Jiao, A. Spannenberg, W. Baumann, R. Ludwig, K. Junge, M. Beller, *J. Am. Chem.* **2016**, *138*, 8809–8814.
[71] V. Zubar, Y. Lebedev, L. M. Azofra, L. Cavallo, O. Sepelgy, M. Rueping, *Angew. Chem. Int. Ed.* **2018**, *57*, 13439–13443.
[72] J. Rana, P. Nagarasu, M. Subaramanian, A. Mondal, V. Madhu, E. Balaraman, *Organometallics* **2021**, *40*, 627–634.
[73] F. Freitag, T. Irrgang, R. Kempe, *J. Am. Chem. Soc.* **2019**, *141*, 11677–11685.
[74] I. Buslov, S. C. Keller, X. Hu, *Org. Lett.* **2016**, *18*, 1928–1931.
[75] X. Wu, G. Ding, W. Lu, L. Yang, J. Wang, Y. Zhang, X. Xie, Z. Zhang, *Org. Lett.* **2021**, *23*, 1434–1439.
[76] A. Obata, Y. Ano, N. Chatani, *Chem. Sci.* **2017**, *8*, 6650–6655.
[77] A. Obata, Y. Ano, N. Chatani, *Chem. Sci.* **2017**, *8*, 6650–6655.
[78] D. Panigrahi, M. Mondal, R. Guptaa, G. Mani, *RSC Adv.* **2022**, *12*, 4510–4520.
[79] T. T. Dang, B. Ramalingam, A. M. Seayad, *ACS Catal.* **2015**, *5*, 4082–4088.
[80] O. Ogata, H. Nara, M. Fujiwhara, K. Matsumura, Y. Kayaki, *Org. Lett.* **2018**, *20*, 3866–3870.
[81] K. Iida, T. Miura, J. Ando, S. Saito, *Org. Lett.* **2013**, *15*, 1436–1439.
[82] M. Chen, M. Zhang, B. Xiong, Z. Tan, W. Lv, H. Jiang, *Org. Lett.* **2014**, *16*, 6028–6031.
[83] Y. Nakamura, Y. Oe, T. Ohta, *Chem. Commun.* **2015**, *51*, 7459–7462.
[84] D. Kim, L. Le, M. J. Drance, K. H. Jensen, K. Bogdanovski, T. N. Cervarich, M. G. Barnard, N. J. Pudalov, S. M. M. Knapp, A. R. Chianese, *Organometallics* **2016**, *35*, 982–989.
[85] L. Le, J. Liu, T. He, D. Kim, E. J. Lindley, T. N. Cervarich, J. C. Malek, J. Pham, M. R. Buck, A. R. Chianese, *Organometallics* **2018**, *37*, 3286–3297.
[86] S. Thiyagarajan, R. V. Sankar, C. Gunanathan, *Org. Lett.* **2020**, *22*, 7879–7884.
[87] T. W. Lyons, D. Bézier, M. Brookhart, *Organometallics* **2015**, *34*, 4058–4062.
[88] Y. Wang, Z. Huang, X. Leng, H. Zhu, G. Liu, Z. Huang, *J. Am. Chem.* **2018**, *140*, 4417–4429.
[89] X. Tang, X. Jia, Z. Huang, *J. Am. Chem.* **2018**, *140*, 4157–4163.
[90] S. Das, R. Mondal, G. Chakraborty, A. K. Guin, A. Das, N. D. Paul, *ACS Catal.* **2021**, *11*, 7498–7512.